AD-A095 971 BATTELLE COLUMBUS LABS OH F/G 13/5
TREND INSPECTION STATION FOR PRINTED CIRCUIT BOARD SOLDER JOINT--ETC(U)
APR 79 D J HAMMAN, D ENSMINGER, R VANZETTI F04606-78-C-0903

UNCLASSIFIED NL

1 OF 2
AD A
09597

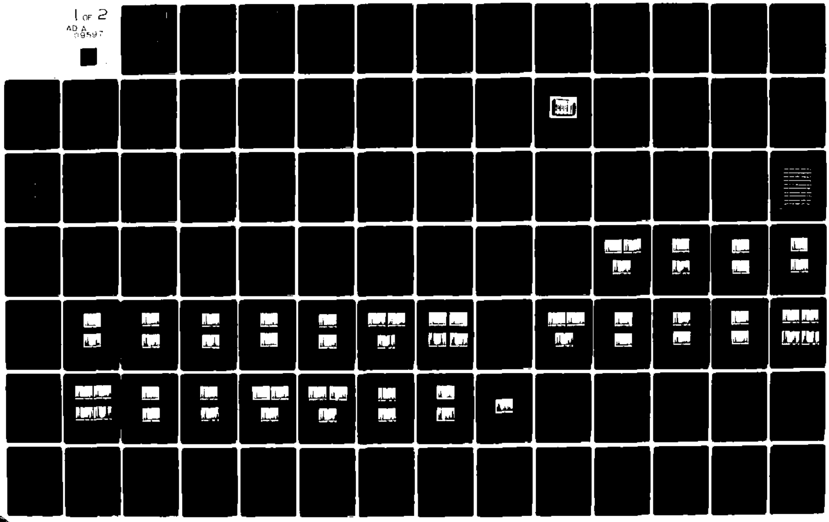

PHOTOGRAPH THIS SHEET

ADA095971

DTIC ACCESSION NUMBER

II

LEVEL

I

INVENTORY

BATTELLE COLUMBUS LABS., OHIO

TREND INSPECTION STATION FOR PRINTED CIRCUIT BOARD
SOLDER JOINTS. FINAL REPT. PHASE I. 7 APR. 79
CONTRACT F04606-78-C-0903

DOCUMENT IDENTIFICATION

DISTRIBUTION STATEMENT A
Approved for public release;
Distribution Unlimited

DISTRIBUTION STATEMENT

ACCESSION FOR		
NTIS	GRA&I	☒
DTIC	TAB	☐
UNANNOUNCED		☐
JUSTIFICATION		
BY		
DISTRIBUTION /		
AVAILABILITY CODES		
DIST	AVAIL AND/OR SPECIAL	
A		

DISTRIBUTION STAMP

DTIC
S ELECTE D
MAR 5 1981
D

DATE ACCESSIONED

"Original contains color
plates: All DTIC reproduct-
ions will be in black and
white"

DATE RECEIVED IN DTIC

PHOTOGRAPH THIS SHEET AND RETURN TO DTIC-DDA-2

DTIC FORM OCT 79 70A

DOCUMENT PROCESSING SHEET

AD A095971

FINAL REPORT

on

TREND INSPECTION STATION
for
PRINTED CIRCUIT BOARD SOLDER JOINTS
(PHASE 1)

to

SACRAMENTO AIR LOGISTIC CENTER

April 6, 1979

by

D. J. Hamman, D. Ensminger and Dr. C. T. Walters
(Battelle-Columbus Laboratories)

and

Dr. R. Vanzetti and Dr. A. C. Traub
(Vanzetti Infrared and Computer Systems, Inc.)

Contract No. F04606-78-C-0903-PZ0001
6 JULY 1978 - 7 APRIL 1979

Approved for public release - Distribution unlimited

BATTELLE
Columbus Laboratories
505 King Avenue
Columbus, Ohio 43201

81 3 04 019

Battelle
Columbus Laboratories
505 King Avenue
Columbus, Ohio 43201
Telephone (614) 424-6424
Telex 24-5454

April 6, 1979

Headquarters
Sacramento Air Logistic Center
McClellan Air Force Base, CA 95652

Attn: MMIREA (John Ele)

Dear Sir:

Final Report - Phase 1

Two (2) copies of the Final Report on "Trend Inspection Station for Printed Circuit Board Solder Joints - Phase 1" are enclosed. The report is submitted in accordance with Contract No. F04606-78-C-0903-PZ0001 as required by DD Form 1423, Line Item 0002, Sequence No. A007, 18 April 1978.

This report covers the contractual period of the program, 6 July 1978 to 7 April 1979.

It was the objective of this Phase 1 effort to demonstrate the feasibility of using:

(1) An Ultrasonic technique and/or
(2) Laser heating with subsequent cooling measurement technique and/or
(3) A multilens microvideo visual technique

to produce a significant improvement in the ability to detect defective lap-type solder joints on printed circuit boards.

Three major efforts were required to meet this Phase 1 objective. One effort was carried out at Vanzetti Infrared and Computer Systems, Inc., (the Laser/IR effort); the other two efforts were conducted at Battelle (the Ultrasonics effort and the preparation of a set of "standard" solder joints containing known good and selected defective joints). The microvideo effort was not considered major for Phase 1 since the capabilities, advantages and limitations of visual systems already were well known.

The results of the Phase 1 program presented in the enclosed Final Report show that all the techniques are feasible with an expected detection accuracy for open, cracked or cold solder joints in excess of 90 percent. Further, the results indicate that the continuation of this program into the Phase 2, "Use-Size Model Fabrication", would be a practical and economical decision for the Sacramento ALC. Therefore, we also will be submitting our proposed program for Phase 2 and are looking forward to the continuation.

If you have any questions concerning this report please call me at 614/424-5799.

Sincerely,

Donald J. Hamman

Donald J. Hamman
Engineering Physics and
Electronics Section

DJH/kv

xc: DCASMA, Dayton
Defense Electronics Supply Center
Attn: Robert E. Reed, DCRO-GDCA
Bldg. 5, 1502 Wilmington Pike
Dayton, Ohio 45444 (letter only)

Dr. R. Vanzetti, President
Vanzetti Infrared and Computer System, Inc.
607 Neponset Street
Canton, Massachusetts 02021

REPORT DOCUMENTATION PAGE

READ INSTRUCTIONS BEFORE COMPLETING FORM

1. REPORT NUMBER

2. GOVT ACCESSION NO. AD-A095 971

3. RECIPIENT'S CATALOG NUMBER

4. TITLE (and Subtitle)
TREND INSPECTION STATION FOR PRINTED CIRCUIT BOARD SOLDER JOINTS (PHASE I)

5. TYPE OF REPORT & PERIOD COVERED
FINAL--PHASE I
6 Jul 78 - 7 Apr 79

6. PERFORMING ORG. REPORT NUMBER

7. AUTHOR(s)
HAMMAN, D.J. and ENSMINGER, D. (BATTELLE)
VANZETTI, DR. R., and TRAUB, DR. A.C. (VANZETTI)

8. CONTRACT OR GRANT NUMBER(s)
F04606-78-C-0903-PZ0001

9. PERFORMING ORGANIZATION NAME AND ADDRESS
BATTELLE COLUMBUS LABORATORIES
505 KING AVENUE
COLUMBUS, OHO 43201

10. PROGRAM ELEMENT, PROJECT, TASK AREA & WORK UNIT NUMBERS
Project No.
FD2040-78-35481-01

11. CONTROLLING OFFICE NAME AND ADDRESS
SACRAMENTO ALC/PP
PMWFA; MCCLELLAN AFB, CA 95652

12. REPORT DATE
7 April 1979

13. NUMBER OF PAGES

14. MONITORING AGENCY NAME & ADDRESS (if different from Controlling Office)

15. SECURITY CLASS. (of this report)
Unclassified

15a. DECLASSIFICATION/DOWNGRADING SCHEDULE

16. DISTRIBUTION STATEMENT (of this Report)

Distribution unlimited--approved for public release

17. DISTRIBUTION STATEMENT (of the abstract entered in Block 20, if different from Report)

18. SUPPLEMENTARY NOTES

19. KEY WORDS (Continue on reverse side if necessary and identify by block number)

Ultrasonic Inspection, Laser Inspection, Visual Inspection, IR Inspection, Solder Joint Inspection, Color Video Inspection

20. ABSTRACT (Continue on reverse side if necessary and identify by block number)

Three techniques, ultrasonic, laser/IR and video were evaluated for feasibility as solder joint defect detectors. All three were found to be feasible with a combined detection accuracy of approximately 90 percent for 19 types of defects. Detection of severe defects is near 100 percent.

All three techniques should be continued for development under Phase 2 to the extent of fabricating use-size models of equipment to use the three techniques.

DD FORM 1 JAN 73 1473 EDITION OF 1 NOV 65 IS OBSOLETE

TABLE OF CONTENTS

Page

SUMMARY 1

BACKGROUND. 1

INTRODUCTION. 2

OBJECTIVE 3

DISCUSSION. 3

- STANDARD SOLDER JOINT PREPARATION. 4
  - Solder Joint Types. 5
  - Equipment 6
  - Solder Joint Preparation Procedures 6
  - Summary 8
- ULTRASONIC STUDIES 9
  - Introduction. 9
  - Theory of the Ultrasonic Inspection Technique 10
  - Experimental Program. 16
    - Feasibility Analysis With Candidate Defects. 16
    - Development of Physical Set-Up and Preliminary Experiments. 17
    - Effects of Ultrasonic Intensity. 20
    - Effects of Coupling. 21
    - Experimental Procedures. 22
    - Experimental Results - Standard Test Boards. 24
    - Typical Spectra of Test Solder Joints. 32
- THEORY OF LASER/INFRARED SOLDER JOINT INSPECTION 63
  - Definition of the Problem 64
  - Selection of Laser Beam Parameter Values. 67
  - Numerical Solution of the Heat-Transfer Problem 69
  - Study of Pulse Length Effects 75
  - Study of Effect of Void Configuration 81
  - Study of Excess Solder Effects. 82
  - Conclusions 84
  - References. 86

TABLE OF CONTENTS
(Continued)

Page

EXPERIMENTAL LASER/IR STUDIES. 87
  Laser/IR Test Results 90
  Joint Description and Detactability 95
    Lead Detached from Joint 95
    Cold Joints. 96
    Dewetted Joints. 101
    Granular Surfaces. 101
    Exposed Gold 101
    Excessive Heat 103
    Insufficient Solder. 103
    Lead Half Off Pad. 103
    Moveable Joints. 106
  Discussion. 109
    Non-Detectable Defects 109
    Laser Pulse Stability. 110
    Pulse Duration and its Effects 110
    Variations Along a Joint 112
    Variations Among Joints. 114
    Effects of Absorptivity. 114
    The Micro-Reflectometer. 120
    Automatic Sample Centering and Surface Characterization. . . 120
  Continued Efforts 123
  Technical Discussion. 124
    Description of Test Arrangement. 124
    Targeting Considerations 128
    Choice of Laser. 128
    Projected System Performance 129
  Conclusions and Recommendations 130
MICROVIDEO STUDY 132
CONCLUSIONS AND RECOMMENDATIONS 133
GENERAL CONCLUSIONS AND RECOMMENDATIONS. 133
SPECIFIC CONCLUSIONS 133

TABLE OF CONTENTS
(Continued)

Page

Accuracy of Defect Detection 133
  Ultrasonic Technique 133
  Laser/IR Technique 134
  Visual Technique 136
  Overall System 136
Processing Capabilities 136
  Accuracy of Platform Movement 136
  Throughout Capability, 1000-Joint PCB 137
  Number of Allowable PCB Configurations 137
  Data Storage Method 137
  Operator Training Requirement 138
  Marking Methods Considered 138
Risk Statement 138
  Sensor Techniques 138
  Platform Movement Accuracy 138
  Maintenance Calibration 139
Station Information 139
  General Description 139
  Data Processing Considerations 139
SPECIFIC RECOMMENDATIONS 141

LIST OF TABLES

Table 1. Preliminary Estimates of the Capabilities of the Ultrasonic Inspection System to Detect Defects in Solder Joints on Flat Pack PC Boards 18
Table 2. Summary of Ultrasonic Inspection of Solder Joints in Test Section of Standard Printed Circuit Board 27
Table 3. Spectral Characteristics of Solder Joints on Standard Board 35
Table 4. Thermal Properties Assumed for Solder-Joint Heat-Transfer Calculation 66
Table 5. Summary of Experimental Results 91
Table 6. Main Components of Laser/IR System 127
Table 7. Overall Detective Capability 135

LIST OF FIGURES

Figure 1. Photograph of Completed Set of Standard Soldered Joints. 7

Figure 2. Basic Configuration of Ultrasonic Inspection Of Soldered Joints On PC Boards. 12

Figure 3. Block Diagram of the Experimental Setup For Inspecting Solder Joints on PC Boards. 23

Figure 4. Map of the Standard Baord Showing the Key Section and the Test Section 25

Figure 5. Typical Spectra of Good Joints Showing Extremes. 36

Figure 6. Typical Spectra of Cold Solder Joints Showing Two Extremes 37

Figure 7. Typical Spectra of Joint With Irregular Spreading [illegible] Solder Up The Lead Due to Excessive Heat 38

Figure 8. Typical Spectra of Irregular Spreading of Solder Up The Lead Due to Insufficient Heat 39

Figure 9. Typical Spectra of Toe of Lead Bent Up Showing Two Extremes 41

Figure 10. Typical Spectra of Lead Soldered Half Off Pad Showing Two Degrees of Seriousness 42

Figure 11. Typical Spectra of Tipped Lead Showing Two Extremes. 43

Figure 12. Typical Spectra of "Yellow Flat Top of Lead Viewed". 44

Figure 13. Typical Spectra of Voids in Solder Showing Extremes. 45

Figure 14. Typical Spectra of Cracks at Heel of Joint 46

Figure 15. Typical Spectra of Joints with Granular Appearance Showing Extremes 47

Figure 16. Spectra of Joints with $AuSn_4$ and $AuSn_2$ Entrapped In Solder Joint Microstructure 49

Figure 17. Spectra of Joints With Insufficient Solder 50

LIST OF FIGURES
(Continued)

Figure 18. Spectra of Joints With Excess Solder. 51

Figure 19. Spectra of Joints Subjected to Excessive Heat Showing Two Extremes 52

Figure 20. Spectra of Joints With Nol Fillet At The Heel/Lead Showing Extremes 53

Figure 21. Spectra of Dewetted Joints Showing Extremes 55

Figure 22. Typical Spectra Caused by Holes and Pits In Solder Joints. 56

Figure 23. Extremes in Spectra of Joints Containing Solder Peaks. 57

Figure 24. Spectra of Solder Joints Containing Inclusions. 58

Figure 25. Additional Spectra of Solder Joints Containing Inclusions 59

Figure 26. Spectra of a Good Solder Joint Verified By Destructive Examination. 60

Figure 27. Spectrum of a Solder Joint Containing a 15 Percent Crack at The Heel But Which Is Otherwise Solid. 61

Figure 28. Spectrum of a Solder Joint Which is Barely Tacked At The Heel and At The Toe 62

Figure 29. Idealized Geometry for Heat Transfer Calculations 65

Figure 30. Comparison of TRAHT2 Results to Analytical Solutions For 4 ms Pulse 72

Figure 31. Spatial Distribution of Surface Temperature for 4 ms Pulse. 74

Figure 32. Transient Temperature Response for 1 ms Pulse 76

Figure 33. Transient Temperature Response for 4 ms Pulse 77

Figure 34. Transient Temperature Response for 10 ms Pulse. 78

Figure 35. Power Density Required to Achieve 200C Surface Temperature Rise. 79

TABLE OF CONTENTS
(Continued)

Figure 36. Defect Temperature Contrast for
Various Pulse Lengths 80

Figure 37. Thermal Classification of Various
Solder-Joint Defects, Relative to Normal
Joints. Hypothetical Curves Based on Phase 1
Test Results. 94

Figure 38. Thermal Profile of a Detached Lead (Upper Trace)
And Of A Normal Joint (Trace Close To Baseline) 97

Figure 39. A Vanzetti-Prepared Cold Joint (Upper) and A
Normal Joint (Lower) 97

Figure 40. Five Vanzetti Cold Joints (Upper Two Groups
Of Traces) And Five Normal Joints (Lower Group) 99

Figure 41. A Repeat Of The Figure 4 Tests. Five Cold Joints
(Above First Division) and Five Normal Joints (Below).
Differences From Figure 4 May Be Due to Target-Point
Differences 99

Figure 42. Cold Joints With Shorter Pulse Durations. Two Cold
Joints Are Shown By The Two Upper Traces. The
Nearly Flat Trace Represents A Normal Joint.
120-Hz "Pickup" is Seen 100

Figure 43. Five Dewetted Joints (Upper Group of Traces) And
Two Normal Ones (Lower Group) 101

Figure 44. Five Granular Joints (Upper Group) And Two
Normal Ones (Two Lower Traces). 102

Figure 45. One Normal Joint (Upper) And Three "Yellow Flat
Tops" (Lower Group. 102

Figure 46. An Excessively Heated Joint (Upper)
And A Normal One (Lower). 104

Figure 47. An "Insufficient Solder" Joint (Upper) And A Normal
One (Lower). Abnormally High Difference May Signify
A Lead Detachment 104

Figure 48. Another "Insufficient Solder" Joint (No. C1-11),
Upper Trace) And A Normal One (Lower) 105

TABLE OF CONTENTS
(Continued)

Figure 49. Lead Half Off Pad (Upper Trace). Lower Group Is Two Superposed Traces At Other Points On Same Joint. (Upper Trace Is For Overhang). 105

Figure 50. A Different Lead Half Off Pad. Upper Trace Is Overhang: Lower Is At Another Point On Same Joint 107

Figure 51. Anomalous Result For Lead Half Off Pad. Upper Trace Is A Normal Joint (No. E2-1). Lower Is Overhang On No. E-2.2. 107

Figure 52. Example Of Heating-Rate Discontinuity. Detached Lead On Joint No. E1-12. Movement Of Lead During Heating Apparently Causes Change In Thermal Contact With Joint. 108

Figure 53. Repeatability Of Peak Thermal Signal At Fixed Point On A Joint. Multiple Exposures With 10-Second of V: 20. H: 5,000. E: 240. 113

Figure 54. Variability Of Thermal Signal At Different Points On The Same Joint. Twelve Seconds Of Cooling Between 113

Figure 55. Variability At Centers Of Two Normal Joints 115

Figure 56. Early Attempt To Normalize Cooling Curves Of Figure 19. 116

Figure 57. An Ink-Blackened (Upper) And A Shiny (Lower) Virgin Solder Pad 118

Figure 58. Early Attempt To Normalize Cooling Curves Of Figure 57. 119

Figure 59. Distinctive Reflection Patterns Of HeNe Laser Beam From Various Solder Surfaces 122

Figure 60. Present State Of Laser/Thermal Experiment Arrangement . . .125

Figure 61. Two Views Of Target Area In Laser/Thermal Test System . . .126

SUMMARY

The purpose of this first phase of the Trend Inspection Station (TIS) for Printed Circuit Board Solder Joints has been to evaluate the feasibility of using one or more of three techniques to give a more accurate inspection procedure than is currently available. The three techniques that were evaluated were ultrasonic, laser/IR and visual (color microvideo). The visual system is similar to the current inspection technique except that the TIS will use a multilens concept to display the entire solder joint in several views simultaneously. The ultrasonic and laser/IR techniques will permit the inspection of the hidden characteristics of a solder joint such as non-obvious cold solder joints, incipient cracks (particularly under the lead), voids, inclusions, etc.

The laser/IR technique uses the energy in a laser pulse to heat a solder joint, and then an IR sensor monitors the heating curve and/or the peak temperature and/or the cooling curve and compares them to the corresponding characteristic of a known "good" solder joint.

The ultrasonic technique injects a pulse of ultrasonic energy into the "toe" end of a lead, monitors the ultrasonic signal received at the "heel" end and compares it with the signature of a known "good" joint.

The three techniques were evaluated independently with the major efforts being on the ultrasonic and laser/IR techniques. The major criterion used in the evaluation was the ability to discriminate between defective solder joints, that may be of 19 types of defects, and "good" solder joints. It is not required to differentiate between defect types. The test vehicle was a specially prepared printed circuit board (PCB) containing 280 solder joints (20, 14-pin flat packs). These included 200 defective joints and 80 "good" joints.

The major effort was expended on the ultrasonic and laser/IR techniques since the visual technique already is well established. The results of this feasibility study indicate that all three techniques are technically feasible. Further, although the ultrasonic technique currently appears to be somewhat more sensitive than the laser/IR technique, neither is totally adequate by itself. Both the ultrasonic and laser/IR techniques will detect severe defects (opens or major cracks, voids or inclusions) with near 100 percent accuracy. Further, the ultrasonic technique will detect smaller cracks (down to as little as 15 percent of the joint area) with at least 90 percent accuracy. However, the ultrasonic technique is weak in detecting defects such as excess solder, irregular spreading or exposed gold while the laser/IR technique does indicate that such joints are suspect.

Granular appearing joints are easily detectable by the laser/IR technique because of high absorptivity, but the ultrasonic may miss that fault if it is otherwise solid. If the granularity is due to a "cold" solder joint, both techniques will detect it with an estimated 70-90 percent accuracy.

The current estimate of overall detection accuracy, considering all defects, is at least 90 percent for the combined ultrasonic-laser/IR. This should improve with the addition of the complementary visual subsystem. The accuracy figures are subject to minor refinement depending on the results of correlating the reported detection results with the results of an actual physical analysis of the inspected joints.

In brief, the current concept has the TIS consisting of:

(1) An accurate, x-y programmable stage to hold and move the PCB under inspection

(2) An ultrasonic transceiver assembly

(3) A low power (5-10 watt) laser with shutter to control pulse width
(4) An infrared detector to monitor heating and/or cooling of the solder joint under test
(5) A multilens, color microvideo subsystem to provide visual inspection capability
(6) A computer (probably microcomputer) to control stage motion, to analyze sensor data, and to provide limited temporary storage capability
(7) A floppy-disc storage for permanent retention of joint location programs and limited trend data.

The responses of solder joints to the inspection techniques are amenable to digital processing and lend themselves quite well to automated classification procedures. Either of the ultrasonic or laser/IR techniques can classify a joint as defective (to be resoldered) outright. If both classify a joint as suspect (marginal), the joint would be resoldered. A classification of suspect by one technique and of good by the other automatically would call for visual inspection to provide the final decision.

The results of the Phase 1 feasibility study demonstrate that all the inspection techniques evaluated are technically sound. Further, their use in combination with each other will provide a significantly more accurate system for detecting defective solder joints than the current practices.

This feasibility study supports the recommendations that this program be authorized for continuing with Phase 2, the individual usage size model fabrication and integrated system design.

FINAL REPORT

on

TREND INSPECTION STATION
for
PRINTED CIRCUIT BOARD SOLDER JOINTS
(PHASE 1)

to

SACRAMENTO AIR LOGISTIC CENTER

from

BATTELLE
Columbus Laboratories

April 3, 1979

BACKGROUND

A significant portion of the time and money spent for keeping U. S. aircraft readily available is devoted to the repair of electronic equipment. Defective solder joints on printed circuit boards (PCB's) are a frequent cause of malfunction and/or failure of electronic equipment. Therefore, it is extremely important to be able, quickly and accurately, to inspect for and detect defective solder joints on PCB's.

The current, primary method of solder joint inspection is visual and depends heavily on the experience and judgement of the inspector. The inspector makes a decision on the acceptability of the solder joint based on color, shininess, granularity and visible cracking (cracks also may be detected by UV techniques). Although not extensive, there is a certain amount of subjective influence in this technique. However, the most serious drawback to the visual technique is that the inspector cannot see inside or under the solder joint. Thus, the inspector cannot detect voids, foreign inclusions or internal cracks. These hidden defects also can cause malfunction, early failure or degradation of electronics. Therefore, following discussions with Sacramento ALC (SM/ALC) concerning the need for a more complete and accurate solder joint inspection technique, Battelle (BCL) submitted to SM/ALC a proposal "Trend Inspection Station for Printed Circuit Board Solder Joints". This proposal resulted in Contract No. F04606-78-C-0903-PZ0001.

INTRODUCTION

This Final Report on Trend Inspection Station for Printed Circuit Board Solder Joints - Phase 1 presents the results of the efforts under the above Contract. This Phase 1 was a feasibility study covering the period July 6, 1978 to April 7, 1979. The successful completion of the feasibility study would be followed by Phase 2 - Design and Fabricate Usage Size Models and Phase 3 - Construction of Prototypical System.

The proposed automatic system suggested the use of one or more of three sensing and display techniques to be evaluated for observing solder joint integrity. First, is a technique previously developed by Battelle (patent still pending) that makes use of the ultrasonic properties of the solder joint and how they vary depending on the joint structure. The technique may use either acoustic transmission or reflection or change in acoustic impedance. Display is rapid and can be either via visual, meter reading or pictorial (CRT), or automated means. Second, is a technique developed and patented by Vanzetti Infrared and Computer Systems, Inc. (a subcontractor to Battelle) in which the solder joint is to be heated by laser injected IR. The resulting cooling characteristic (using IR sensing) then is compared graphically and rapidly to the cooling curve of a known good solder joint of the same type. Good thermal characteristics usually denote good mechanical and electrical characteristics. Third, is visual examination using a multilens (probably three or four) color video system. The actual number of lenses and other attributes of the color video system were to be determined, in part, with the aid of CIRCON Corp. of Santa Barbara, CA, a leading supplier of micro-video systems. The total system would feature display options as well as a keyboard entry system.

The combining of one or more of these techniques into a single inspection station, when coupled with historical data comparison (not meant to imply mass data storage) would provide the Air Force with a rapid and accurate means of detecting solder joint defects and defect trends.

This Final Report covers only the results of the Phase 1 - feasibility study.

OBJECTIVE

The objective of this feasibility study was to evaluate each of the three detection methods described as to their feasibility for use as techniques to enhance inspection of lap-type solder joints. The results of the evaluation suggest the conclusion that all of the techniques are feasible for continuation into Phase 2. The remainder of this report presents the rationale for this conclusion.

DISCUSSION

All three of the above techniques have been used and proven in applications similar to that of solder joint inspection. The concept of heat injection by laser to determine thermal signatures has been described in "Practical Applications of Infrared Techniques", Dr. Riccardo Vanzetti, John Wiley and Sons, New York, (1972). The laser IR technique also has been demonstrated as an inspection method for plated-thru-holes in PCB's as reported in "A Dynamic Thermal Test Station for Multi-Layer Printed Circuit Boards", R. W. Woodgate (Hamilton Standard), a summarization of RADC-TR-88. Similarly, the use of ultrasonic techniques to examine the internal structure of materials and material interfaces has been well known for some time, and visual techniques have been used for many years, as is well known.

The completion of the Phase 1 feasibility study initially was expected to require the performance of two major tasks and two minor tasks. Instead, three major tasks and one minor task were required to evaluate the feasibility of the Trend Inspection Station (TIS). They were:

Major Tasks

(1) Prepare set of "standard" solder joints for use in sensor evaluation

(2) Evaluate feasibility of Ultrasonic technique

(3) Evaluate feasibility of Laser/IR technique

Minor Task

(1) Consider preliminary aspects of use of multilens, color-microvideo subsystem.

All of the above tasks were pursued concurrently, however, they will be discussed individually.

STANDARD SOLDER JOINT PREPARATION

An Auxiliary Task described in Battelle's original proposal for this Phase 1 effort was to prepare a set of "standard" lap-type solder joints with 14-lead, integrated circuit flat packs for use in evaluating the three proposed detection techniques. It was expected that this would be a minor effort, but it rapidly grew to major proportions. The making of consistently "good" solder joints is not normally a severe problem with reasonable quality control practices. Similarly, it is not difficult to make certain types of "bad" solder joints. However, the preparation of the "standard" set of solder joints required the ability to make a specified type of defect when and where desired. It required an extensive amount of developmental experimentation to attain this ability.

Solder Joint Types

The following types of defects were specified by Battelle's proposal and by Engineering Specification, Sacramento ALC, MMIRE, 782, 2 May 1978 (both incorporated as part of the Contract) as being desired for study and detection.

(a) Cold solder joint
(b) Irregular solder spreading due to excessive heat
(c) Irregular solder spreading due to insufficient heat
(d) "Toe" of lead bent up
(e) Lead soldered one-half off pad
(f) Tipped lead
(g) Yellow flat top of lead
(h) Lead pressed down too hard thus squeezing out solder (Deleted because of redundancy)
(i) Voids in solder
(j) Cracks at heel of joint
(k) Granular appearance
(l) $AuSn_4$ and/or $AuSn_2$ entrapped in solder joint
(m) Copper abietate (green)
(n_1) Insufficient solder
(n_2) Excess solder
(o) Excessive heat
(p) No fillet at heel of lead
(q) Dewetted joint
(r) Holes and/or pits
(s) Solder peaks
(t) Inclusions
(z) Good solder joints.

The defect (m) copper abietate was not produced because the formation of the compound is a relatively long term process and our acceleration techniques were unsuccessful. All other joint types were prepared using 14-lead, flat-pack style integrated circuit packages on a printed circuit board (PCB) as shown in the photograph of Figure 1.

Equipment

The equipment used in preparing the solder joints was a Hughes Microgap Welder, Model MCW-550 incorporating a Model VTA-60 attachment with a spacing of 0.040 in between the parallel tips. This equipment permits a wide range of pulse voltages and pulse durations. The voltage may be varied from 0 to 1.99 volts in steps of 0.010 volt and is a constant voltage supply for a given pulse. The duration of the voltage pulse can be varied from 0 to 9.99 seconds. The pulse steps are 1 millisecond from 0 to 100 milliseconds, 10 milliseconds from 100 milliseconds to 1 second, and 100 milliseconds from 1 second to 9.9 seconds.

Solder Joint Preparation Procedures

Extensive experimental effort was involved in developing the procedures used in preparing the PCB pictured in Figure 1. It was necessary to determine not only the characteristics of the voltage pulse, but, also the other physical and chemical requirements necessary to produce a particular type of defect.

The development of the procedures to prepare all of the joint types had three things in common:

(1) The leads and pads had to be properly tinned except in the cases of "g" and "q" which required that the lead be suitably masked to prevent proper solder coating

(2) The leads and pads had to be properly cleaned except in the cases of "i", "k", "l", "r" and "t" which required the deliberate contamination of the joint with particular foreign materials

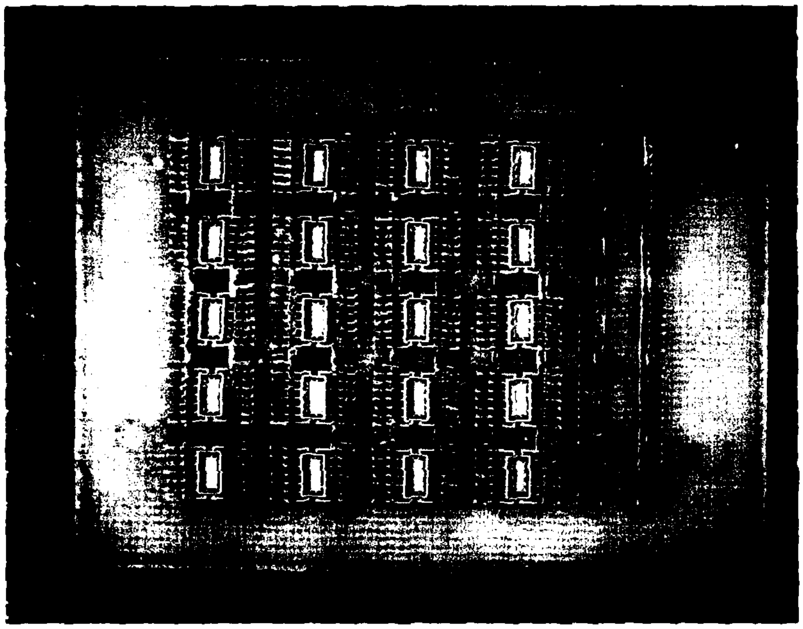

FIGURE 1. PHOTOGRAPH OF COMPLETED SET OF STANDARD SOLDERED JOINTS

(3) A variety of pulse conditions (voltage and duration) had to be tried for each joint type. There were many joints prepared under each set of conditions with subsequent destructive analysis to discover the conditions that consistently gave the desired results. In general, this procedure was repeated for each different contaminant type tried for "i", "k", "l", "r" and "t".

Three printed circuit boards (PCB), each consisting of 20, 14-lead flat packs (280 solder joints) were prepared using the results of the procedures described above. One board was sent to Dr. Traub of Vanzetti for use in the Laser/IR Study, one was sent to D. Ensminger at Battelle for use in the Ultrasonic Study and one was retained at Battelle for later use in visual detection. The preparation of these "standard" solder joint PCB and the conditions for their preparation are documented in "Interim Report on Standard Solder Joint Documentation" submitted to SM/ALC on January 15, 1979.

Summary

It is always the intent, when making solder joints for electronics, that the completed joint be electrically continuous and mechanically strong. A joint that is defective is always the result of defective materials, improper techniques or poor workmanship. However, the intent of this Auxiliary Task was to produce known types of defects, not once, but consistently. Some of the defect types were quite easy to produce, such as those requiring only mechanical displacement or distortion, (d, e, f, j, n_1, n_2, p, q, s). Others such as those requiring excessive or insufficient heat (b, c, o) were a little more difficult in that the power pulse deviations from nominal needed to be determined. Still others, particularly those involving voids, holes and pits, foreign inclusions, granular appearance, cold joints and gold-tin compounds (a, g, i, k, l, r, t) were extremely difficult to produce consistently. These required the identification of special materials (suitable contaminants), deviant power pulse conditions and/or unusual mechanical techniques.

This Auxiliary Task was considerably more difficult and entailed much more effort than expected at the beginning of the program. However, we believe the resulting sets of "calibrated" or "standard" solder joint defects are quite satisfactory for the needs of the program.

ULTRASONIC STUDIES

Introduction

The objective of the ultrasonic portion of Phase 1 of this program was to adapt the principles proven in previous laboratory work to the inspection of soldered joints on the sponsor's flat-pack printed circuit boards. The elements of the study include (1) an evaluation of the proposed principles to determine which ones are feasible for meeting the inspection requirements, (2) an evaluation of the structures of the conductors, coatings, solder joints, or any other parameter that will determine the sensitivity of the inspection procedure to defective solder joints, (3) a determination of design parameters relative to transducer and probe dimensions, power and loading, (4) a review (including laboratory experiments) of single and multilayer PC boards to be supplied by the sponsor which contain suspected defective solder joints, and (5) construction and laboratory evaluation of experimental transducers and probes to determine the sensitivities of the proposed methods, the characteristics of the signals produced, and the methods of processing the data in an automated system.

The basic theory of the ultrasonic inspection method has been confirmed experimentally. Definitely bad solder joints can be detected by the technique with a very high degree of confidence. We believe that destructive examination in Phase 2 will prove that the method is very sensitive to less serious defects as well.

The results of the ultrasonic study are very encouraging.

Theory of the Ultrasonic Inspection Technique

The prior laboratory work referred to earlier had been conducted in-house at the Battelle Columbus Laboratories. In the prior research by BCL, three principles were applied simultaneously. These were (1) transmission of ultrasonic energy across or through a soldered joint, (2) reflection of the acoustic impedance of a soldered joint into a transmitting ultrasonic transducer and (3) modulation of an electrical current through a soldered joint by means of ultrasonic excitation. Any one of the three principles offers the potential for evaluating solder joints for specific types of defects. Therefore, each could be applied separately or in combination with either of the other two. Due to the differences in sets of defects to which each principle applies, combining two or more principles ovbiously enhances the reliability of the test. This prior research was aimed at evaluating soft-solder joints in any of those applications.

The sponsor's PC boards provide only one lead, or one side, of the solder joints to the inspection probes. This immediately restricts the test methods to two principles: (1) reflection of acoustic impedance into a transmitter thus affecting its vibratory characteristics and (2) transmission of ultrasonic energy across the joint. In both cases, the reaction of the joint to ultrasonic excitation is associated with constraints which are controlled by the conditions at the joint. These conditions include, but are not limited to, the quality of the solder joint.

The specifications require that the inspection be accomplished without adding a coupling fluid. This restriction determines the upper limit of frequency that can be applied and in a sense dictates the technique, if ultrasonic inspection is to be used.

The basic principles of the inspection method may be explained with the assistance of Figure 2. The ultrasonic energy is produced through a transmitter, T, which responds as a function of frequency, T(f), to an electrical excitation. As a result of the ultrasonic excitation by the transmitter, which might be compared with the action of a phonograph pickup in reverse, the joint responds over the same frequency range according to a function H(f). The response of the joint is detected by an ommidirectional receiver, R, which has a response function R(f). The total response of the joint, the transmitter, and the receiver is

$$Z(f) = T(f)\ H(f)\ R(f)$$

From the analytical viewpoint, the ideal condition is to maintain no variance in T(f) and R(f) from joint to joint. In this case, the function H(f) can be derived by extracting the components T(f) and R(f) from Z(f) for each joint. Since H(f) describes the reponse of the joint and since the response is controlled by the conditions within the joint, the function H(f) is also a function of the joint condition. This is the basic theory of the inspection system for evaluating solder joints on flat-pack PC boards.

The response of the joint may be analyzed according to three different mechanisms. The first mechanism may be related to an elastic rod which is constrained along its length. This rod is a composite of the solder and the lead. If the rod is long and slender and if it is constrained so that no flexural modes can be established, it will act like a mechanical filter which passes only those signals at frequencies which

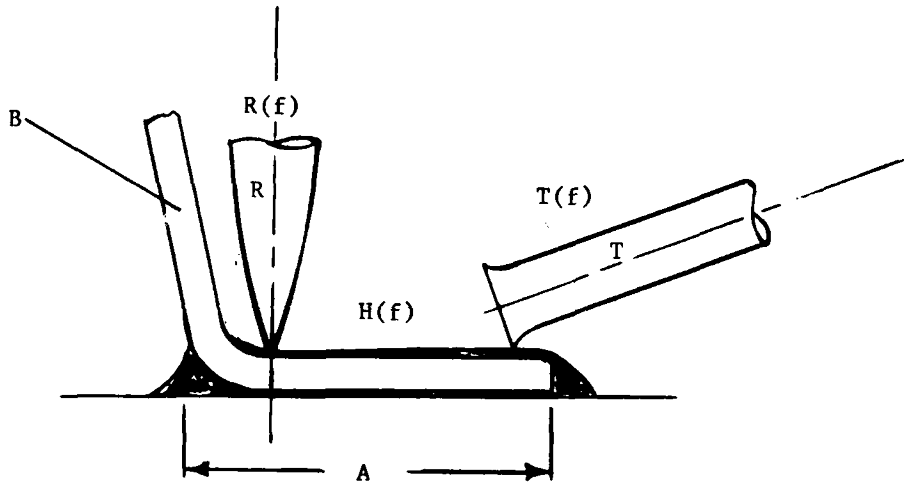
B
R(f)
R
T(f)
T
H(f)
A

FIGURE 2. BASIC CONFIGURATION OF ULTRASONIC INSPECTION OF SOLDERED JOINTS ON PC BOARDS

are at or near its longitudinal resonances. The shapes and heights of the resonance curves will be functions of the Q (or losses) of the lead and the joint materials. The longitudinal vibratory characteristics of the lead itself will be fairly consistent for a given type and size. Variations in the internal structure of the solder will affect the characteristics of the composite. Losses at internal boundaries, such as grain boundaries and interfaces between inclusions and solder, will affect the shape of the response curve, and if the internal structure affects the stiffness of the joint, the amplitude of the displacements also may be affected. In an otherwise well-anchored, well-filled joint, this may be the only evidence of a defective bond. The resonance peaks observed may not differ in location from those of a good joint, especially if the peaks are related to the response of the transmitter, but the widths and shapes of the peaks would be affected.

The second mechanism may be related to a mass on a flexural spring which is anchored at one end and which carries a mass at the other end. The mass corresponds to the lead and any solder which lies on top of it. The spring corresponds to the solder attaching the lead to the pad. In a well-anchored joint, this spring is so stiff that the flexural resonance would occur only at an extremely high frequency (which is beyond the range used in the interrogation). However, severe defects may weaken the constraint so drastically that flexure along the joint may occur under the excitation of the transmitter with relatively large displacements compared with those associated with good joints.

The third mechanism relates to the lead between the heel of the joint and the electronic component. An excitation at the base of the lead parallel to the surface of the board will promote flexure in the lead in this region (region B of Figure 2). Two basic conditions may be observed in the flexure in these leads: the stiff joint condition and the loose joint condition. The first is produced as a result of mode conversion promoted by the longitudinal motion of a well-anchored lead. If the joint is very good, the motion will be slight and no significant flexural vibration will be detected. However, if the joint is weakened by grain boundary or similar conditions, the motion may be slightly larger and additional resonances attributable to flexure may be observed. If the bond is broken in any manner (including cracks and poor filleting) the flexural constraint is more severely weakened and flexural modes may increase in number and in amplitude according to the conditions within the joint. Not only will the lead between the heel and the electronic component flex, but this flexure and the excitation of the transmitter may induce any number of flexural modes in the lead within the joint area.

Obviously, interactions will occur involving all three basic mechanisms of the joint reaction, the characteristics of the receiver, and the characteristics of the transmitter.

Starting at the receiver (Figure 2) and working backwards, coupling between the joint and the receiver probably is easier to hold constant from joint-to-joint than coupling between the transmitter and the joint. The receiver is mounted in a vertical position through a constant force spring. The end is pointed. The only variations in the effect that the receiver might cause on the vibration of the joint, if the force and angle of contact are held constant, will result from variations in the position of the transducer relative to the heel of the joint. Slight changes in angle produce little effect because the transducer is onmi-directional. The load constitutes an acoustic impedance on the joint. It will, therefore, influence the response of the joint. However, since the loading force is a constant from joint to joint, the acoustic impedance of this load is also a constant. If this impedance can be made very small compared with that of the joint and if it is held constant, its effect on the response of the joint will be minimal. Therefore, the contributions of H(f) and T(f) should be readily extractable and some leeway in the position of the receiver on the joint is permissible. However, the receiver should be located as close to the heel as possible because it responds to the ultrasonic conditions which exist at the point of contact.

The combined response of the joint and the transmitter will depend upon the degree of acoustical coupling between the two elements. In a tightly coupled system, the signal produced by the transmitter is partially controlled by the load (reflected impedance). This control of the signal may range from small to large depending upon its magnitude relative to that of the transmitter. In this case, the transfer of energy into the joint is at its highest efficiency. In a loosely coupled system, the transmitter may have the response of an unloaded transducer and the joint will respond according to its condition and excitation. In either case, the total response is a function of the condition of the joint.

If the transmitter has a high impedance compared with that of the joint, defects in the joint will be difficult to detect in a tightly coupled system. On the other hand, if coupling is too light, only a small amount of energy can be transferred to the joint and the sensitivity of the system will be very low.

The approach taken during the Phase 1 study was to design a very small transducer comparable in size and frequency response to that of a good joint and to couple to the joint with modest pressure. Thus, the response of the entire system could be related to the condition of the joint.

As described previously, interactions between modes of vibration and the joint response are used to advantage in analyzing the solder joints. For example, the low amplitude longitudinal vibrations excited by the transmitter into the joint may induce low amplitude flexural vibrations into the lead above the heel. These flexural modes would tend to induce flexure in the joint. If the joint is well bonded, flexure in the joint is insignificant. If it is weak (dewetted, cracked, etc.) flexure may have a significantly high-amplitude. In the latter case, the joint stiffness is low so that the amplitude of the vibrations that excite the flexure is correspondingly higher. Resonances in addition to those associated with the transmitter will be generated corresponding to the potential modes of vibration within the lead and joint.

The previous discussion covers two extremes of conditions corresponding to good joints and to failed joints. Another type of indication is related to frictional losses at boundaries within the joint. Various degrees of seriousness also are associated with conditions of this type. In this case, the first symptoms are the broadening of resonance indications in the spectrum, i.e., lowered Q or sharpness of resonance. As the condition becomes more severe, the joint is weakened, the displacement increases, and more and higher amplitude resonances occur associated both with the primary modes and with those produced by mode conversion. Flexural indications (of which many are possible) may be present in the most severe case.

These are general statements regarding the characteristics of a solder-joint on a printed-circuit board which make ultrasonic inspection of the joint possible. Any resonances of a transmitter that occur within the spectral range of the test will produce a corresponding indication in the spectrum produced by the receiver.

Experimental Program

Feasibility Analysis With Candidate Defects

A list of the types of defects of interest to ALC were provided for study at the beginning of the feasibility program. This list of defects was used as a guide in designing the experimental ultrasonic system. The list was reviewed and an estimate was made of those defects that might be detected by an ultrasonic method working from one lead only.

The initial estimate was made without prior knowledge of the effects of most of the defects upon the actual physical characteristics of the joint. They were based upon nomenclature alone. This initial estimate was essential to estimating the feasibility of the technique and to designing the experimental apparatus.

After micrographs of suitable "defective" joints had become available, a new estimate of the capabilities of the technique was made based upon an analysis of the micrographs. Each of these analyses were based upon intuitive estimates without the benefit of the knowledge of actual physical properties. The results are given in Table 1.

Development of Physical Set-Up and Preliminary Experiments

Early in the research program, it was anticipated that experiments would be conducted within the frequency range 20 to 100 kHz. An important objective was to determine an optimum inspection frequency which was expected to lie within that range of frequencies. We intended to use high-Q transducers as transmitters. This would require fabricating a number of transducers which would resonate at preselected frequencies in order to cover the frequency range of 20 kHz to 100 kHz. The frequency was chosen to compensate for having to couple to the joint without adding coupling fluids. At this stage, it was believed that dry coupling at higher frequencies would be too inefficient.

The early experimentation was hampered somewhat by the fact that no suitable "standard" solder joints were available at that time. Instead, simulated flat-pack configurations were made using Lucite to represent the board and IC's. Crude, fairly large solder joints were prepared containing various conditions ranging from no-solder to good joints. Although these joints were large, it was rather easy to fabricate known defects and to determine accurately their condition from their

TABLE 1. PRELIMINARY ESTIMATES OF THE CAPABILITIES OF THE ULTRASONIC INSPECTION SYSTEM TO DETECT DEFECTS IN SOLDER JOINTS ON FLAT PACK PC BOARDS

	Defect Type	Initial Estimate	Estimate Based on Micrographs
a.	Cold solder joints	F-G	Q
b.	Irregular spreading of solder up lead due to excessive heat	Q	Q
c.	Irregular spreading of solder up lead due to insufficient heat	Q	Q
d.	Toe of lead bent up	Q	Q
e.	Lead soldered 1/2 off pad	F-G	P-E
f.	Tipped lead	F	Q-G
g.	Yellow flat top of lead viewed	P-F	Q-F
i.	Voids	F-G	Q-G
j.	Cracks at heel of joint	F-G	G
k.	Granular appearance	Q	Q
l.	$AuSn_4$ and $AuSn_2$ entrapped in solder joint microstructure	Q	Q-G
m.	Copper Abietate Green	Q	Q
n_1.	Insufficient solder	F	Q
n_2.	Excess solder	F	Q
o.	Excessive Heat	F-G	Q-G
p.	No fillet at heel/lead	F-G	G
q.	Dewetted joint	G	G-E
r.	Holes and Pits	F-G	F-G
s.	Solder Peaks	Q	Q
t.	Inclusions	F-G	Q-G
x.	Open joints	G	E
z.	Good joints	G	G

The interpretation of the codes is as follows:

E = excellent; G = Good; F = Fair; P = Poor or Impractical; Q = not sure; and O = no.

ultrasonical response. Both the electrical conductivity and the acoustical response of the joints were studied.

Several stages of miniaturizing the ultrasonic transducers followed. Refinement was aimed toward adopting the transducers to the particular circuit-boards specified for the project. The electrical aspect of the test was omitted for two reasons: (1) the two sides of the joints are frequently unavailable to the probes which are operated from the open surface and (2) indexing may introduce problems.

During the miniaturization, additional attention was focussed on increasing the bandwidths of the transmitters and the receivers. This would reduce the number of separate transducers required and would provide the potential for using either a constant amplitude sweep frequency mode or a broad-band pulse mode of inspection. These probes were found to provide sufficient dry coupling potential to frequencies exceeding 550 kHz.

Considerable effort was consumed in mounting the transducers in such a manner that constant coupling could be maintained from joint to joint. During one of the final stages of developing the laboratory inspection, coupling was done by making pointed contact tips on the two transducers so that each would penetrate the solder under controlled, constant applied force. This approach was aimed at insuring constant coupling conditions. The technique no longer requires actual penetration of the solder. Only a 5-10 gm force is necessary. The receiver, an omnidirectional transducer, was mounted in a vertical position. The transmitter was placed at an incident angle. The vertical component of thrust was primarily for controlling coupling. The horizontal component of the ultrasonic displacement was primarily for energizing the solder joint. The same broadband receiver was used in the final system but the transmitter was improved so that the axis of the transducer could be placed at an angle of 20 degrees or less with the surface of the PC board and maintain good coupling. This was made possible by adding a small flange to the end of the transmitter for coupling to the solder joint.

These early experiments also indicated the need to overcome the "human" element in coupling. After several experiments, a technqiue was devised by which the coupling force of both the transmitter and the receiver could be held constant and in a fixed position on the joint. These elements were mounted on a phonograph pickup arm. The force that the transmitter applies to the joint is 10 grams and the receiver force is 5 grams.

Prior to designing the transducers which have been used in all of the recent "standard" PC board tests, a theoretical evaluation was used to estimate a frequency at which the ultrasonic method would be most sensitive to variations in the solder joints of the sizes found on the flat-pack printed circuit boards. With an assumed velocity of sound in the solder of 2.4×10^5 cm/sec (a typical value for lead-tin solder), the estimated effective frequency range is 500 to 550 kHz. This is fortunate because we had already proven that coupling at these frequencies into the solder was adequate using the latest miniature transducers. As a result of this study, a new transmitter and receiver combination were designed for full wave operation at 520 kHz (half-wave frequency was 270 kHz). These transducers were evaluated using flat-pack frame trimmings.

Thus the preliminary investigation prior to performing studies of the characteristics of the joints included controlling coupling conditions for consistency, determining the points of contacts and directions in which the waves should be transmitted, and controlling the uniformity of the coupling from joint-to-joint.

Effects of Ultrasonic Intensity

One prepared set of solder joints was used for establishing the test parameters. Occasionally, a joint was damaged and this was attributed to handling and manual accidents. However, the question naturally arose as to whether damaging ultrasonic stresses could be generated during the experiments. Consequently, the theoretical power into the transducers was calculated for the voltage levels used during the experimental work. Perhaps, under some of the earlier studies, stresses might have exceeded the fatigue limit of the solder. However, the results of the calculations suggested that even under the most severe conditions, the intensity in the joints would not exceed 10 mw/in^2 (1.6 mw/cm^2) with the present levels of intensity.

In order to verify this conclusion, experiments were conducted with the transmitter operating at rated voltage and placed against a solder joint. The transducer was operated for 3 minutes in each test. The tips of the transducers are not sharp. The only indication of damage discovered under a microscope at magnifications of 90X, 135X, and 300X was a slight polishing of the surface of the solder--an effect that was difficult to locate even under the microscope.

Effects of Coupling

Coupling is a most important factor in "sounding" the solder joints for quality. The reactions are so small that inconsistencies in coupling could obscure the details required to analyze the responses of joints. For this reason considerable effort went into developing the coupling system and method. The three coupling conditions which were considered included (1) transmitting from the knee of the lead and detecting the signal at the toe, (2) the reverse of (1), and (3) transmitting from the toe of the joint and detecting at a point near the heel of the lead. It was supposed that transmitting from the knee of the lead or vice-versa would more completely evaluate the response of the entire joint. It was very quickly determined that transmission from near the toe and detection near the heel provided adequate indication of the acoustic constraints of the joint and in many ways was preferred over the other two approaches. For this reason, all of the evaluation studies on the "standard" PC board used this third method.

Experimental Procedures

The preliminary studies have led to a test procedure which appears to be good. This procedure was used on flat-pack PC boards containing both good solder joints and designed defective solder joints. The original plans were to restrict studies to frequencies within the frequency range 500 to 575 kHz. During the early measurements on the PC boards, it was determined that a broader spectrum including much lower frequencies had to be covered. At that time, it was hoped that a window around which studies could be concentrated would be revealed. However, at the present time, the spectrum from 150 to 650 kHz appears to be important to a complete evaluation of solder joints on flat-pack PC boards.

Data taking over the given frequency range was facilitated by using the following electronic apparatus:

(1) A Wavetek 114 Sweep frequency Generator to drive the transmitter through the desired range of frequencies.

(2) A Tektronix 434 Storage oscilloscope for monitoring the voltage to the transmitter. Voltage into the transmitter is restricted to 1 volt peak-to-peak. (This voltage has been calculated to produce a stress within the solder which is well below 1 psi.)

(3) A Tektronix 7L5 Spectrum Analyzer and Tektronix 7613 oscilloscope for monitoring the response of the transducer/solder-joint system.

Figure 3 is a block diagram of the experimental setup.

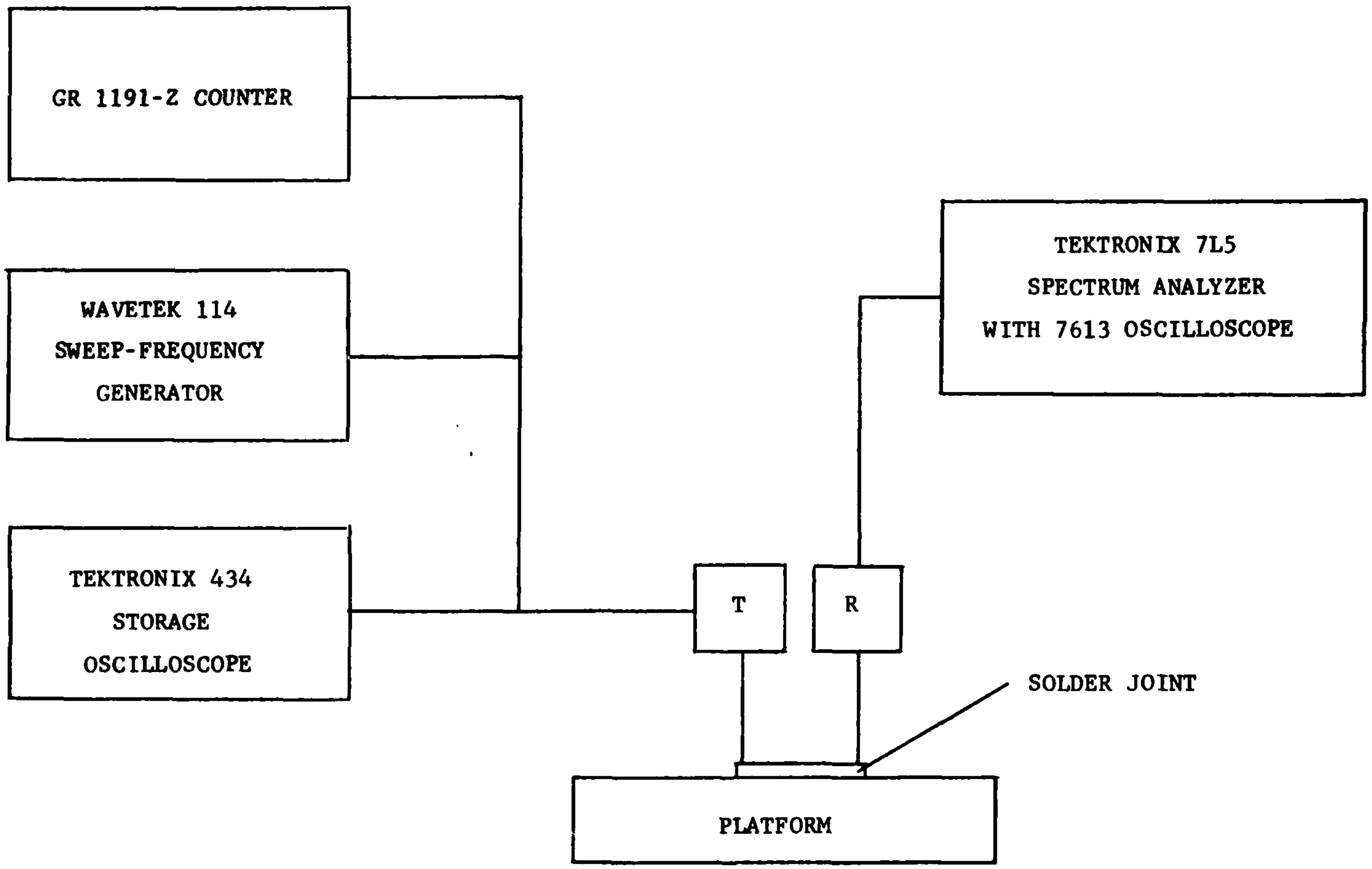
GR 1191-Z COUNTER
WAVETEK 114 SWEEP-FREQUENCY GENERATOR
TEKTRONIX 434 STORAGE OSCILLOSCOPE
T
R
TEKTRONIX 7L5 SPECTRUM ANALYZER WITH 7613 OSCILLOSCOPE
SOLDER JOINT
PLATFORM

FIGURE 3. BLOCK DIAGRAM OF THE EXPERIMENTAL SETUP FOR INSPECTING SOLDER JOINTS ON PC BOARDS

The spectra show major resonances in the transmitter at frequencies of approximately 200 kHz, 270 kHz, and 520 kHz. These resonances are not strictly harmonics because of the shapes and constrictions involved in the design. However, they can be identified as half wave resonance (270 kHz), a structurally controlled resonance (200 kHz), and a full wave resonance (520 kHz), which is the design frequency.

Experimental Results - Standard Test Boards

A standard test board as described earlier, was prepared containing 140 solder joints of designed "known" conditions corresponding to most of the items listed in Table 1. A key was provided to identify the condition of these joints. We have called this section of the board the "key" section. A second set of 140 joints was prepared on the same board containing all of the identified (or known) defects but in various arrangements that were not revealed to the investigators until after they had been inspected and classified. We have called this section of the board the "test" section. Figure 4 is a map of the standard board identifying the "key" section and the "test" section. This map was included in the Interim Report on Standard Solder Joint Documentation, submitted January 15, 1979, and is repeated here in order to simplify the explanation of the evaluation of the experimental results. All joints were inspected identically. The investigators made visual inspections of all of the joints under a microscope and made complete notes of their observations. This was done in order to identify any spectral variations that might be attributed to geometrical differences or other obvious condition at the joint. The ultrasonic response spectrum of each joint was photographed and labeled.

The integrated circuits are identified by letter row and number columns. The leads on each IC are identified in counter-clockwise order--from lower right to lower left. For example, lead number A1-1 is the lead at the lower right corner of IC A-1. Lead number A1-8 is the lead at the upper left corner of IC A1.

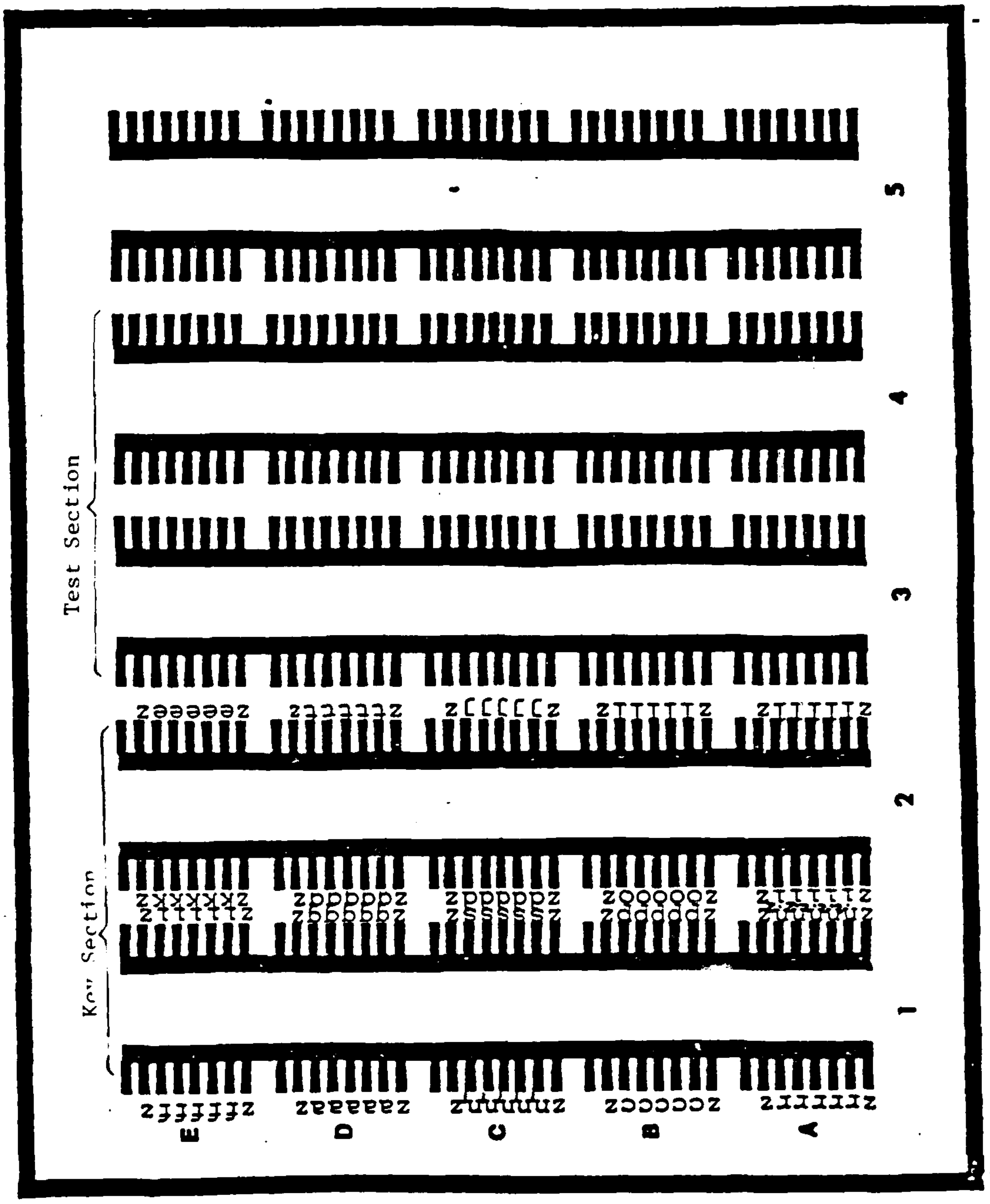
Key Section
Test Section
A
B
C
D
E
1
2
3
4
5

FIGURE 4. MAP OF THE STANDARD BOARD SHOWING THE KEY SECTION AND THE TEST SECTION

The spectra of the known defects were catalogued according to whether they were supposed to be good or defective and according to the alleged types of defects which they contained.

Spectra of the unknowns were compared with those of the knowns and thus categorized. In evaluating the results, it is necessary to recognize that several types of "defects" may appear as good joints ultrasonically. These might include such types as solder peaks, excess solder and toe of lead bent up. Also, the test includes a learning factor for the evaluator.

Table 2 is a summary of the results. In Table 2, the column headed "Ultrasonic Test Spectra" indicates the type of defects that may fit the observed spectrum for the joint inspected. The column headed "Actual Joint Condition" is the actual joint type as prepared on the test board.

An examination of Table 2 shows, tentatively, that there were 125 correct and 11 incorrect decisions for 136 of 140 joint conditions (good or defective). The condition of 4 joints is unknown. These results indicate that the ultrasonic inspection technique is at least 90 percent accurate in defining the condition of a solder joint (good versus defective). This is considering _all_ of the defect type, some of which are only marginal defects. The expectation of detecting an extremely poor solder joint (50 percent or more of the lead separated from the pad for whatever reason, e.g., voids, cracks, inclusions, etc.,) is virtually 100 percent.

All of the 11 "errors" were solder joints intended to be defective, but were classified "good" by the ultrasonic method. This would indicate that these joints contain, at worst, only minor defects.

All of the above results are subject to minor revision in the early part of the Phase 2 program, when the results will be correlated with

TABLE 2. SUMMARY OF ULTRASONIC INSPECTION OF SOLDER JOINTS IN TEST SECTION OF STANDARD PRINTED CIRCUIT BOARD

IC NO.	PIN NO.	*ULTRASONIC TEST SPECTRA	**ACTUAL JOINT CONDITION	CORRECT DECISIONS (GOOD vs. DEFECT)	CONFIDENCE LEVEL (DEFECT vs. GOOD)
A3	1	i.z	z	yes	low
	2	n_2,q	q	yes	high
	3	z	k	no	low
	4	n_2, i, l	l	yes	high
	5	p,j,n,	j	yes	medium
	6	z,o,q,l,t	?	(a)	unknown
	7	z	z	yes	high
	8	z	z	yes	high
	9	l,j	l	yes	high
	10	d,i,k,j	d	yes	medium
	11	t,r,l,i	t	yes	medium
	12	t,r,l,i	e	yes	medium
	13	i,l,k	i	yes	medium
	14	z	z	yes	high
A4	1	z	z	yes	high
	2	g,n	n_1	yes	high
	3	n_2, l,i	f	yes	medium
	4	z,c,n,g	g	yes(a)	low
	5	l,o,i,k	o	yes	medium
	6	z	b	no	low
	7	z,i,r	z	yes(a)	low
	8	z,n_2,o,e	z	yes(a)	low
	9	o,d,q,t	t	yes	medium
	10	z,r,i,l	i	yes(a)	low
	11	s	s	yes	medium
	12	z,s,a,n_1	a	yes(a)	low
	13	n_1	n_1	yes	high
	14	z	z	yes	high

---

* Spectra in key section which closely matches test spectra.

**Joint condition according to key.

(a)Gray scale indication--could be good joint or defective.

TABLE 2. SUMMARY OF ULTRASONIC INSPECTION OF SOLDER JOINTS IN TEST SECTION OF STANDARD PRINTED CIRCUIT BOARD (Continued)

IC NO.	PIN NO.	*ULTRASONIC TEST SPECTRA	**ACTUAL JOINT CONDITION	CORRECT DECISIONS (GOOD vs. DEFECT)	CONFIDENCE LEVEL (DEFECT vs. GOOD)
B3	1	z	z	yes	high
	2	l,n_1,g,i	q	yes	high
	3	k,i	k	yes	high
	4	k,l,z	l	yes	high
	5	j	j	yes	high
	6	z,t,l,s	t	yes(a)	low
	7	z,r	z	yes	low
	8	z,n_2	z	yes	low
	9	z,l	l	yes(a)	low
	10	d	d	yes	high
	11	o,l,q	t	yes	high
	12	e	e	yes	high
	13	i	i	yes	high
	14	z	z	yes	high
B4	1	r,z,l	z	yes(a)	low
	2	c,n_1	c	yes	high
	3	i,l,p	f	yes	high
	4	g,z	g	yes(a)	low
	5	i,o	o	yes	high
	6	z,l,i,c,o,n_1, t	b	yes(a)	low
	7	z,n_2,p,d,t	z	yes(a)	low
	8	z	z	yes	high
	9	l,n_2,i	t	yes	high
	10	i	i	yes	high
	11	l	s	yes	high
	12	(BAD)	a	yes	high
	13	n_2,a	n_2	yes	high
	14	z,p	z	yes(a)	low

---

* Spectra in key section which closely matches test spectra.

**Joint condition according to key.

(a)Gray scale indication--could be good joint or defective.

TABLE 2. SUMMARY OF ULTRASONIC INSPECTION OF SOLDER JOINTS IN TEST SECTION OF STANDARD PRINTED CIRCUIT BOARD (Continued)

IC NO.	PIN NO.	*ULTRASONIC TEST SPECTRA	**ACTUAL JOINT CONDITION	CORRECT DECISIONS (GOOD vs. DEFECT)	CONFIDENCE LEVEL (DEFECT vs. GOOD)
C3	1	z	z	yes	high
	2	r,l,i,q	q	yes	high
	3	z	k	no	low
	4	l,i,t	l	yes	high
	5	j,p	j	yes	high
	6	z,l,i,j	?	(a)	unknown
	7	z	z	yes	high
	8	z	z	yes	high
	9	z	l	no	low
	10	c,l,s,n_1,d	d	yes	high
	11	t,i	t	yes	high
	12	t,l,r,i	e	yes	high
	13	l,i,n_2	i	yes	high
	14	r,a,z	z	yes(a)	low
C4	1	z	z	yes	high
	2	l,p,c,i,f,t	c	yes	high
	3	l,p,c,i,f,t	f	yes	high
	4	l,p,c,i,f,t	t	yes	high
	5	o	o	yes	high
	6	l,t	b	yes	high
	7	l,z	z	yes(a)	low
	8	z,r,i,j,t,k	z	yes(a)	low
	9	n_2,l,t,i	t	yes	high
	10	n_2,l,t,i	i	yes	high
	11	s,z	s	yes(a)	low
	12	9	a	yes	high
	13	n_2	n_2	yes	high
	14	z	z	yes	high

---

* Spectra in key section which closely matches test spectra.

**Joint condition according to key.

(a)Gray scale indication--could be good joint or defective.

TABLE 2. SUMMARY OF ULTRASONIC INSPECTION OF SOLDER JOINTS IN TEST SECTION OF STANDARD PRINTED CIRCUIT BOARD (Continued)

IC NO.	PIN NO.	*ULTRASONIC TEST SPECTRA	**ACTUAL JOINT CONDITION	CORRECT DECISIONS (GOOD vs. DEFECT)	CONFIDENCE LEVEL (DEFECT vs. GOOD)
D3	1	z	z	yes	high
	2	q	q	yes	high
	3	k	k	yes	high
	4	z,l,r	l	yes(a)	low
	5	z,i	j	yes(a)	low
	6	t,z	t	yes(a)	low
	7	z	z	yes	high
	8	z,n_2,i,c,p	z	yes(a)	low
	9	n_1,l	l	yes	high
	10	n_2,l,d	d	yes	high
	11	l,t,i	t	yes	high
	12	l,t,i	e	yes	high
	13	l,i	i	yes	high
	14	z,a,r	z	yes(a)	low
D4	1	z,n_2,r,k	z	yes(a)	low
	2	i	r	yes	high
	3	i,j,q,e	f	yes	high
	4	z,r,l,s,t	t	yes(a)	low
	5	l,i,o	o	yes	high
	6	z	b	no	low
	7	z,l	z	yes(a)	low
	8	z	z	yes	high
	9	t	t	no	low
	10	z,i,l,t	i	yes(a)	low
	11	i,l,s	s	yes	high
	12	(BAD)	a	yes	high
	13	z	p	no	low
	14	z,l,t	z	yes(a)	low

---

* Spectra in key section which closely matches test spectra.

**Joint condition according to key.

(a)Gray scale indication--could be good joint or defective.

TABLE 2. SUMMARY OF ULTRASONIC INSPECTION OF SOLDER JOINTS IN TEST SECTION OF STANDARD PRINTED CIRCUIT BOARD (Continued)

IC NO.	PIN NO.	*ULTRASONIC TEST SPECTRA	**ACTUAL JOINT CONDITION	CORRECT DECISIONS (GOOD vs. DEFECT)	CONFIDENCE LEVEL (DEFECT vs. GOOD)
E3	1	z	z	yes(a)	medium
	2	r,p,n,i	q	yes	high
	3	z,l,i,t	k	yes(a)	low
	4	z	l	no	low
	5	j	j	yes	high
	6	r,l,i,o,d,t	?	yes	high
	7	z	z	yes	high
	8	z	z	yes	high
	9	a,l	l	yes	high
	10	d,i,l	d	yes	high
	11	z,i,l,n_1,t	t	yes(a)	
	12	e	e	yes	high
	13	z,l,i	i	yes(a)	low
	14	z	z	yes	high
E4	1	z,p,l,i	z	yes(a)	low
	2	i,l,r	r	yes	high
	3	f	f	yes	high
	4	l,i,t	t	yes	high
	5	l,i,t	?	yes	high
	6	o,z,t,i	b	yes(a)	low
	7	z	z	yes(a)	medium
	8	z,t,i	z	yes(a)	low
	9	z	t	no	low
	10	z	i	no	low
	11	z	s	no	low
	12	z,a	a	yes(a)	low
	13	j,p	p	yes	high
	14	z	z	yes	high

---

* Spectra in key section which closely matches test spectra.

**Joint condition according to key.

(a)Gray scale indication--could be good joint or defective.

the laser/IR results and then compared to the results of a definitive destructive analysis of the solder joints.

One conclusion is clear from Table 2. Although the ultrasonic technique will differentiate well between good and defective, it will not describe accurately the type of defect. However, such an ability is not needed for a practical inspection technique.

Several joints were inspected several times for repeatability. The intervals between inspections were sometimes as long as four days. The objective of these experiments was to determine the degree to which variances in coupling due to positions or surface conditions might influence the spectra. Generally the only noticeable differences in these spectra were slight differences in amplitudes. The forces applied to the transducers were held constant as was the driving voltage across the transmitter.

Typical Spectra of Test Solder Joints

Figures 5 through 25 are representative of the spectra obtained while examining solder joints on the "standard" board. This board includes a total of 280 solder points. The investigators were given a key identifying 140 of these joints as being either good or as containing "known" defects. This key and corresponding spectra were then used to identify the unknown joints by their spectra. The experimental results were then compared with the defect key for the joints.

Figures 5 through 25 show three categories of spectral characteristics. These categories are (1) low energy spectra, (2) medium energy spectra, and (3) high energy spectra. Generally, the resonance indication at 270 kHz corresponding to half-wave resonance of the transmitter remains fairly constant in width and off-scale. In cases such as severe cracks, dewetting, etc., this peak may broaden considerably. If coupling is poor, the amplitude at 270 kHz will drop considerably so that this indication might be used as an indicator of coupling.

The evaluations based upon the spectra of Figures 5 through 25 are preliminary. The only verifications at the present time that the joints are "defective" or "good" are visual observations under the microscope and the word and skill of the person making the joints. The preliminary analysis was based upon the following interpretative key:

- Low energy spectra - probably good
- Medium energy spectra - gray area. These might be good or defective to an intermediate degree
- High energy spectra - defective.

A second step in the analysis involved investigating both the obvious and also the more subtle features of the spectra. These include the following in order of increasing difficulty:

1. High energy throughout the spectrum
2. High energy concentrations in only certain portions of the spectrum
3. Resonance indications other than those associated with normal spectra - especially at the low frequency end of the spectrum (These are not necessarily high-amplitude resonances)
4. Distinctive shapes of the spectra, i.e., broadening of high-frequency peaks, irregularities, etc. These may be of low-amplitude but their shapes show high-damping characteristics of conditions usually not associated with good solder joints.

A definite statement regarding the seriousness of defects producing signatures in the "gray" category is premature. Acoustic theory and the fabricator's key were the basic guides in the analyses. The conditions in the "standard" joints have not been verified destructively. This is planned for Phase 2 after IR and Ultrasonic tests have been completed on the two available boards. The criteria for ascribing defects to joints producing spectra in the gray area may be too rigid. For the present, these restrictions were necessary in order to obtain a thorough analysis of the spectra. Spectra from conditions that have been fairly well-defined are presented later in this section.

The results of the tests on the "standard" solder joints (Figures 5 through 25) are summarized in Table 3 which is interspersed with Figures 5 through 25.

In addition to the studies using the "standard board, spectra were obtained from joints in which the condition was verified.

Figure 26a and b are spectra of a good joint on an unused, commerical circuit board. Figure 26a is the spectrum of the joint before a conformal coating was removed. Figure 26b is the spectrum of the same joint with the conformal coating removed. Note that the shapes of the two spectra are similar. The amplitude is slightly higher after the coating is removed, as would be expected. Note that the spectrum is relatively clean, showing only resonances associated with the transmitter at 200, 270, 515 and 610 kHz with no indication of spurius modes appearing. This joint was subsequently opened and found to contain less than 1 percent voids--a very good joint.

Figures 27 and 28 are spectra of additional defective joints. Figure 27 is from a joint with a crack extending approximately 15 percent into the heel of the joint. Otherwise, it was well bonded. Figure 28 is from a joint which is barely soldered at the heel and at the toe with the central portion of the joint unsoldered.

TABLE 3. SPECTRAL CHARACTERISTICS OF SOLDER JOINTS ON STANDARD BOARD

Figure No.	Condition (according to key)	Comments
5a	Good	Low amplitude resonance at 200 kHz (Transmitter structural resonance); normal (off-scale) transmitter resonance at 270 kHz. No significant indication at 500 kHz or above.
5b	Good	Significant resonance amplitudes at 200 and 270 kHz and multiple but regular low amplitude resonances at frequencies above 400 kHz. The shape of the spectral envelope causes one to guess that this represents a good joint.
5c	Good	The high peaks and the broad shapes of these peaks at frequencies above 400 kHz plus enlargement of the low frequency peak places this indication in the gray area. Until a better definition of limits can be defined, this joint must be suspect.
6a	Cold solder joint	Only distinctive feature (from a good point) is a minor resonance peak at 240 kHz.
6b	" " "	Major resonance peak at 240 kHz plus very high amplitudes in spectrum above 400 kHz. Typical of anticipated spectra from cold solder joints
7a,b	Irregular spreading of solder up lead-excessive heat	These are the two extremes from this type of joint. Both are gray scale. Would anticipate no difference between this and a good joint. Subtle differences might be observed in the bandwidths and spectral shape at frequencies centered around 615 kHz.
8a,b	Irregular spreading of solder up lead-insufficient heat	Characteristics both at low frequencies and at frequencies above 500 kHz were not anticipated. Possibly indicate weak bonds between solder and lead.

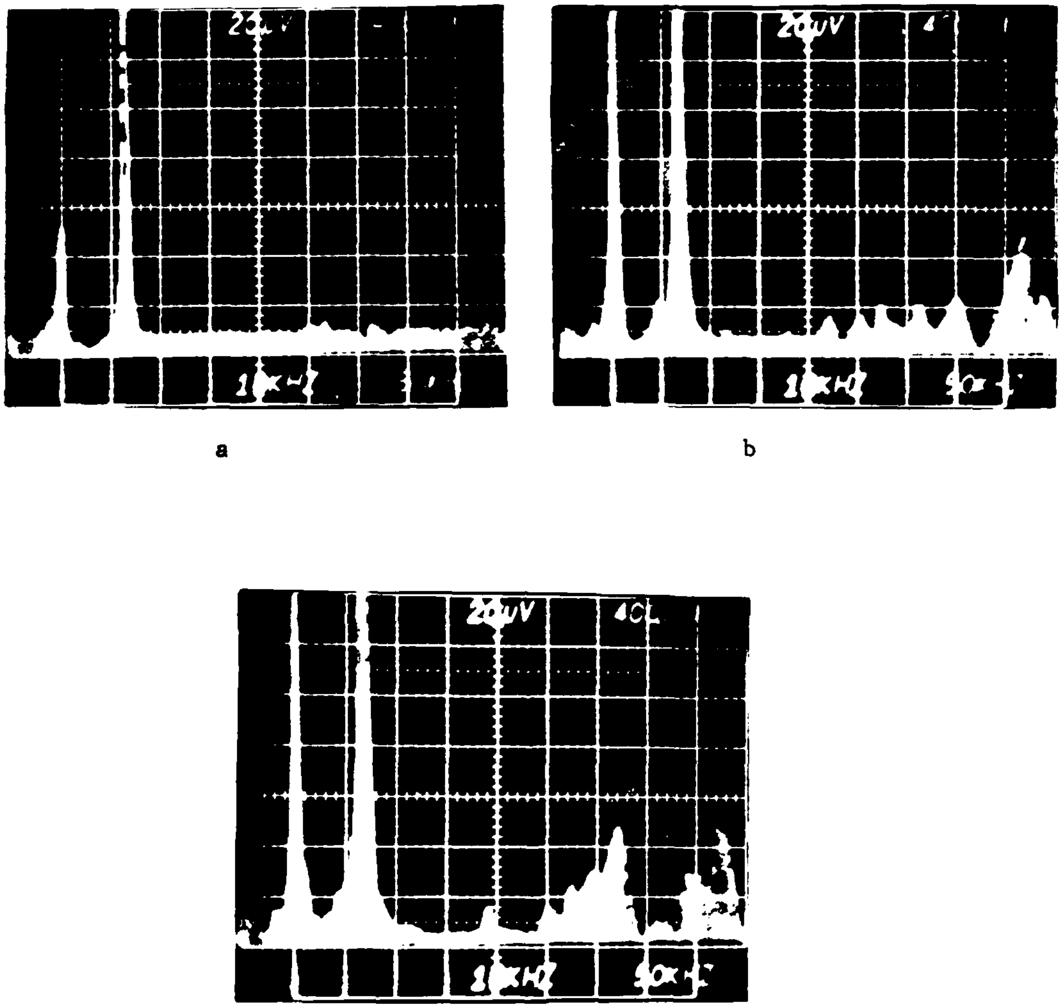

a

b

c

FIGURE 5. TYPICAL SPECTRA OF GOOD JOINTS SHOWING EXTREMES

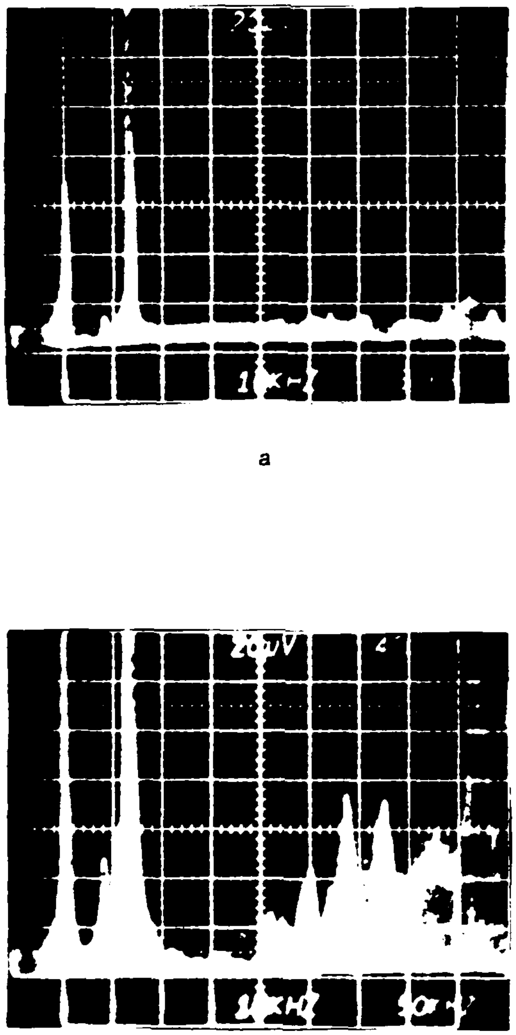

a

b

FIGURE 6. TYPICAL SPECTRA OF COLD SOLDER JOINTS SHOWING TWO EXTREMES

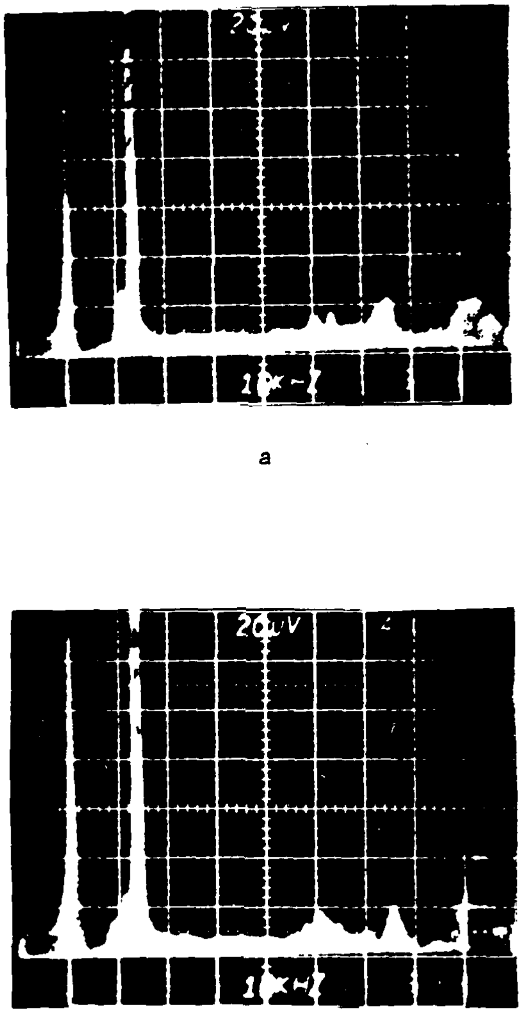

a

b

FIGURE 7. TYPICAL SPECTRA OF JOINT WITH IRREGULAR SPREADING OF SOLDER UP THE LEAD DUE TO EXCESSIVE HEAT

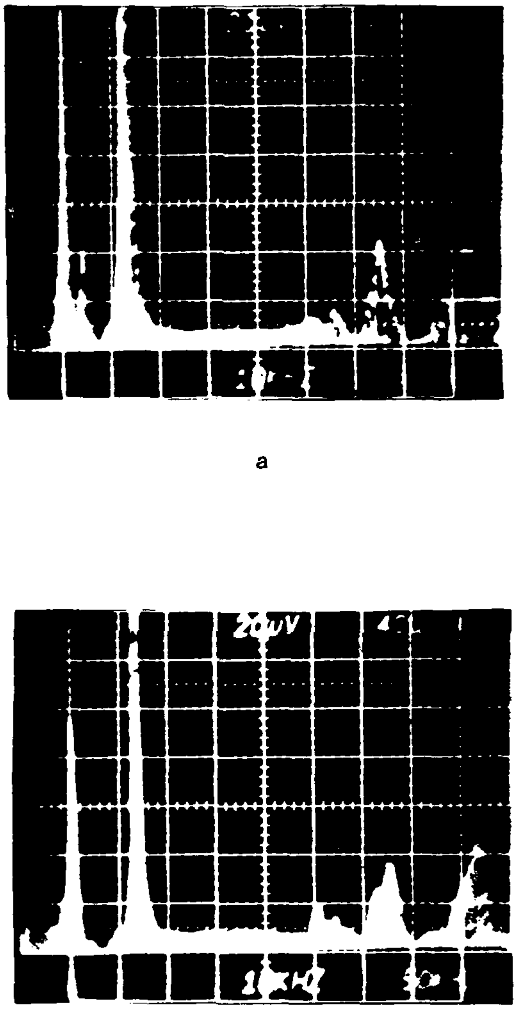

a

b

FIGURE 8. TYPICAL SPECTRA OF IRREGULAR SPREADING OF SOLDER UP THE LEAD DUE TO INSUFFICIENT HEAT

TABLE 3. (Continued)

Figure No.	Condition (according to key)	Comments
9a, b	Toe of lead bent up	The two extremes are indicative of the anticipated spectra. Figure a could pass as a good joint. Figure b shows extremely large resonance conditions indicating that the toe is not constrained by solder.
10a, b	Lead soldered half off pad	Figure a shows more solder rigidity than Figure b. These are anticipated spectra. Spectra from this type of joint can indicate additional resonances and higher amplitudes.
11a,b	Tipped lead	Figure a could pass as a good joint. The spectrum indicates a lead well imbedded in solder. Figure b is less constrained. High peaks at 510 kHz and 610 kHz are indicative of defective joint.
12a, b	Yellow flat top of lead viewed	Both indicate fairly good constraint by solder. Sometimes if bond is not complete beneath the lead, resonances indicative of such a condition appear.
13a, b	Voids in solder	Figure a is similar to a good joint. Resonances at 180 kHz, 520 kHz, 590 kHz and 620 kHz in Figure b are indicative of a weakened joint. The spectra obtained from voids depends upon where they are located--beneath the lead or to a side, for instance.
14a, b,c	Cracks at heel of joint	All three spectra are indicative of a broken solder condition of various degrees. The spectra may vary some with the position (and therefore loading) of the receiver with respect to the crack but the spectra will always indicate a defect is present.
15a,b,c, d	Granular appearance	No difference between good and defective had been anticipated. Most spectra indicate a weakened joint. Only a would pass for good but this spectrum is seldom seen on the test boards. Most range from Figure b to the indication of an extremely weak joint such as c and d.

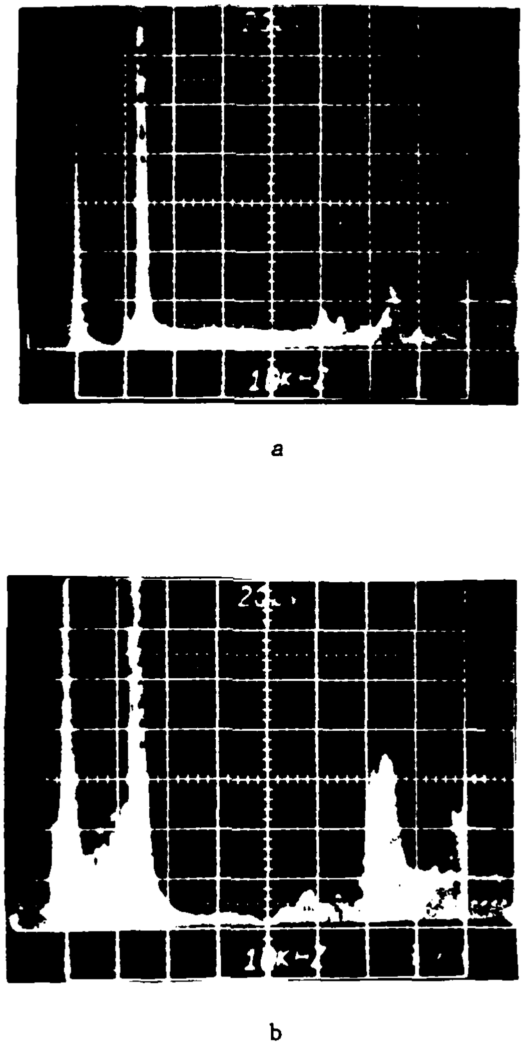

FIGURE 9. TYPICAL SPECTRA OF TOE OF LEAD BENT UP SHOWING TWO EXTREMES

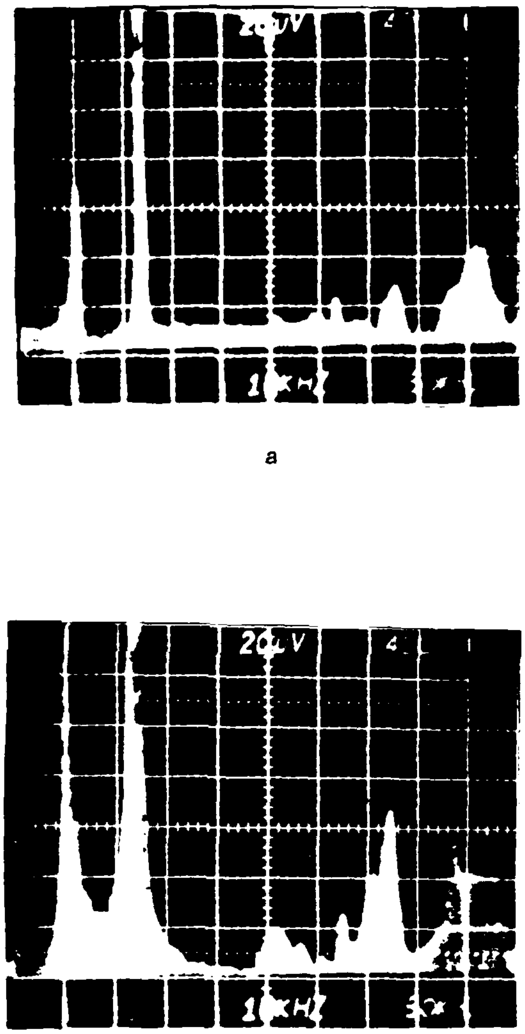

a

b

FIGURE 10. TYPICAL SPECTRA OF LEAD SOLDERED HALF OFF PAD SHOWING TOW DEGREES OF SERIOUSNESS

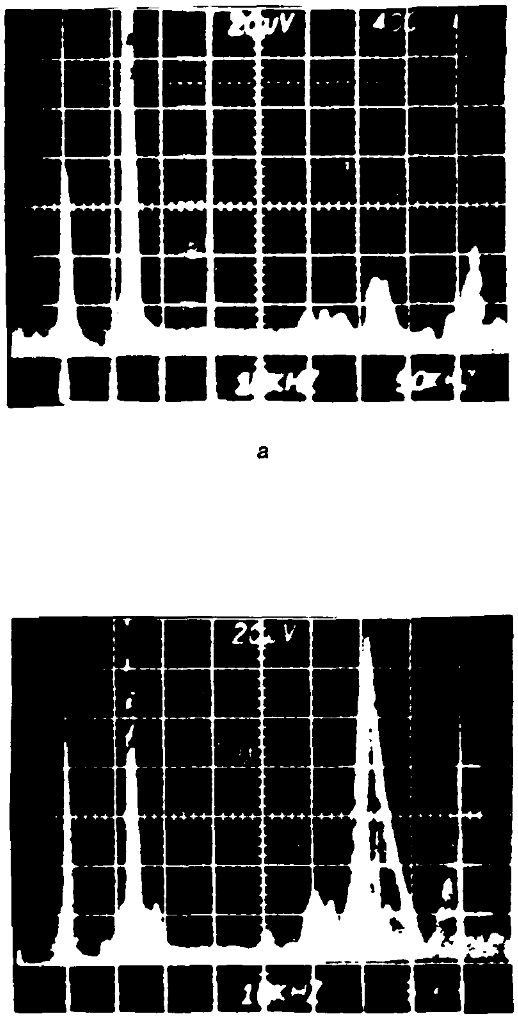

a

b

FIGURE 11. TYPICAL SPECTRA OF TIPPED LEAD SHOWING TWO EXTREMES

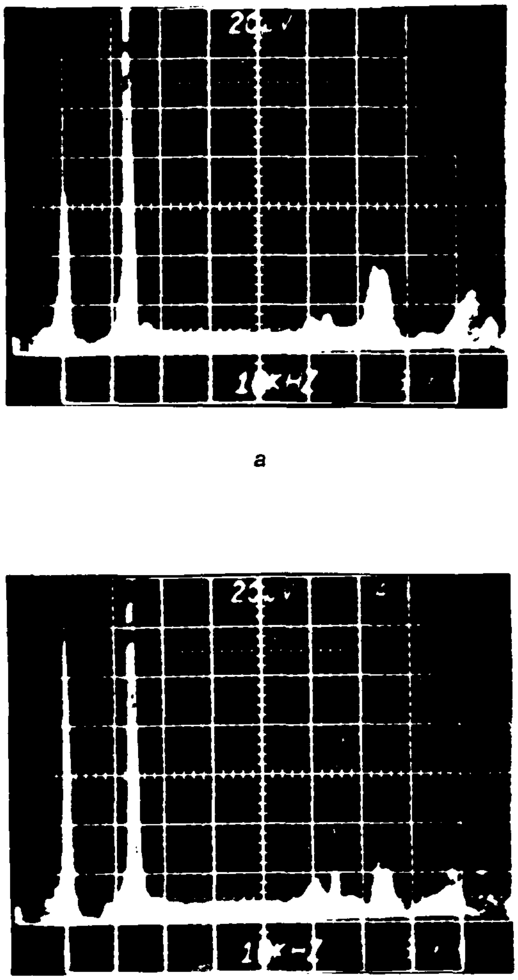

a

b

FIGURE 12. TYPICAL SPECTRA OF "YELLOW FLAT TOP OF LEAD VIEWED"

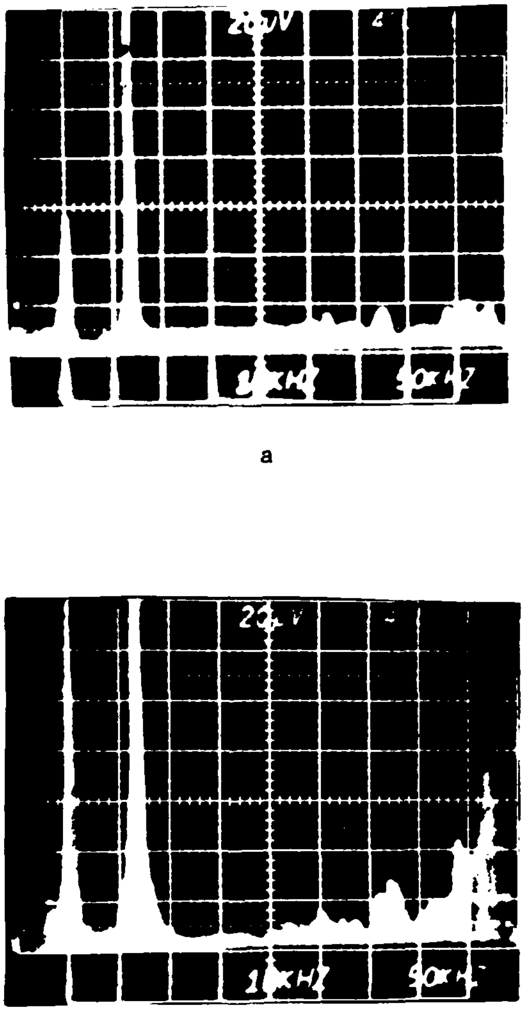

a

b

FIGURE 13. TYPICAL SPECTRA OF VOIDS IN SOLDER SHOWING EXTREMES

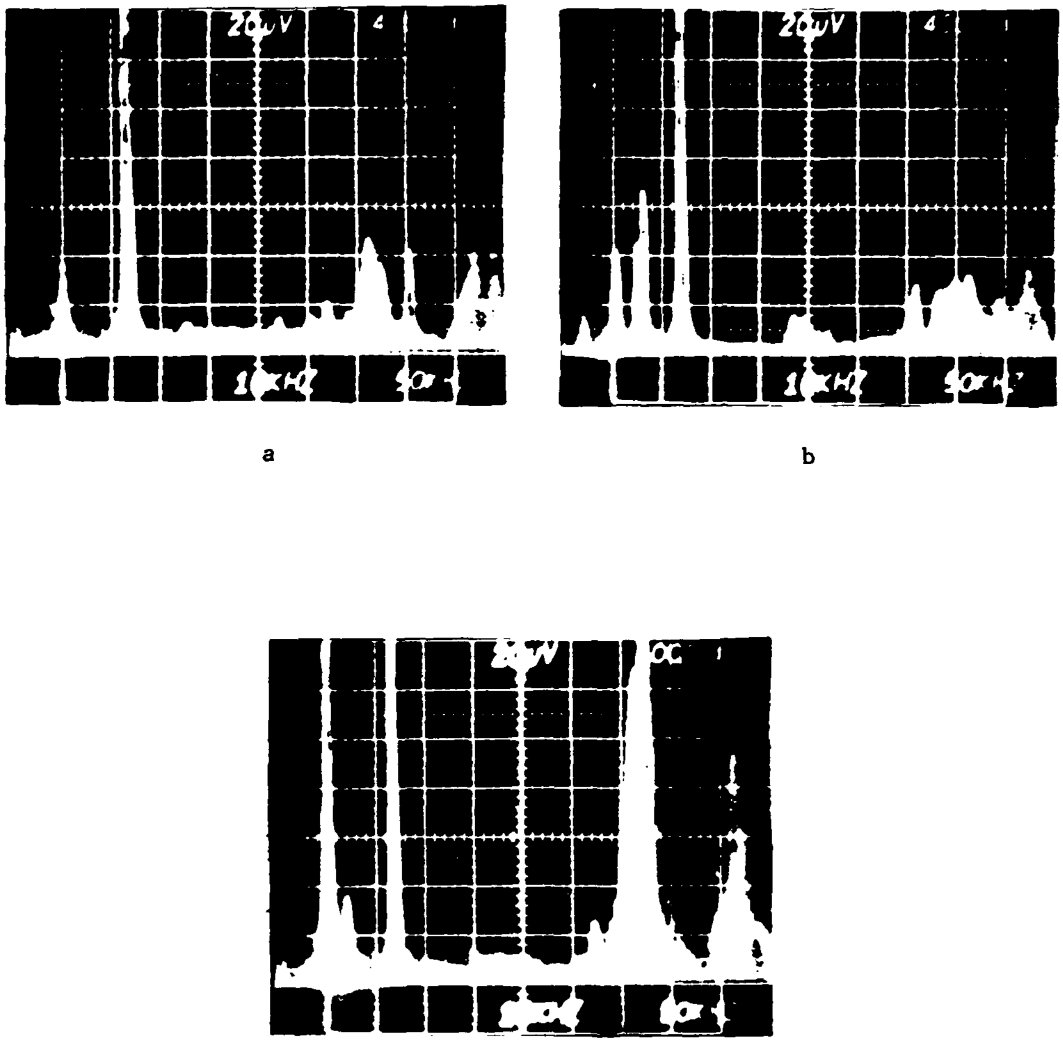

a

b

c

FIGURE 14. TYPICAL SPECTRA OF CRACKS AT HEEL OF JOINT

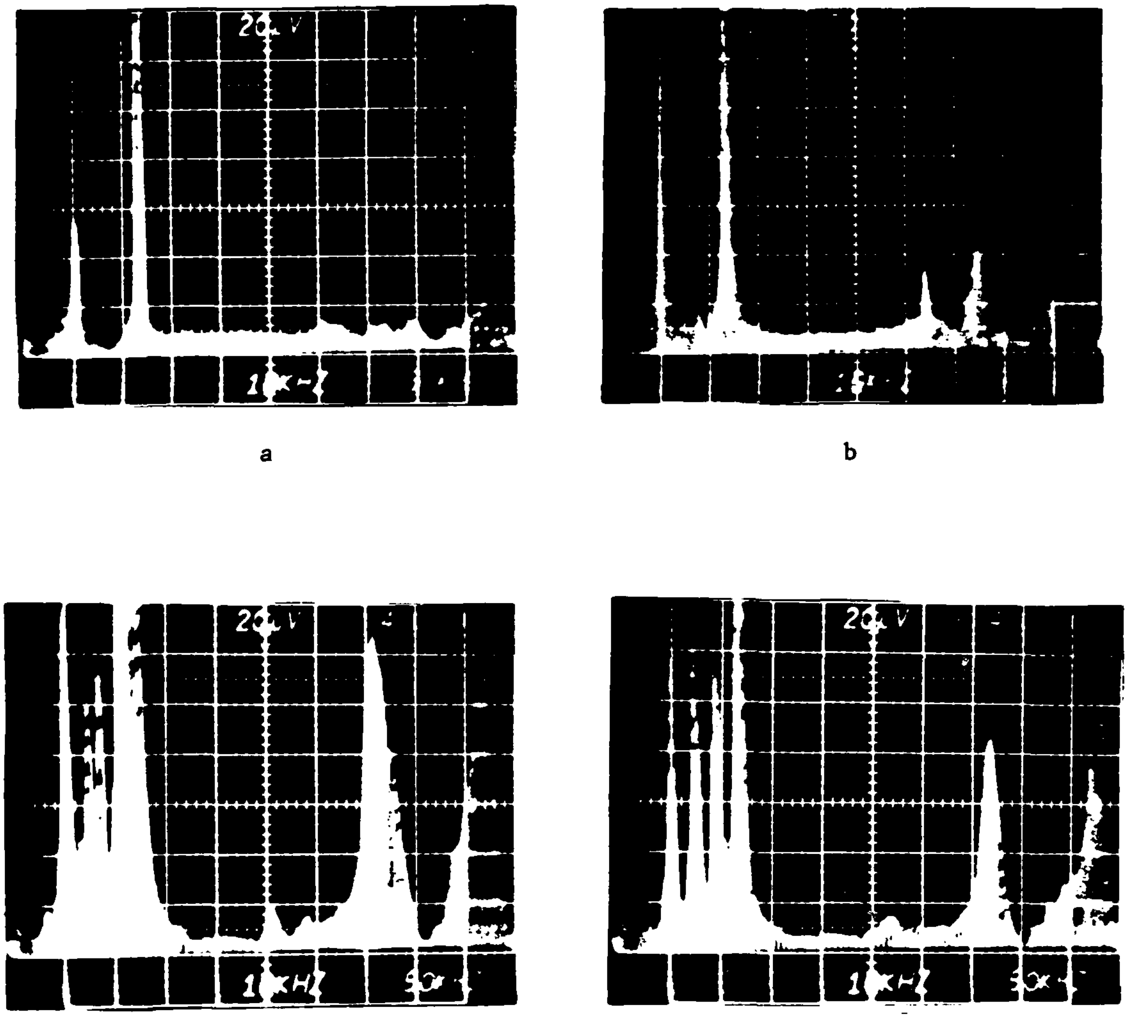

a

b

c

d

FIGURE 15. TYPICAL SPECTRA OF JOINTS WITH GRANULAR APPEARANCE SHOWING EXTREMES

TABLE 3. (Continued)

Figure No.	Condition (according to key)	Comments
16a,b,c	Gold entrapped	No difference between good and defective had been anticipated. Most joints produced spectra similar to a which would pass as a good joint. Occasionally, indications of weakness occur, as with the low frequency resonances at 210, 235, and 250 kHz in Figure b or large high-frequency responses and enlarged 200 kHz and 270 kHz peaks as in Figure c.
17a,b	Insufficient solder	These spectra are typical of this condition. The distinguishing feature is the fairly large amplitude resonance at 240 kHz. These conditions probably are not extremely poor. Conceivably, this defect could produce many high-amplitude resonances in severe cases.
18a,b	Excess solder	This condition, as anticipated, does not produce very severe indications. However, the spectra are more distinctive than had been anticipated.
19a,b	Excessive heat	Except in the severest cases, detecting this condition ultrasonically had not been anticipated. However, all of the spectra of "excessive heat" joints show at least the characteristic broad-band around 600 kHz and, in extreme cases, the indications of weakness associated with the high peak at 620 kHz.
20a,b,c,d	No fillet at the heel/lead	These spectra show various degrees of poor-filleting. The only feature distinguishing a from a good joint is the low amplitude resonance at 250 kHz. This would pass as a good joint indication. The remaining spectra show increasingly severe resonances within the 200 to 270 kHz range and around 520 kHz with little significant effect at higher frequencies.

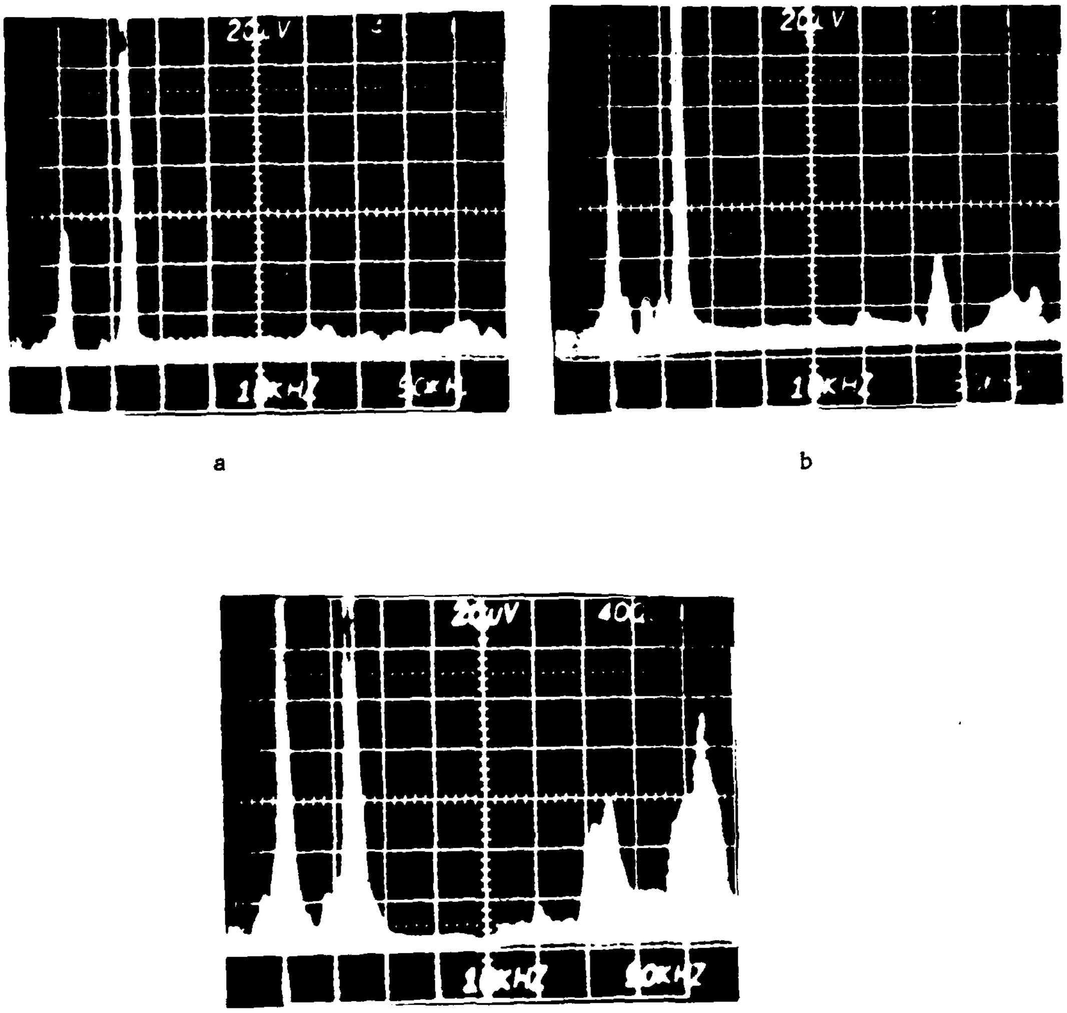

a

b

c

FIGURE 16. SPECTRA OF JOINTS WITH $AuSn_4$ AND $AuSn_2$ ENTRAPPED IN SOLDER JOINT MICROSTRUCTURE

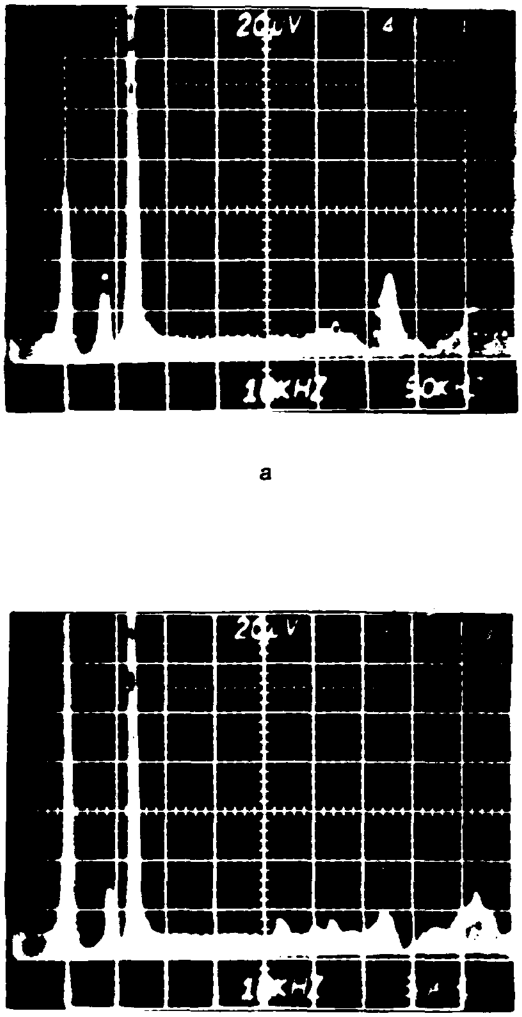

a

b

FIGURE 17. SPECTRA OF JOINTS WITH INSUFFICIENT SOLDER

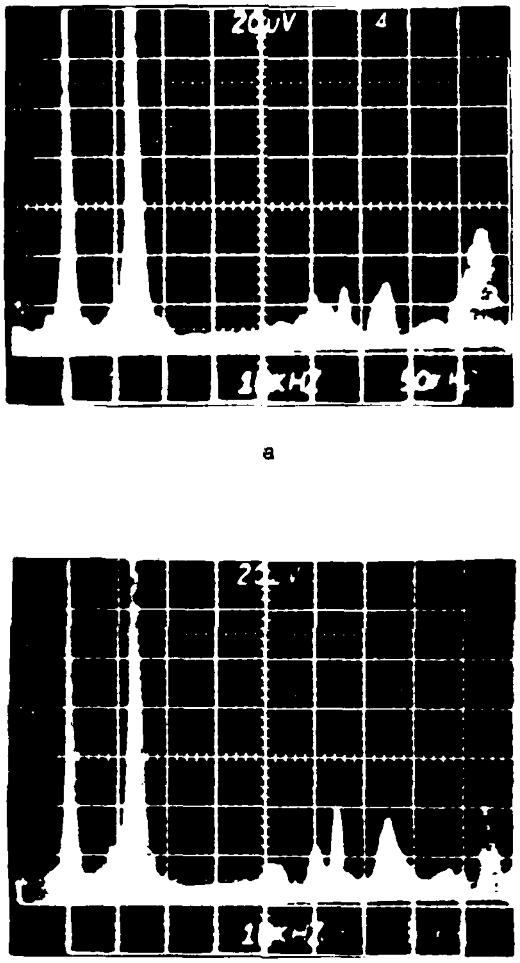

a

b

FIGURE 18. SPECTRA OF JOINTS WITH EXCESS SOLDER

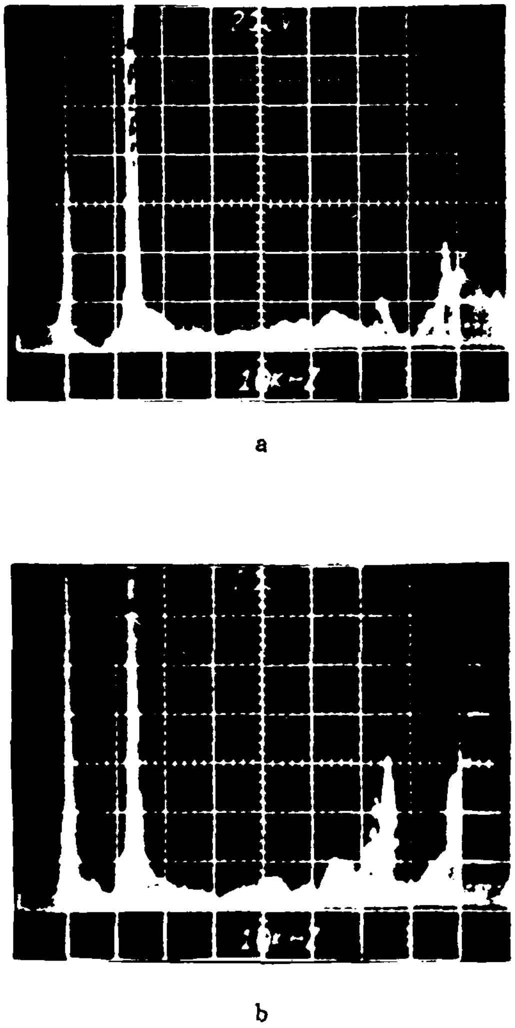

FIGURE 19. SPECTRA OF JOINTS SUBJECTED TO EXCESSIVE HEAT SHOWING TWO EXTREMES

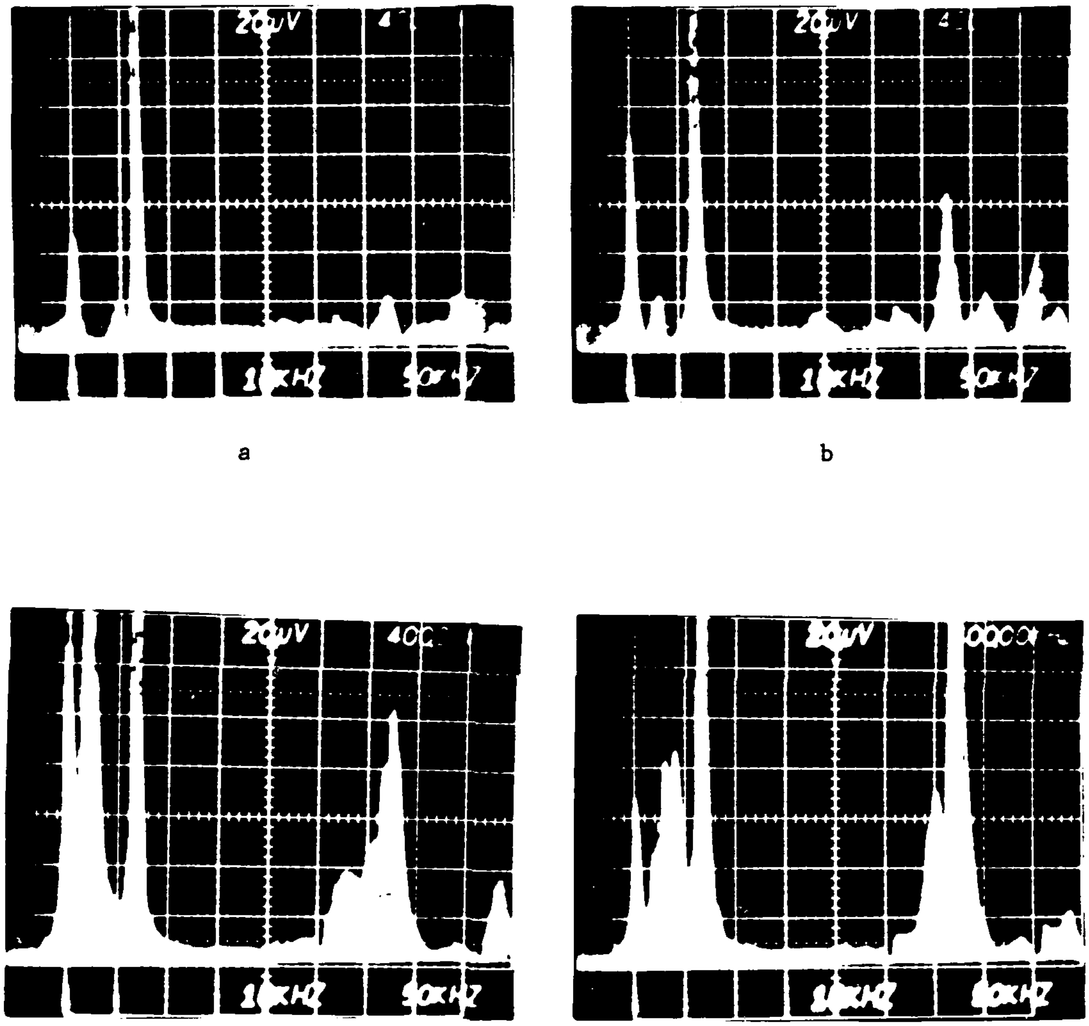

a

b

c

d

FIGURE 20· SPECTRA OF JOINTS WITH NO FILLET AT THE HEEL/LEAD SHOWING EXTREMES

TABLE 3. (Continued)

Figure No.	Condition (according to key)	Comments
21a,b, c,d	Dewetted	Figures a-d are increasing in severity. Occasionally, extra peaks occur between 200 and 270 kHz. As the condition worsens, the amplitudes of high-frequency peaks increase.
22a,b	Holes and Pits	As with voids, the severity depends upon the location of the defects. Both a and b are typical of this defect type.
23a,b	Solder peaks	Figure a has appearance of a good joint. Figure b is in questionable area. Optics would verify this one. The shapes and magnitudes of the high frequency resonances of b may indicate fairly good coupling into the side of a peak.
24 and 25	Inclusions	Inclusions may cause any number of responses according to severity, as Figures 24a through 25a show. Particularly, the high-frequency resonances are affected. Except in the worst cases, the low frequency end is not affected severely.

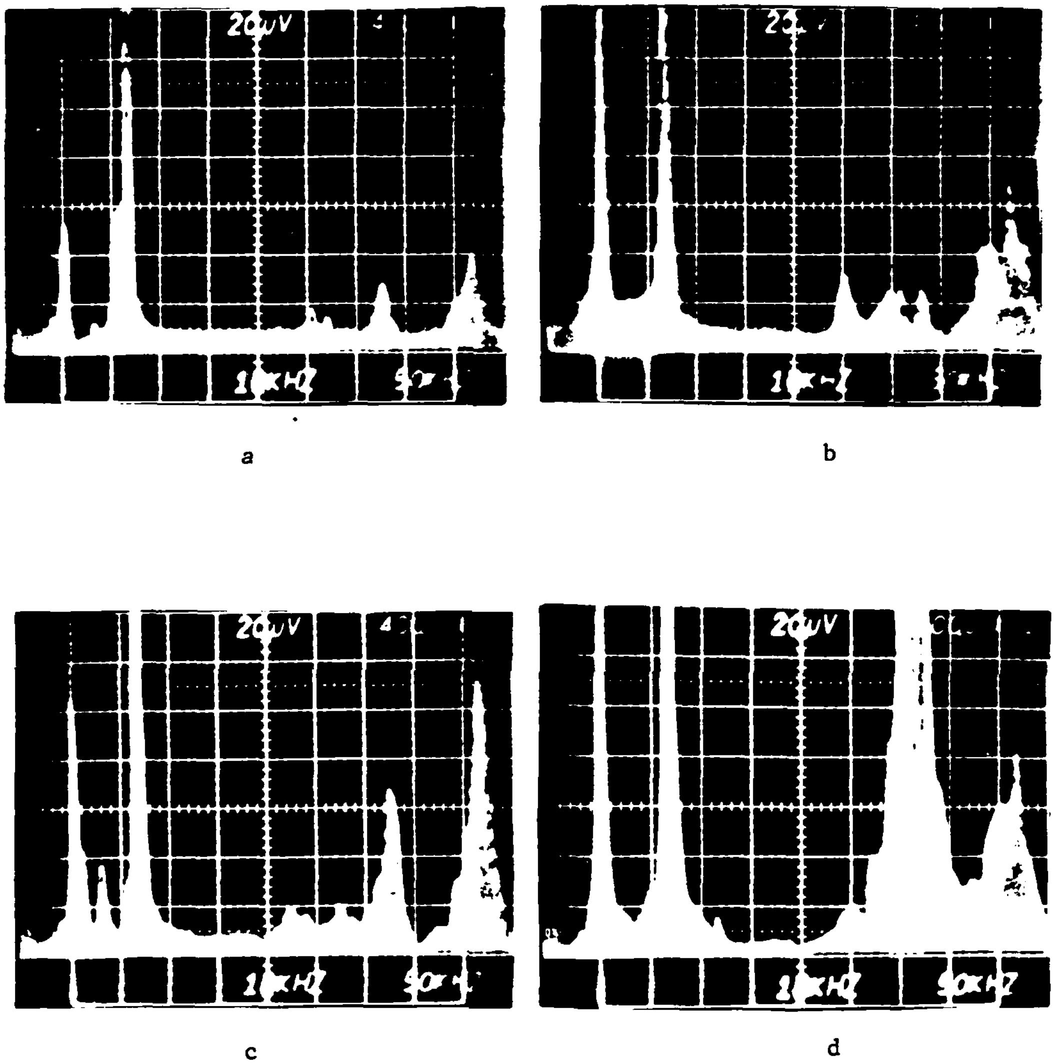

a

b

c

d

FIGURE 21. SPECTRA OF DEWETTED JOINTS SHOWING EXTREMES

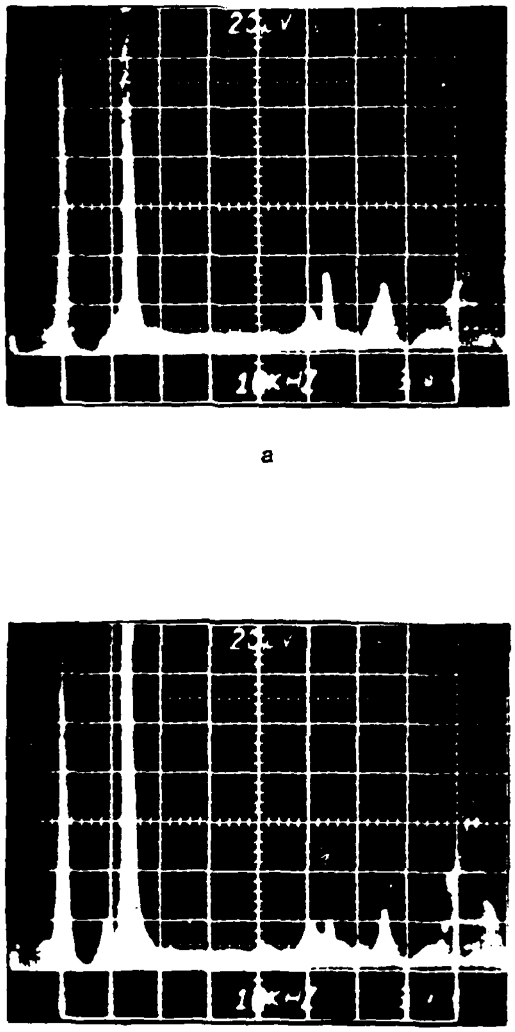

a

b

FIGURE 22. TYPICAL SPECTRA CAUSED BY HOLES AND PITS IN SOLDER JOINTS

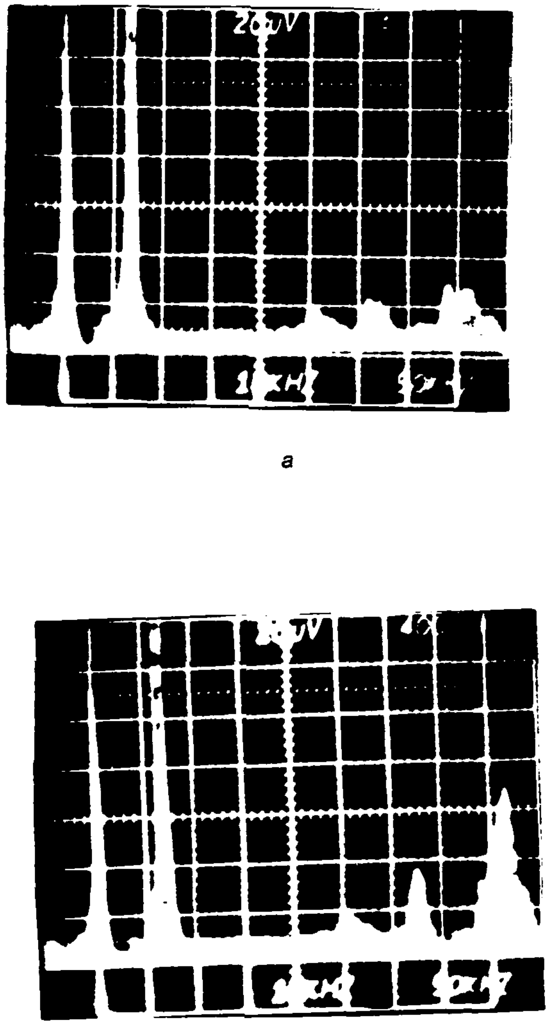

a

b

FIGURE 23. EXTREMES IN SPECTRA OF JOINTS CONTAINING SOLDER PEAKS.

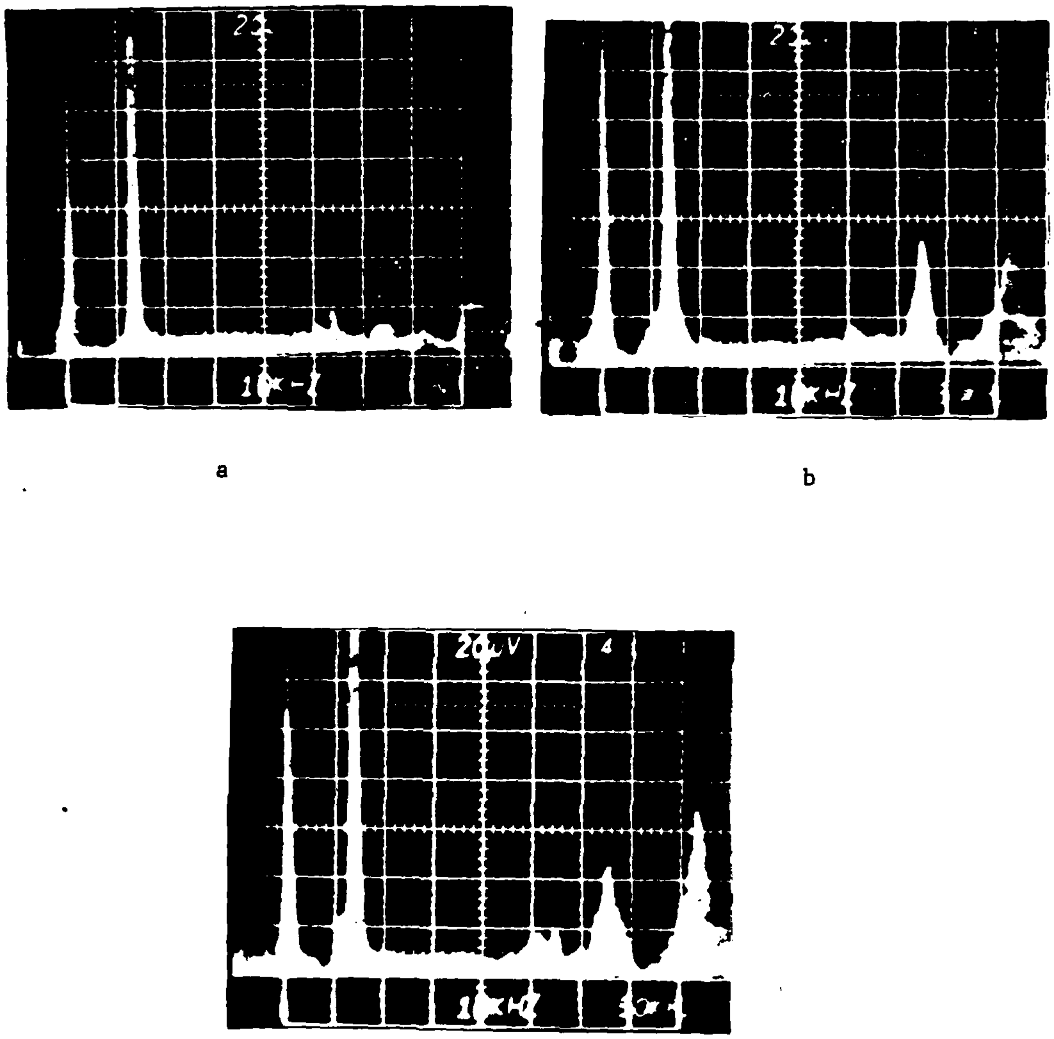

a

b

c

FIGURE 24. SPECTRA OF SOLDER JOINTS CONTAINING INCLUSIONS

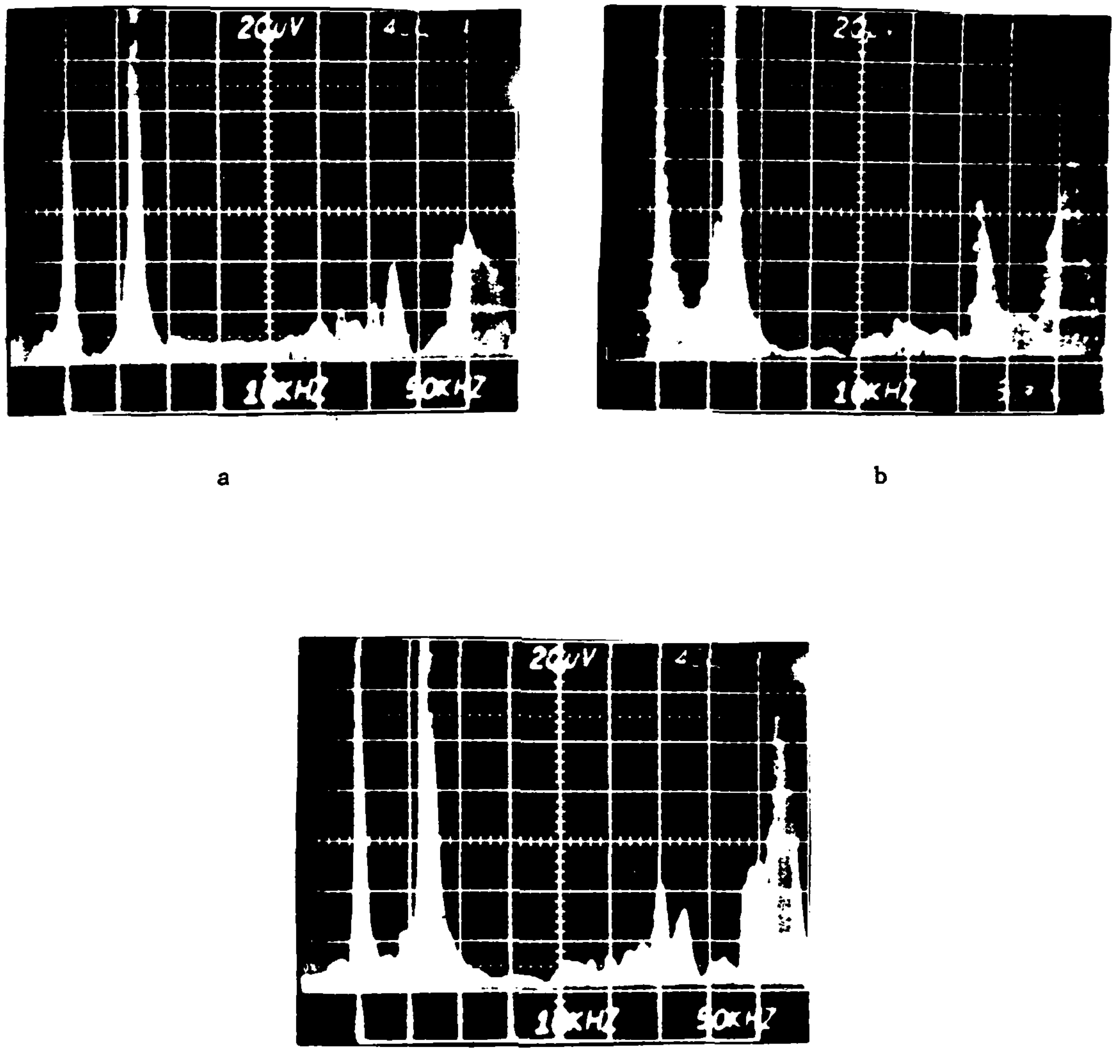

a

b

c

FIGURE 25. ADDITIONAL SPECTRA OF SOLDER JOINTS CONTAINING INCLUSIONS

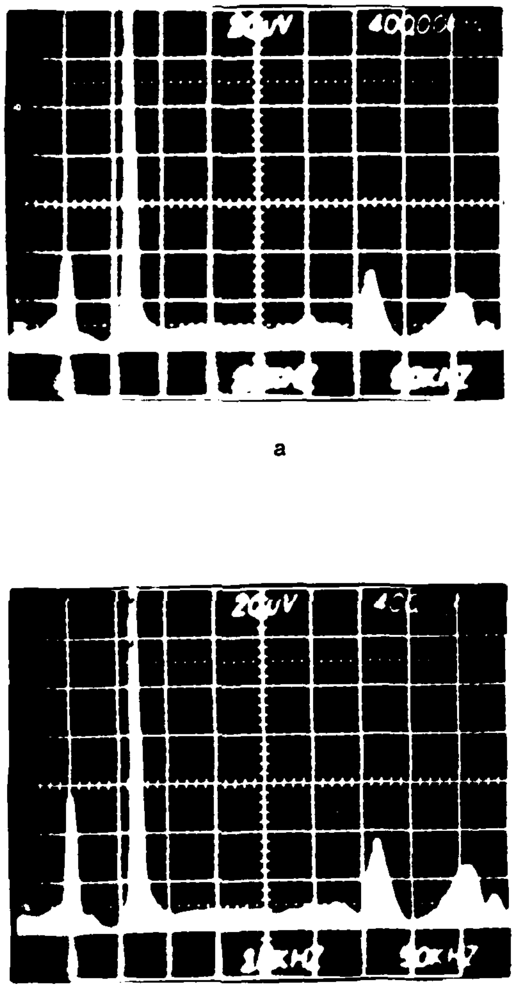

a

b

FIGURE 26. SPECTRA OF A GOOD SOLDER JOINT VERIFIED BY DESTRUCTIVE EXAMINATION. (a) With conformal coating. (b) With conformal coating removed.

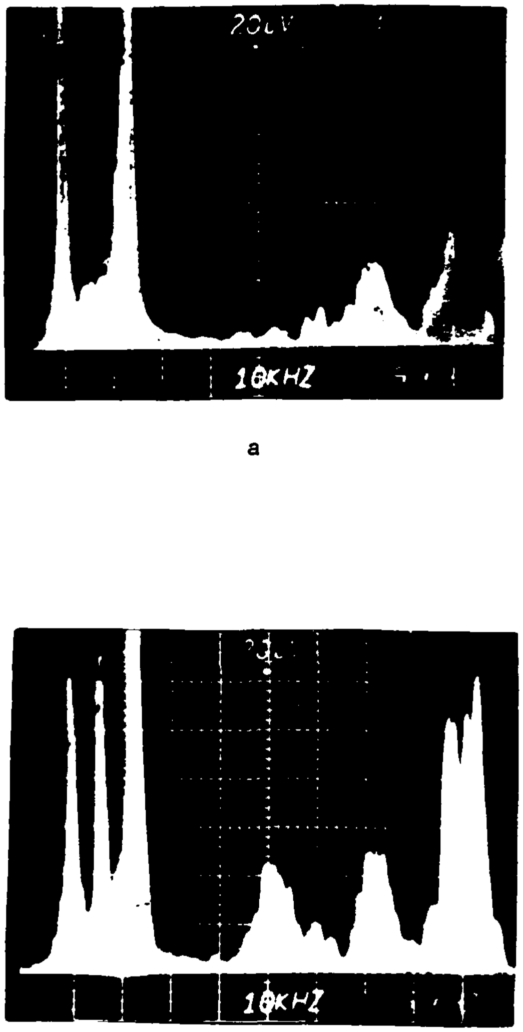

a

b

FIGURE 27. SPECTRUM OF A SOLDER JOINT CONTAINING A 15 PERCENT CRACK AT THE HEEL BUT WHICH IS OTHERWISE SOLID
(a) Transducers over solid portion of solder.
(b) Receiver over crack.

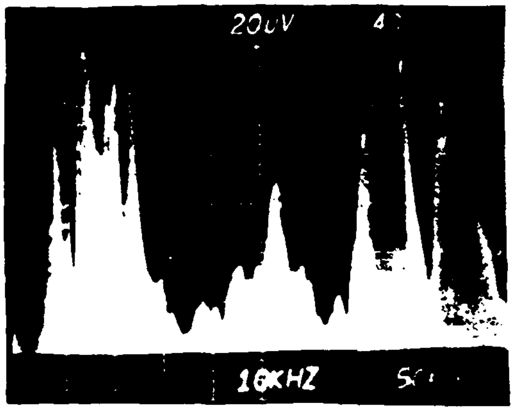

FIGURE 28. SPECTRUM OF A SOLDER JOINT WHICH IS BARELY TACKED AT THE HEEL AND AT THE TOE

In Figure 27a, the receiver is located over a solid portion of the solder joint. In Figure 27b, the receiver is moved closer to the heel and over the crack. Note that both show significant responses both at the low frequency end of the spectrum (200 to 270 kHz) and at the high-frequency end of the spectrum.

The spectrum of Figure 28 is extremely severe. The joint from which it was obtained would be rejected without question.

THEORY OF LASER/INFRARED SOLDER JOINT INSPECTION

The use of surface temperature monitoring in nondestructive testing is well known, but not in as wide-spread use as other standard techniques such as ultrasonics and radiography. A review by Vavilov et al.(1)* of recent journal literature on thermal methods of inspection cited only 36 references in the area. Most of the research that has been performed to date has been related to infrared imaging of passive objects or of actively heated objects in the steady-state. The use of a laser as a heat source and infrared detection of the temperature transient has had only limited study.

In view of the novelty of the laser heating/infrared inspection method and its application to detection of microscopic flaws in flatpack solder joints, theoretical effort was undertaken to guide experiment parameter selection and data interpretation. Most theoretical work to date on the transient thermal method of inspection has been carried out by Soviet researchers(2-5), but none of their results are directly applicable to the geometry of interest for the case of both heating and cooling. A general conclusion they have reached, however, confirms the intuitive view that the transient method is much more sensitive to small defects than is the steady-state method(1). The remainder of this section of the report describes the theoretical approach taken in the current research and numerical results for cases of interest. Implications of the results for use of the laser/infrared inspection method in practical solder joint inspection are discussed.

---

*References are listed at the end of this section.

Definition of the Problem

The geometry of interest consists of a long narrow Kovar lead (from an integrated circuit flat-pack) which is soldered to a copper pad which in turn is bonded to an epoxy-fiberglass substrate. A laser beam impinges on the top surface of the Kovar lead which is coated with a thin layer of solder. In reality, the flow of heat in this system is three-dimensional and there may be considerable geometrical variation from the ideal configuration. Considerable understanding of the thermal behavior of the solder joint can be obtained, however, by solution of the heat-transfer problem in a two-dimensional geometry which approximates the real case. Because of the heat sink capability of the lead and the copper pad, the plane chosen for study was that which sections the lead along its length. The idealized geometry is illustrated in Figure 29. While not shown in the figure, the right-hand boundary extends to 11.8 mm from the left boundary. This was found necessary to permit proper calculation of the heat sink effect of the copper for the longest laser pulse length studied. The geometry shown is that used for the initial calculations and was varied in some cases as discussed in subsequent sections. Properties assumed for the materials are given in Table 4.

The only serious deviation from two-dimensionality in the problem is the variation in laser beam energy deposition over the width of the lead arising from beam axisymmetry. This will lead to small systematic

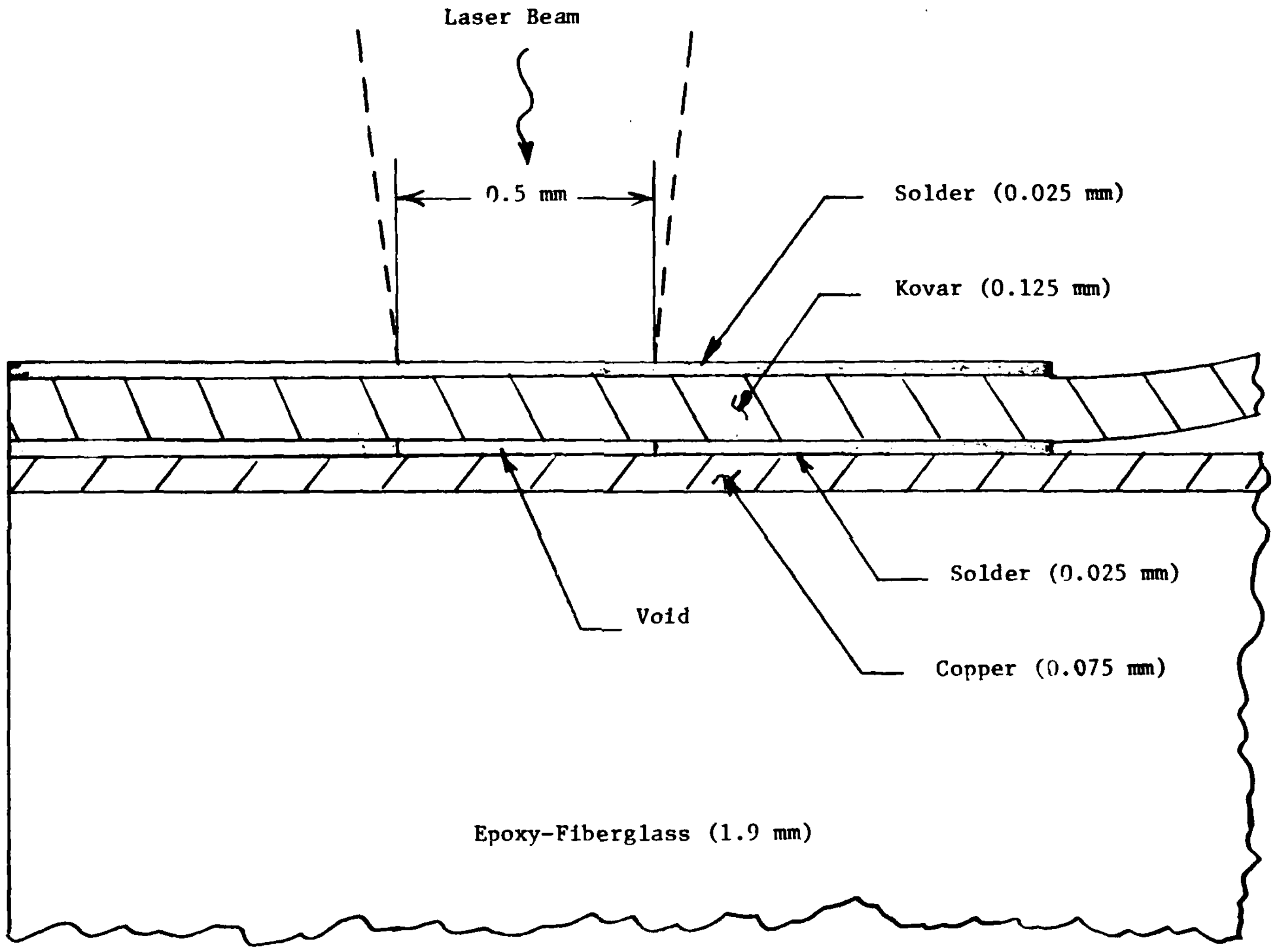
Laser Beam
0.5 mm
Solder (0.025 mm)
Kovar (0.125 mm)
Solder (0.025 mm)
Void
Copper (0.075 mm)
Epoxy-Fiberglass (1.9 mm)

FIGURE 29. IDEALIZED GEOMETRY FOR HEAT TRANSFER CALCULATIONS

TABLE 4. THERMAL PROPERTIES ASSUMED FOR SOLDER-JOINT HEAT-TRANSFER CALCULATION

Material	Thermal Conductivity, k (W/cm/C)	Specific Heat C_p (J/gm/C)	Density ρ (gm/cm^3)	Thermal Diffusivity, η (cm^2/sec)
solder	0.35	0.13	11.3	0.24
Kovar	0.14	0.42	8.4	0.039
copper	3.9	0.39	8.9	1.12
epoxy-fiberglass	0.008	0.92	1.8	0.0048

errors in the temperature results, but will not alter the main conclusions of the study. Lateral spreading of heat in the epoxyfiberglass substrate will contribute only negligible errors. Also it should be noted that only voids which cut completely across the joint can be treated in this geometry. This does not particularly limit the results, because the primary intent of the analysis is to determine trends in anticipated temperature transients in the presence of defects and guide selection of some of the laser beam parameters for experimental studies.

Selection of Laser Beam Parameter Values

Values of laser beam parameters used in the calculations were those believed to optimize detectivity of voids in solder joints. The laser beam parameters of interest are:

- wavelength
- spot size
- beam power
- pulse duration.

Wavelength is determined by the laser type and is limited to only a few specific values based on practical considerations (0.35 - 0.53, 1.06, and 10.6 μm). The impact of wavelength on the heat-transfer calculations is solely through the surface absorption coefficient for laser radiation, α_o. To minimize laser power requirements, generally the shorter wavelengths are preferable because α_o increases with decreasing wavelength. Since a 1.06 μm laser was selected for the experiments, this wavelength was used for the calculations. No data on solder absorptivity were available, however, a value of 0.30 at 1.06 μm was estimated based on lead and tin properties.

The laser beam spot size selected for the study was based upon using a circular beam. Given this constraint, the spot diameter was fairly well fixed at a value close to the width of the Kovar lead. A smaller spot diameter would require an excessive number of pulses to completely cover the lead, while a larger spot would require excessive power and might burn the epoxy. Use of an elliptical or rectangular spot was not considered in detail, but is discussed subsequently.

The beam power used in the calculation was varied depending on the case under consideration. Two factors limit beam power for a given spot area. If the power is too great, the solder on the top surface will melt (solidus 182 C, liquidus 238 C). If the power is too low, detection by the infrared method becomes difficult. In practice, a compromise power density will be selected which gives good defect discrimination without solder melt. For the calculations, a maximum temperature rise of 200 C in the absence of voids was arbitrarily selected for setting the beam power. This value for temperature rise is unimportant because all results can be scaled. The beam power density is then determined from the predicted surface temperature rise in a semiinfinite body subjected to a constant heat pulse of duration, t_p,(6)

$$\Delta T = 200\ \mathrm{C} = 2\ G\alpha_o \left[\frac{t_p}{\pi\ k\ \rho\ C_p} \right]^{1/2} , \qquad (1)$$

where G is incident laser power density. Using the Kovar properties, α_o = 0.3, and t_p = 10 ms, it is found that the required incident power density for a 200 C rise is $G = 4.15 \times 10^3$ W/cm^2. Assuming an effective beam-spot area of 0.0025 cm^2, it is found that a beam power of about 10 W would be required to produce this temperature rise. For the heattransfer analyses performed in this study, the beam power density was scaled for display convenience according to Equation (1), i.e., $G \sim t_p^{-1/2}$.

The remaining beam parameter, pulse duration, was a principal parameter of variation in the study. A range of interest for this parameter was easily determined by considering the characteristic time for heat to diffuse through the Kovar lead to the solder joint interface defect,

$$t_c \sim \frac{d^2}{\eta} \sim 4 \text{ ms}, \qquad (2)$$

where d is the thickness of the Kovar lead and η is thermal diffusivity. Pulse durations in the range 1-40 ms were used in the study.

Numerical Solution of the Heat-Transfer Problem

Solutions of the transient heat-transfer problem described above were obtained numerically because the complexity of the problem precluded analytical treatment. A previously developed, Battelle computer code, TRAHT2, was employed which solves the transient heat-conduction equations in two-dimensions for a multiregion geometry with general boundary conditions. An explicit finite-difference algorithm is used in the code with a time step automatically calculated to ensure numerical stability. For the calculations of this study, an insulating boundary condition was imposed at the limits of the conducting regions and a prescribed heat-flux boundary condition was imposed over the boundary region corresponding to the laser beam impingement area. No phase change was considered and thermophysical properties were held constant. The finite difference mesh consisted of a 29 x 17 array of nodes with varying mesh intervals selected to optimize computing time consistent with required accuracy.

Results of initial baseline calculations with TRAHT2 are illustrated in Figures 30 and 31. The case considered is that given by the geometry of Figure 29, an ideal joint with a single void located directly under the beam spot and having the same width dimension (0.5 mm). The void thickness is the same as that of the solder in the gap (0.025 mm) and is assumed to be completely nonconducting. The incident laser-beam power density is assumed to be constant to 6.57 x 10^3 W/cm^2 for a duration of 4 ms. the initial temperature of the conducting region is assumed to be 25 C for display purposes. The temperature transient for a point on the surface at the center of the laser-beam spot (maximum temperature) is given by the upper solid curve in Figure 30, For comparison, a TRAHT2 case was run with no void for the same conditions and results are given by the lower solid curve of Figure 30. Initially both curves rise together according to Equation (1), which is expected for time short compared to the characteristic time required for the heat to diffuse to the defect. Approximately 30 C difference in temperature develops by the end of the pulse. On the cooling portion of the curves, the difference increases to a maximum of about 60 C at 8 ms. It is this temperature difference or "contrast" which would be used in the inspection system to infer the presence of a solder-joint defect.

Also shown in Figure 30 are dashed lines corresponding to simple analytical solutions of single-region one-dimensional problems which may be used for reference and which provide a consistency check for the numerical results. For a semiinfinite region of thermal diffusivity, n, and thermal conductivity, k, the temperature at depth x is (6)

$$T_s(x,t) = \frac{2F\,(\eta t)^{1/2}}{k} \quad \mathrm{ierfc}\,[\,x/(\eta t)^{1/2}] \,, \qquad (3)$$

where F = α_oG, the absorbed (constant) power density, and ierfc is the first integral of the complementary error function. Using Duhamel's theorem, the surface temperature for a heat pulse of duration, t_p, becomes

$$T_s(0,t) = \left[\begin{array}{l} \frac{2F}{k}\left(\frac{\eta t}{\pi}\right)^{1/2}, \text{ for } t \le t_p \\ \frac{2F}{k}\left(\frac{\eta}{\pi}\right)^{1/2}\left(t^{1/2} - (t - t_p)^{1/2}\right), \text{ for } t > t_p \end{array}\right] \qquad (4)$$

Similarly, it can be shown that the surface temperature of a slab of the same material of finite thickness, L, is given by

(See next page)

$$T_f(0,t) = \frac{2F(\eta t)^{1/2}}{k} \left\{ \frac{1}{\pi^{1/2}} + 2 \sum_{n=1}^{\infty} \text{ierfc} \left[\frac{nL}{(\eta t)^{1/2}} \right] \right\}, \quad (5a)$$

for $t \leq t_p$ and

$$T_f(0,t) = \frac{2F}{k} \left[(\eta t)^{1/2} \left\{ \frac{1}{\pi^{1/2}} + 2 \sum_{n=1}^{\infty} \text{ierfc} \left[\frac{nL}{(\eta t)^{1/2}} \right] \right\} - \eta^{1/2}(t-t_p)^{1/2} \left\{ \frac{1}{\pi^{1/2}} + 2 \sum_{n=1}^{\propto} \text{ierfc} \left[\frac{nL}{\eta^{1/2}(t-t_p)^{1/2}} \right] \right\} \right], \quad (5b)$$

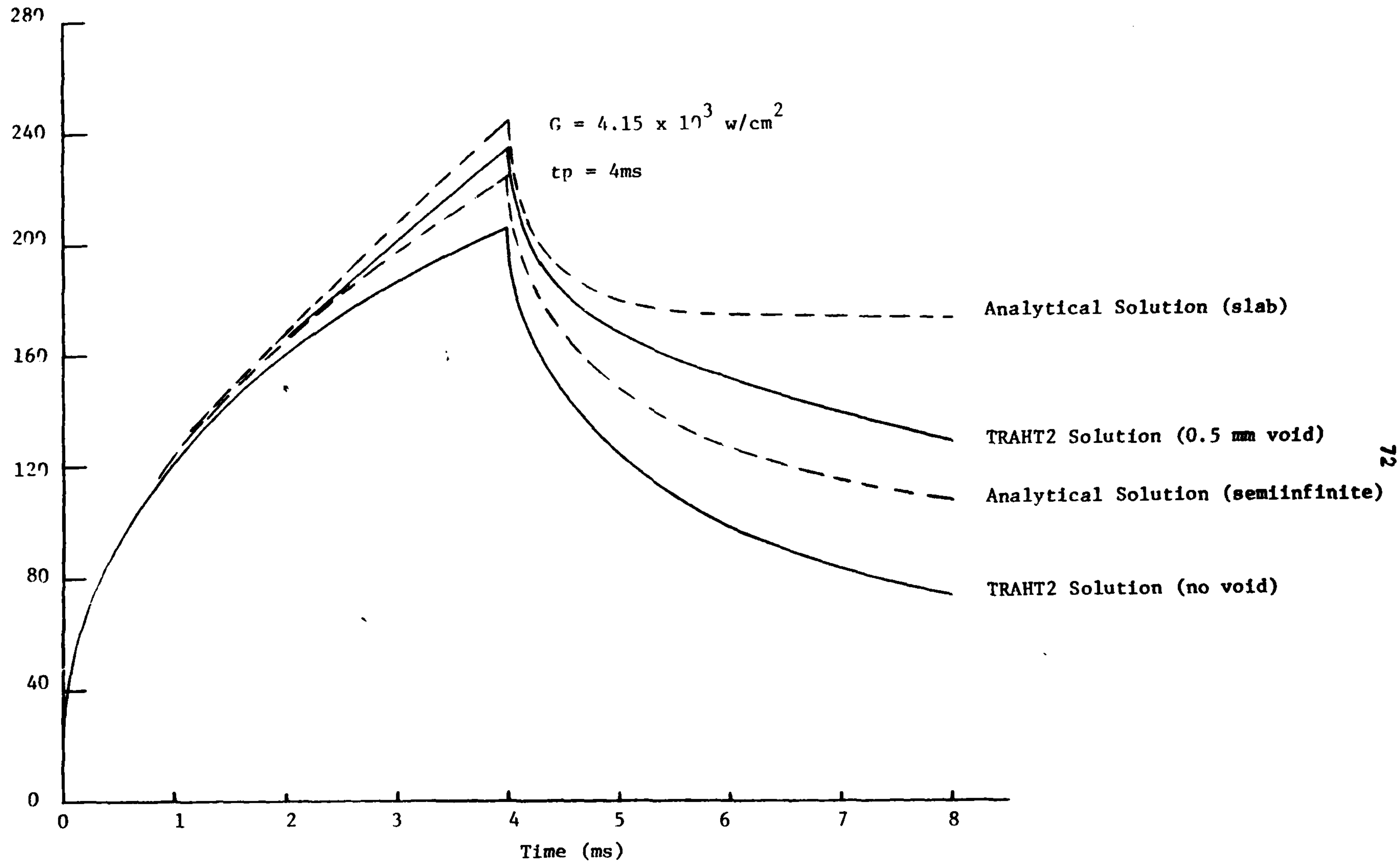

FIGURE 30. COMPARISON OF TRAHT2 RESULTS TO ANALYTICAL SOLUTIONS FOR 4 ms PULSE

for $t > t_p$. The lower and upper dashed curves of Figure 30 are graphs of Equations (4) and (5), respectively, for Kovar properties and beam conditions as above. The upper dashed curve, corresponding to a finite thickness Kovar slab, should be an upper bound to the TRAHT2 solution for a void as is seen to be the case. The temperature calculated with TRAHT2 is seen to continue to drop at long times as two-dimensional heat flow develops around the defect and into the copper pad. The onedimensional analytical solution for an insulated slab exhibits equilibration at long times. The lower dashed curve gives the predicted surface temperatures for a semiinfinite Kovar region with no void. Both two-dimensional effects and the presence of the copper pad cause the temperature to drop faster in the real case (TRAHT2 solution with no void).

The spatial distribution of the surface temperature for the TRAHT2 cases discussed above are presented in Figure 31 for two instants of time, 5 and 10 ms. The solid curves give results for the 0.5 mm void and dashed curves present results of the no-void calculation for comparison. A considerable variation in surface temperature over the laser beam spot area is noted even though the irradiance is assumed constant over the area. The temperature contrast at 5 ms rises from 10 C at the edge of the beam spot to about 45 C at the center. This suggests that the infrared detector image area should be considerably smaller than the laser spot area and should be carefully aligned for maximum sensitivity to defects. The effects of spreading of the heat are noted by comparing the results at the two times. Temperatures in the unirradiated areas are observed to increase with time. An interesting counterintuitive feature is noted in the unirradiated area where at a given point in time, the temperature is lower in the presence of a defect which might be expected for force more heat to flow into the unirradiated area. Examination of the thermal pattern in detail revealed that the high thermal diffusivity copper pad provides the dominant path for heat flow along the length of the lead and blocking the path to the copper

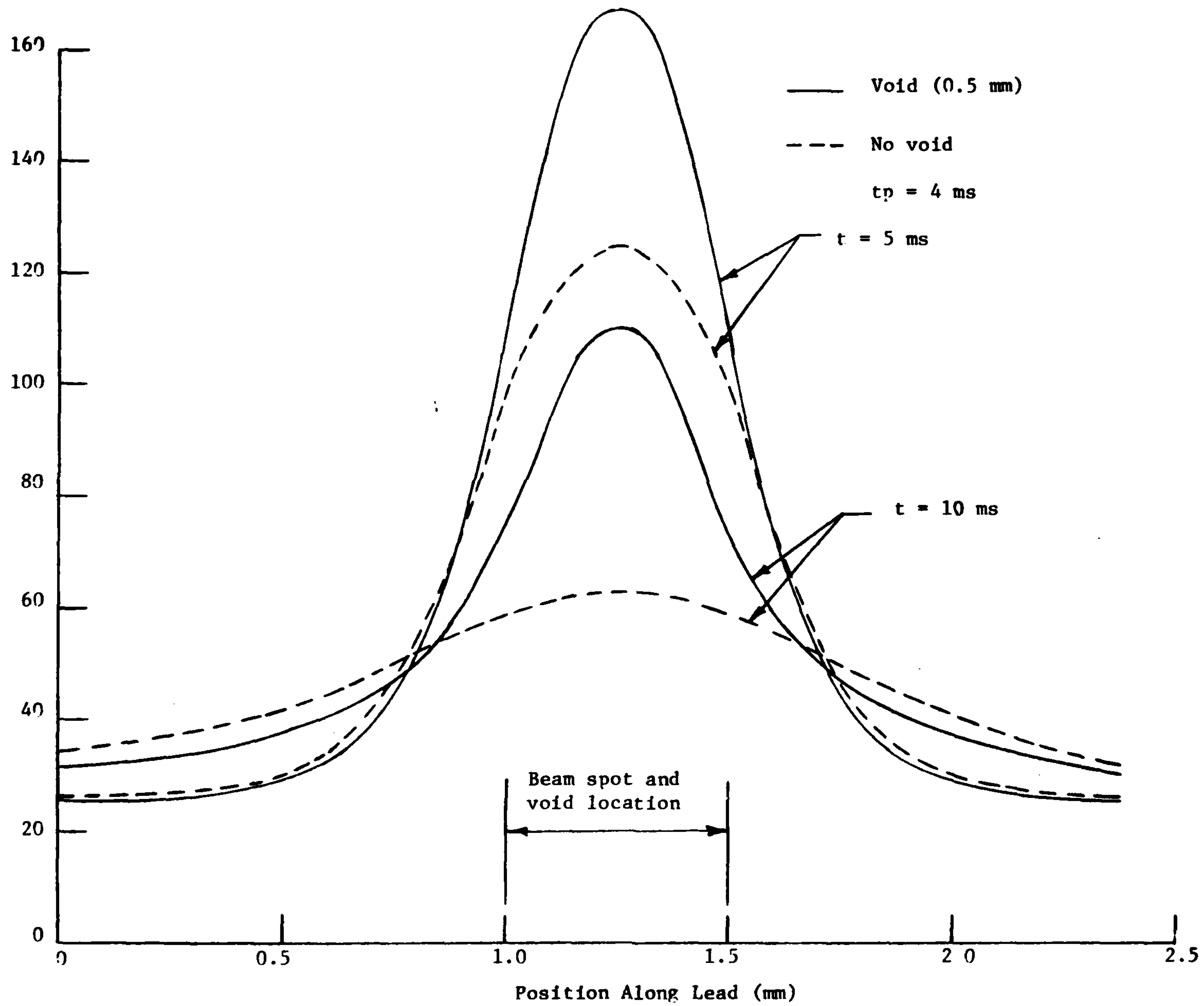

FIGURE 31. SPATIAL DISTRIBUTION OF SURFACE TEMPERATURE FOR 4 ms PULSE

with a defect has the net effect of inhibiting lateral spreading. Thus, the copper pad might have beneficial effect of enhancing defect image contrast if a scanning detection system is used.

Study of Pulse Length Effects

Having established basic characteristics of the temperature response of a solder joint, cases were computed for various laser pulse lengths in an attempt to establish an optimum pulse length for discrimination of solder joint defects. The beam power density was varied according to Equation (1) to provide an approximately constant temperature rise for comparison purposes. Figures 32, 33, and 34 present transients for $t_p = 1$, 4, and 10 ms, respectively. In the figures, the numbers (1), (2), and (3) refer to points on the top surface at the center of the beam, on the top surface at the edge of the beam, and under the void on the copper surface at the center of the beam, respectively. In Figure 32, it may be seen that no difference in surface temperature between the void and no-void case is seen until well after the pulse is over as expected for a short pulse. The contrast which develops is greater at the beam center than at the edge as noted before. From Figures 33 and 34 it is noted that the defect contrast increases with increasing pulse duration and significant contrast exists at the end of the laser pulse.

A more useful way to examine the effects of pulse length is to display the defect temperature contrast directly as a function of time. Temperature differences between the void and no-void cases were extracted from the numerical results. These data were then adjusted to correspond to the same "no-void" temperature rise (200 C) for each pulse length. The adjustment was required because Equation (1) underestimates the power density required to achieve 200 C in the longer pulse cases. Figure 35 presents Equation (1) (dashed line) and the power density required for achieving 200 C as determined by scaling the TRAHT2 results (solid line). The adjusted contrast results are presented in Figure 36. The maximum

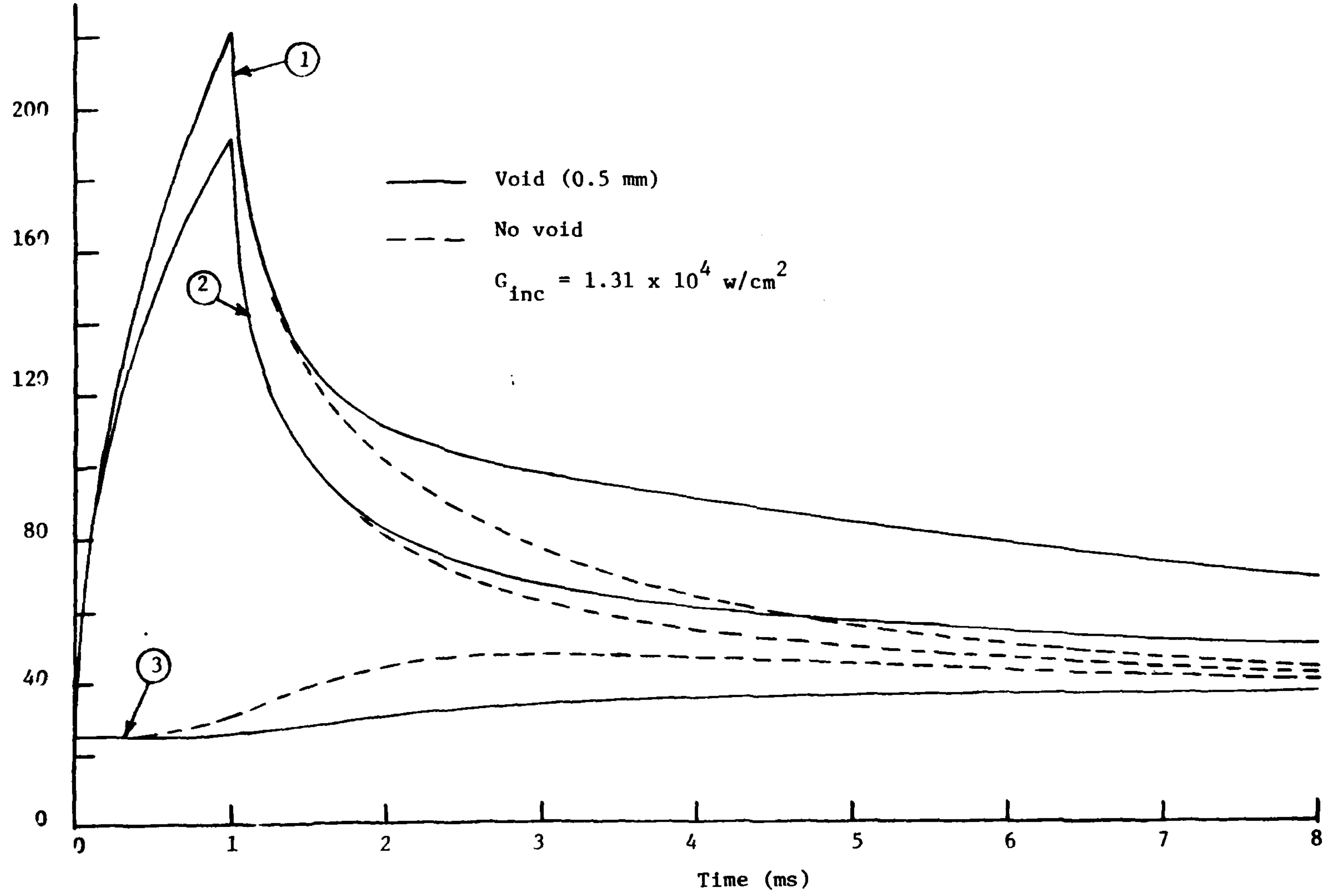

FIGURE 32. TRANSIENT TEMPERATURE RESPONSE FOR 1 ms PULSE

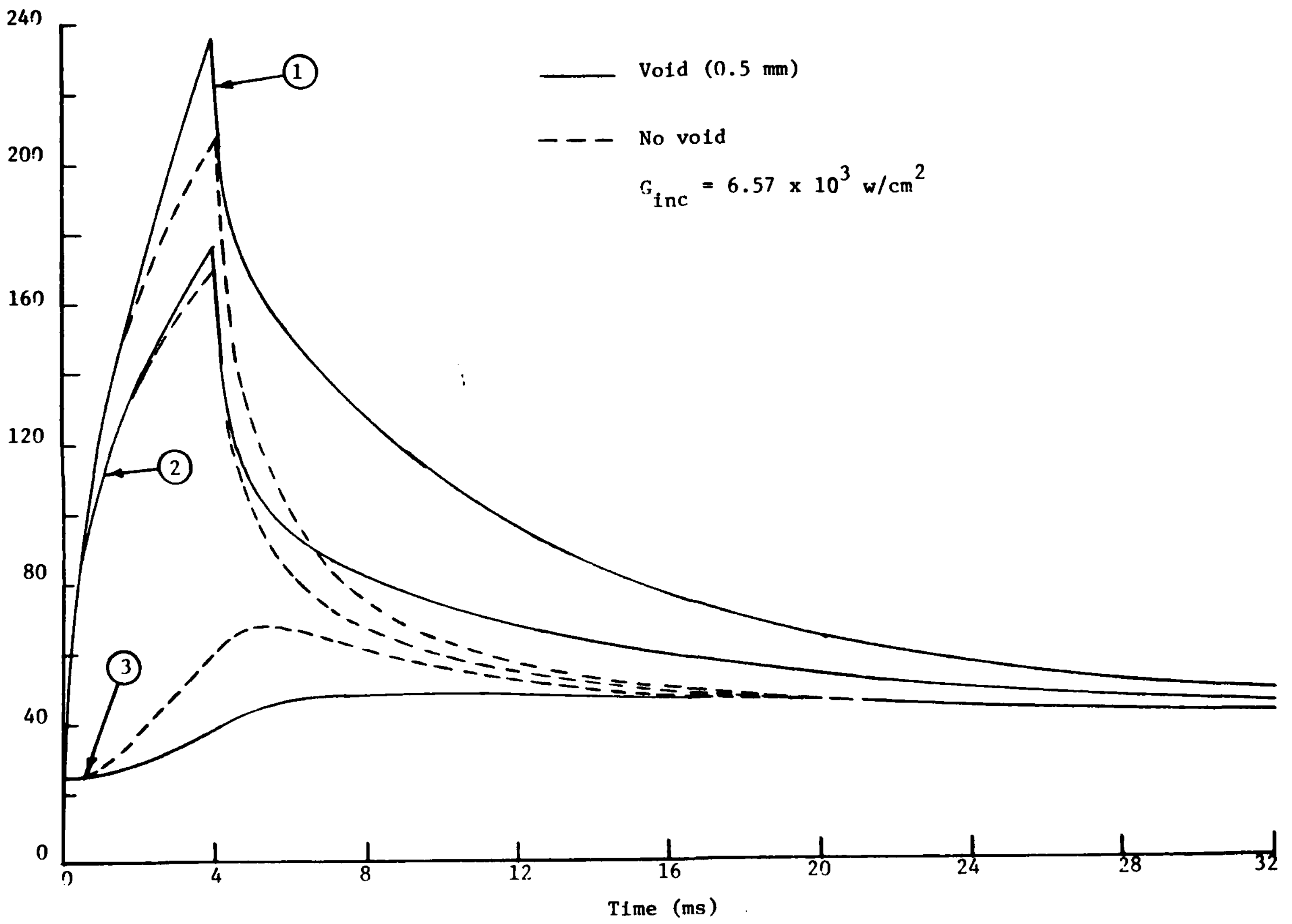

FIGURE 33. TRANSIENT TEMPERATURE RESPONSE FOR 4 ms PULSE

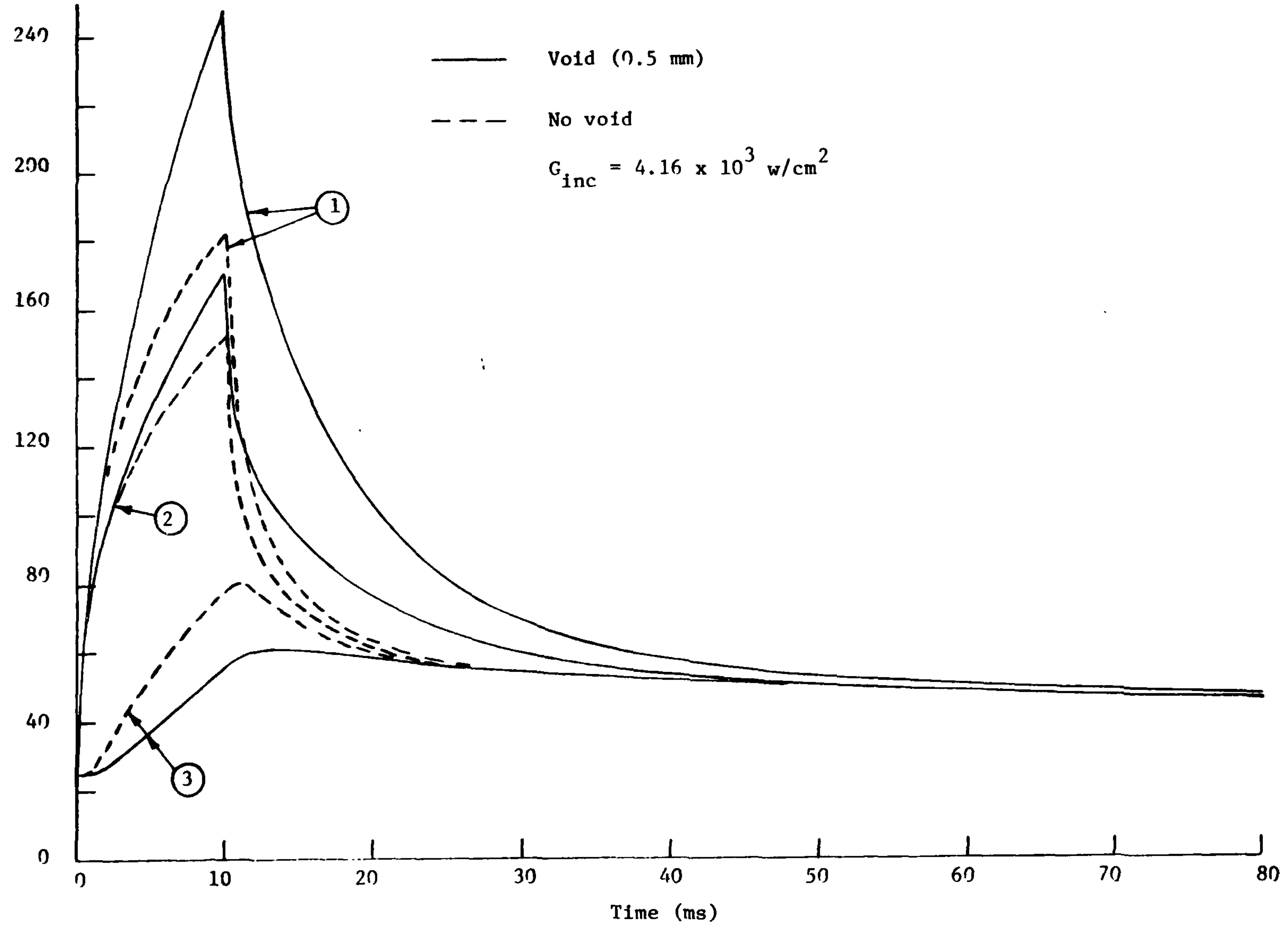

FIGURE 34. TRANSIENT TEMPERATURE RESPONSE FOR 10 ms PULSE

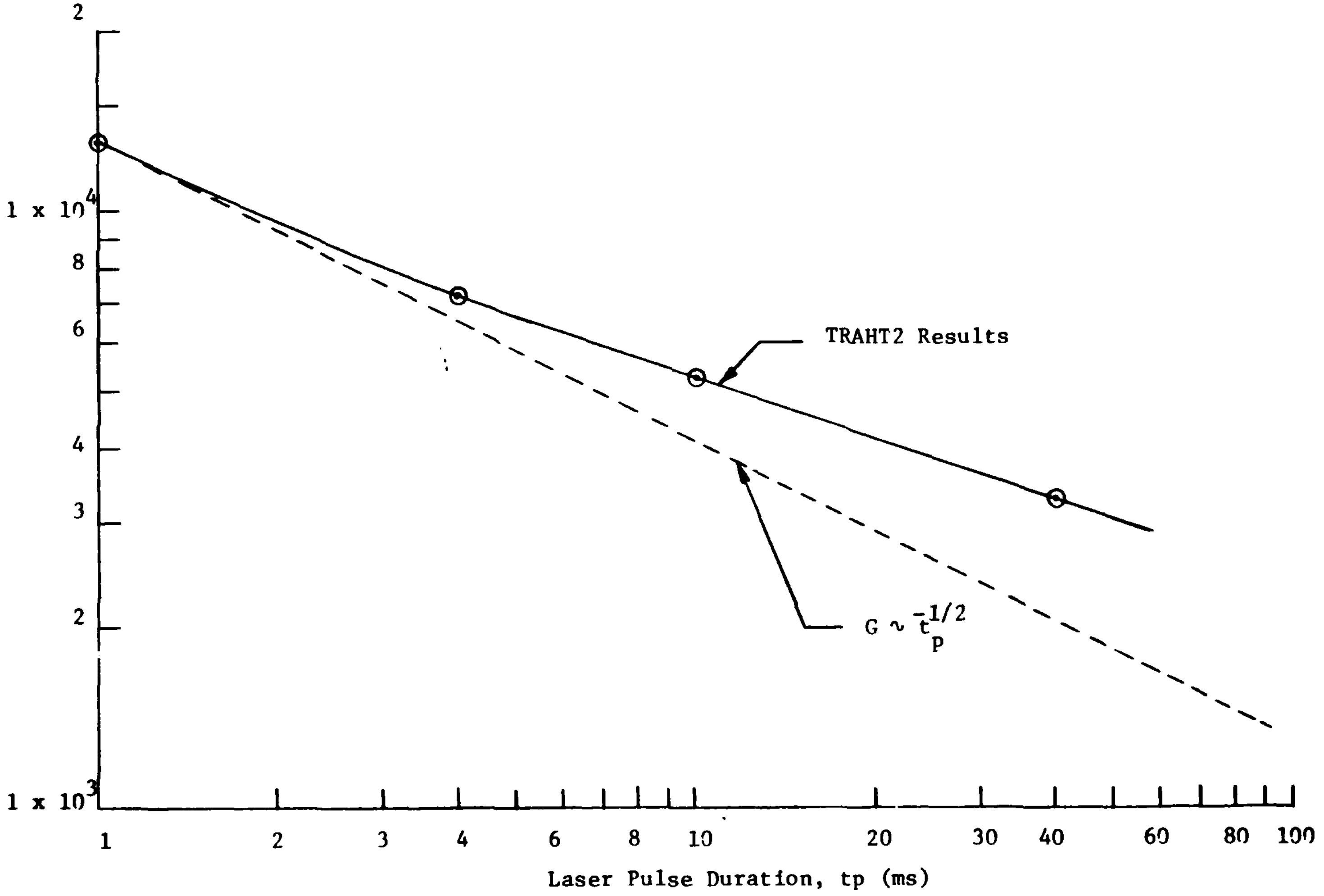

FIGURE 35. POWER DENSITY REQUIRED TO ACHIEVE 200C SURFACE TEMPERATURE RISE (α_o = 0.3)

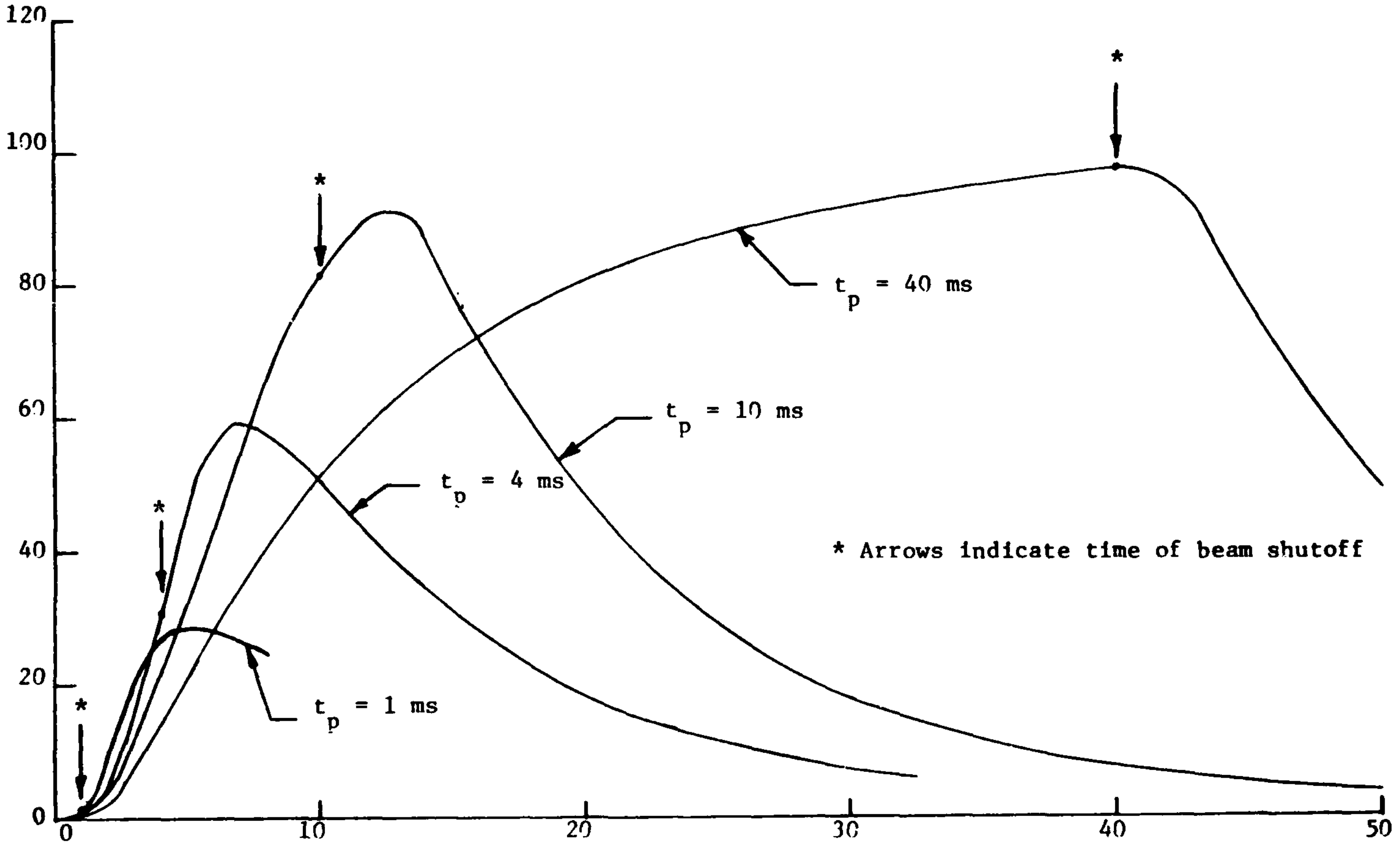

FIGURE 36. DEFECT TEMPERATURE CONTRAST FOR VARIOUS PULSE LENGTHS

contrast rises rapidly with increasing pulse length for short pulses. While a 20 ms case was not run, extrapolation of the results indicates that a maximum contrast probably occurs for a pulse length near 20 ms. As the pulse length is increased to 40 ms, a quasiequilibrium develops in the heat-transfer pattern and the maximum contrast, while still very useful, probably drops below that at the optimum pulse length. It should be noted that in the 10-40 ms pulse regime, the peak contrast occurs near the point of peak temperature. This suggests acquisition of the peak temperature in the infrared inspection system, rather than the cooling curve characteristics, which would be a considerable simplification. This result is in agreement with experimental results achieved under the program, but may not hold for all void configurations.

The contrast results presented above indicate that a wide range of pulse widths are acceptable for detecting large defects when the beam spot is centered on the defect. For smaller defects, it is anticipated that a pulse width less than 20 ms may be optimum. Since the level of contrast will be lower for smaller defects, it may ultimately be necessary to select a shorter pulse length based on the heat-transfer characteristics of the defect which is of a size near the threshhold of detectability. An insufficient number of cases were run to determine all of the optimum pulse lengths for defects of interest, however, a defect size effect was established. For a 0.125 mm defect directly under the beam spot, the peak contrast was 30% greater for a 10 ms pulse than for a 40 ms pulse.

Study of Effect of Void Configuration

A limited number of cases were run to assess some of the variation in surface temperature response to be expected as a function of void location and size. In two cases, the solder gap was left entirely void except in a region centered under the beam spot. In one case, the

AD-A095 971 BATTELLE COLUMBUS LABS OH F/G 13/5
TREND INSPECTION STATION FOR PRINTED CIRCUIT BOARD SOLDER JOINT--ETC(U)
APR 79 D J HAMMAN, D ENSMINGER, R VANZETTI F04606-78-C-0903
UNCLASSIFIED NL

2 OF 2
AD A
095971

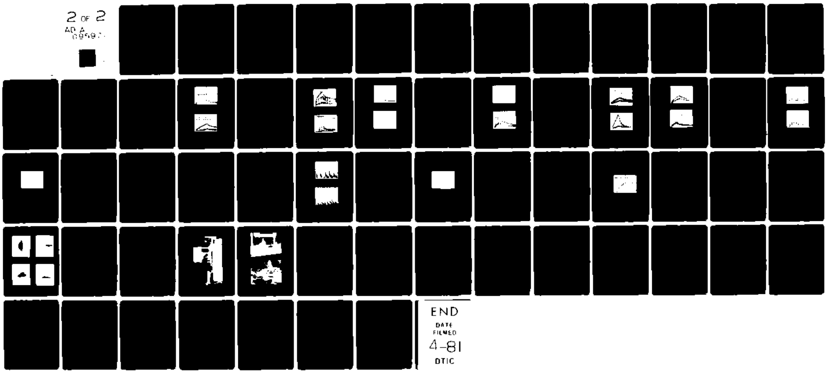

END
DATE
FILMED
4-81
DTIC

remaining solder region was 1.25 mm in length and in the other it was 0.5 mm in length (the same area as the beam spot). The pulse length was set at 4 ms. The peak contrast for the surface temperature at the center of the spot was found to be 2.5 C at 20 ms for the first case and 3.8 C at 18 ms for the second case. The pulse length was increased to 10 ms for the void of the latter case and the contrast increased to 5.8 C. While the threshold contrast level for the inspection system has not yet been determined, it will probably be of order 10-20 C or greater. It is important to note that this level will not be constrained by detector system sensitivity (which should be capable of discrimination at the 0.1 C level) but by normal deviation in "good" solder joint response. It is concluded that the presently conceived system cannot usefully sense void type defects outside the laser beam spot area. Hence, inspection of a single lead will require several passes (about 4) of the currently configured system to insure that at least 2/3 of the gap is filled with solder.

As noted previously, cases were run with a single small void, 0.125 mm in width, located near the center of the beam spot. Pulse lengths of 10 and 40 ms were investigated and results indicated peak contrasts of 3.3 C and 2.5 C, respectively. While some improvement in contrast may result from going to a still shorter pulse, this void size is believed to be below the threshold of reliable detectability. Doubling of the void size, however, would raise the width-to-depth ratio to about two where two-dimensional effects would be strong and detection likely. It is estimated that the threshold void defect width for the type of void studied here is in the range of 0.13-0.25 mm.

Study of Excess Solder Effects

Excess solder can be present in a solder joint and, while acceptable in most cases, must be accounted for in interpreting the measured thermal response. The excess solder may be on top of the lead or in the solder joint proper. A potential problem in the infrared measurement of surface temperature occurs because of irregularities in solder thickness on top of the lead. The method of solder joint production leaves an irregular surface contour in some cases and this in turn may lead to fluctuations in measured surface temperature due to changes in detector collection efficiency and surface emissivity. This part of the excess solder problem is not addressed here but, rather, it is assumed that temperature is measurable and real changes in temperature due to heat-flow alteration are examined. In the baseline case, a uniform 0.025 mm thick layer of solder was assumed to exist on top of the Kovar lead. A case without voids was run wherein this layer was increased in thickness by a factor of three. For a 4 ms pulse, this lead to a maximum surface temperature which was 8.6 C less than that for the thin solder layer under the same conditions. The lower surface temperature results from the slightly higher value of $k_\rho C_\rho$ for solder than for Kovar (see Equation (1)). It is somewhat fortuitous that larger differences in $k_\rho C_\rho$ do not exist, or the normal variations in solder thickness would give rise to an unacceptably high "noise" threshold for defect temperature contrast detection.

A case was also calculated for excess solder in the Kovar/copper interface region. The solder layer was set at a thickness equal to twice that of the Kovar lead or 10 times the nominal value. This joint would be acceptable if otherwise defect free. Surprisingly, for a 4 ms pulse, the excess solder led to only a 6 C difference in surface temperature, and in this case, the temperature was greater than that for a normal layer. The higher temperature likely occurs because, when the excess solder is placed between the Kovar and the copper, the dominant effect is the delay of onset of the copper heat sink effectiveness. This is time dependent and longer pulse times would probably show this temperature difference more dramatically.

It is concluded that temperature differences due to excess solder will be in the 5-20 C range. While these values are small, due to a fortuitous condition, they will be a major factor in setting the threshold temperature deviation level for defect detection.

Conclusions

Based on these limited two-dimensional heat-transfer calculations, it is concluded that the laser/infrared solder joint inspection method is feasible and will be particularly useful for detecting hidden voids in the solder. Specific conclusions for the initial configuration of the system are:

(1) a reasonable laser power level in the 10-20 W range should be adequate for the inspection system if a circular beam *irradiance area is used*,

(2) maximum sensitivity to a void under the beam spot results for a detector image area which is small compared to the laser beam irradiance area and is carefully coaligned,

(3) for a 0.5 mm void under the laser beam irradiance area, maximum defect temperature contrast occurs for a pulse length in the range 10-40 ms, probably near 20 ms,

(4) voids cannot be reliably detected outside the beam irradiance area, which implies that multiple passes (about 4) or a scan procedure will be required to insure that a joint is acceptable,

(5) the minimum width of a transverse void which will be detectable will be greater than 0.13 mm and probably in the range 0.13-0.25 mm,

(6) excess solder does not have a major effect on the solder joint heat-transfer characteristics for sufficiently short laser pulses due to a fortuitous match in certain properties of solder and Kovar.

Because of implications of the fourth conclusion alternate configurations for laser irradiation of the lead and for surface temperature acquisition should be considered. In particular, consideration should be given to irradiation with a single laser pulse which covers the entire lead area. This could be done with a special lens or lens combination which would produce a long narrow elliptical beam irradiance area. Temperature information could be acquired with (1) an elliptical detector-image area, (2) a small circular detector-image area which is rapidly scanned along the length, or (3) multiple detector images. The first technique is the simplest to implement but probably is unacceptable, except for the largest solder voids, because temperature contrast information is averaged. The second method yields the most temperature contrast information, but may be the most difficult to implement because of the rapid, accurate, small-displacement scanning required. The third method would give adequate contrast information and would be reasonably straight-forward to implement. Instead of the single detector now envisioned, a close-packed stationary detector array consisting of 4 or 5 elements would be employed with a corresponding number of data acquisition channels.

References

1. V. P. Vavilov, V. I. Gorbunov, and B. N. Epifantsev, "Some Theoretical and Experimental Problems in Thermal Methods of Nondestructive Testing" Defektoskopiya, No. 6, pp. 67-75 (1975).

2. V. P. Vavilov and V. I. Gorbunov, "Analytical Calculation of Temperature Distributions in the Thermal Flaw Detection of Laminated Components", Defektoskopiya, No. 2, pp. 100-105 (1974).

3. V. I. Gorbunov, V. P. Vavilov, and G. N. Parvatov, "Solution of the Two-Dimensional Problem of Thermal Flaw Detection for a Metal Plate With a Rectangular Internal Defect", Defktoskopiya, No. 5, pp. 74-80 (1974).

4. N. A. Bekeshko, "Calculation of the Transient Temperature Field of a Metal Plate in Active Methods of Thermal Testing", Defektoskopiya, No. 2, pp. 64-68 (1975).

5. V. P. Vavilov, "Calculation of Certain Temperature Drop Parameters When Testing with a Constant Thermal Flux", Defektoskopiya, No. 5, pp. 65-67 (1976).

6. H. S. Carslaw and J. C. Jaeger, Conduction of Heat in Solids, Oxford University Press, London (1959).

EXPERIMENTAL LASER/IR STUDIES

This section discusses the results of the efforts at Vanzetti IR and Computer System, Inc. The program at Vanzetti was initiated with a review of theoretical and practical considerations to lead to a design of experiments. The review extended for several weeks and included:

(1) A literature review of prior work on the laser-heating of surfaces;

(2) Consideration of laser-damage thresholds which must not be exceeded;

(3) A review of criteria for defining faulty solder joints;

(4) A determination of how the theoretical and experimental efforts were to be divided between the Battelle and Vanzetti organizations;

(5) A catalog review of available equipment to be considered for use in the experimental work;

(6) A calculational effort based on theoretical considerations in order to establish optimal laser-beam power densities and exposure times for maximum sensitivity to differences in solder-joint quality.

The calculations from (6) suggested that a radiation source which could deliver between 1 and 10 watts of power to an IC lead or solder joint would be suitable for the program, depending upon the sample heating time desired. This indicated that radiation sources other than lasers might also be considered, and these might be more desirable from the standpoint of economy, compactness, and maintenance. Preliminary evaluation tests were made in August 1978, using ½-millisecond pulses from a 40-watt xenon flashlamp. This was followed by further tests in September using a shuttered 150-watt tungsten-halogen projector lamp. Both devices showed some possibility of being useful, but not without certain problems. Achieving variable pulse lengths with the flashlamp, for example, would be a complicated electronic problem but would be necessary for our tests. The projector lamp offered convenience but achieved slower heating rates than those predicted for a laser. Both lamps, being incoherent, required large-diameter optics for delivering useful power levels to the target, and this would interfere mechanically with other system elements.

Nonetheless, the work done by use of these sources was important in our establishing procedures and in observing actual warmup and cooldown phenomena in metallic targets before going on to the small test-joints which were to be used later in the program.

The work on non-laser sources was set aside in September when tests began with use of a Sylvania Model 607 Neodymium: Yttrium-Aluminum-Garnet (Nd:YAG) laser rated at 8 watts. Early tests from this power level proved to be more than adequate for test purposes on nonmetallic test materials having moderate absorptivity. With most of the beam focused into a 0.020"-diameter disc, surface temperatures of 130°C were attained in a 0.010"-diameter central area with exposures pulses of 5 milliseconds. The tests were interrupted when the laser, which was on loan to Vanzetti for evaluation, had to be returned to the vendor because of other commitments.

In October, attention was turned to experimental measurements of heat-flow phenomena in actual solder joints. While awaiting the receipt of actual-size sample joints from Battelle, Vanzetti prepared their own versions of scaled-up joints containing voids and inclusions, with normal joints as reference standards. These tests again used the tungsten-halogen lamp sources, and demonstrated that void-type and normal joints could be distinguished clearly on the basis of thermal behavior. Oscillograms were prepared showing that a "lead" with a void underneath would reach a higher initial temperature and would cool down more slowly than a "good" joint because of the reduced heat-sinking. These and other results were described at the 19 October USAF/Battelle/Vanzetti meeting in Columbus and appear in Vanzetti's Fourth Status Report in Appendix A.

Also, in October, Vanzetti began the design of a micro-reflectometer in order to be able to measure absoption variations among test joints, should this prove to be necessary.

The tungsten lamp tests continued through November and part of December as Vanzetti awaited shipment of another laser from Sylvania. During this time they continued to refine their experimental techniques as well as to build up their laboratory facilities in preparation for the laser tests. The work included modification of a Vanzetti INSPECT optical system to receive the laser, as well as the fabrication and initial testing of the micro-reflectometer. A thermoelectrically cooled lead sulfide detector was evaluated as a possible alternative to the liquid-nitrogen-cooled indium antimonide INSPECT detector.

The new Nd:YAG laser was received on 20 December and became operational a few days later. Initial heating tests with the laser, plus additions and refinements to the optical and electronics systems, extended through January, by the end of which Vanzetti demonstrated full operation of the integrated/laser/thermal system on Battelle-furnished test samples. At this time, a rare type of laser failure (water coolant leaks) occurred which interrupted the program for two weeks until 22 February 1979. Actual test data recording was resumed at that time.

The laser/IR test results follow.

Laser/IR Test Results

Most of the laser/IR tests were conducted on a sample board prepared by Battelle that contained a diversity (19 types) of intentionally defective solder joints. Samples of "good" joints also were included for reference. Other of the Vanzetti tests were conducted on samples prepared by the Vanzetti Company.

The types of defective joints which Vanzetti has been able to identify by laser/thermal probing, in order of descending detectability, are:

(1) Lead detached from joint(i, j, or q but severe)
(2) Cold joint if having dull appearance (a)
(3) Dewetted joint (q)
(4) Granular-surface joint (k)
(5) Exposed gold lead (yellow flat top) (g)
(6) Discolored joint due to excessive heat (b,o)
(7) Insufficient solder (n_1)
(8) Lead half off pad. (e)

The letter in parentheses in the above list refers back to the defect listing in the section on Standard Solder Joint Preparation.

Vanzetti defines an easily detectable defect as one whose peak thermal signal is several times higher than that for a normal joint. The detectabilities of the above defects cover a range of values, allowing for highly positive identification of Item (1) defects to a lower value for Item (8) defects.

The pertinent information about these defects is summarized in Table 5. In the table, the figure-numbers refer to typical oscillograms which are illustrative of the phenomena which have been observed. The oscillogram traces were highly repeatable for each target point. That is,

TABLE 5. SUMMARY OF EXPERIMENTAL RESULTS

Description of Defect	IC Sample No.	Detection Reliability	Example Shown in Figures Nos.:	Detected by Virtue of:
Lifted lead	Battelle E1	Excellent	38	Low thermal mass
Cloudy cold joint	Vanzetti G1	Very Good	39,40,41,42	Dullness
Dewetted joint	Battelle D2	Good	43	Low thermal mass
Granular surface	Battelle E2	Good	44	Increased absorption
Yellow flat top	Battelle D1	Good	45	Low absorption
Excessive heating	Battelle B2	Fair	46	Darkening
Insufficient solder	Battelle C1	Fair	47,48	Low thermal mass
Lead half off pad	Battelle E2	Random	49,50,51	Low thermal mass at overhang
Moveable joint	Battelle E1	Random	52	Change in thermal mass during heating or cooling.

each photograph was prepared only after it had been ascertained that the same heating/cooling trace was obtained on the oscilloscope several times during identical exposure conditions, with adequate target-cooling being allowed between exposures. These tests were to ensure that the laser power and pulse duration did not vary significantly between exposures and that the target surface did not change (such as due to possible laser overheating).

The last two items of Table 5 lists a different type of phenomenon which Vanzetti observed and which appears to be associated with lifted leads and other mechanical detachments. The phenomenon occurs as a discontinuity in either the heating or cooling rates or in both. Vanzetti interprets this as a thermal deformation of the lead or joint in which it changes its state of thermal contact, reversibly, with other parts of the joint. They have observed this phenomenon on several occasions, during one of which they verified a small amount of physical movement by observing changes in the speckle pattern of the helium-neon laser beam which is reflected from the target.

However, there is yet no evidence that a separated or cracked joint will exhibit such behavior reliably, and so they do not propose this as a primary detection method but rather as a support technique to verify the presence of a defect.

The physical processes which occur during laser-heating and which allow the identification of the above-listed defects are twofold:

(1) The surface absorptivity of the joint in question is different from that of a normal joint, resulting in a different heating rate and a different peak temperature; or

(2) The mass of material which is thermally connected to the target surface differs from that of a normal joint, also affecting the peak temperature.

Absorptivity variations allow distinguishing a good joint from one which is cloudy, granular or crystalline, discolored, or of highly reflective gold. In the former cases, higher peak temperatures are reached than normal; for gold, a lower peak temperature is reached.

In the case of thermal mass variations, normal joints heat more slowly than do detached leads, dewetted joints, joints with reduced solder mass, or the overhanging parts of misaligned leads.

Among other findings, Vanzetti confirms that there is a normal variation in peak temperatures which are reached by different normal joints and even at different points along the length of a given normal joint. These variations establish a tolerance band, outside of which it is possible to assert that a certain test joint is not normal. The variations among good joints are due to the amount of thermal mass, the absorptivity, and the angular inclination of the target point in question. The greater the variations which are observed, the wider must be the acceptance band and the less the sensitivity of the method. This matter will be treated more fully later in this report.

Figure 37 is an idealized drawing illustrating the general nature of these findings. Four bands of thermal signatures are depicted, with each band representing a family of curves which might result from a given type or group of solder-joint characteristics. For example, the uppermost band would include a range of thermal signatures for target areas with air-gaps or detachments directly underneath the joint, implying low thermal masses and rapid heating. Also included would be joints which were mechanically normal but which were darkened by contamination or by excessive heat.

The second band embraces the family of thermal curves resulting from dull or cloudy solder surfaces which generally characterize cold joints.

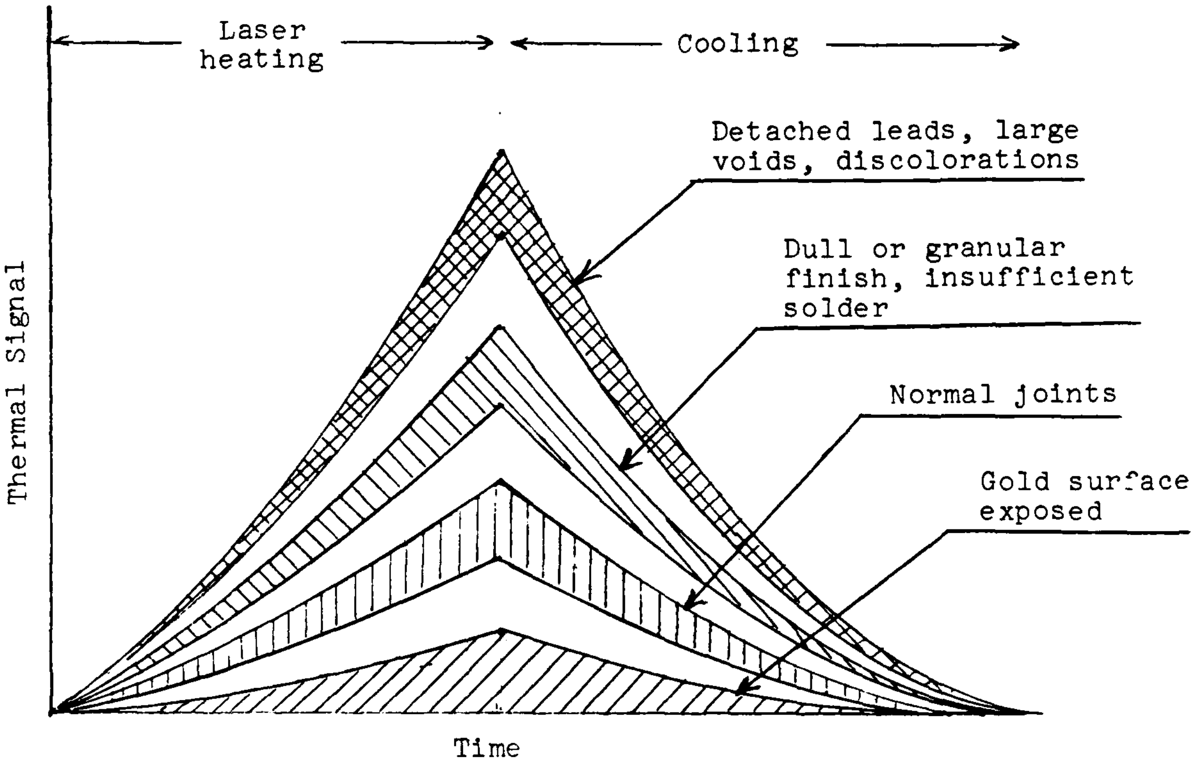

Figure 37. Thermal classification of various solder-joint defects, relative to normal joints. Hypothetical curves based on Phase 1 test results.

The third band includes the range of curves resulting from good solder joints containing normal variations in thermal mass or absorptivity, and the lowest band illustrates the curves obtained with exposed gold or "yellow flat top" leads.

Although the curves are depicted over their entire histories, generally speaking, only one point is of statistical interest on each curve, and that is the peak temperature value which is observed at the moment that the laser shutter closes.

Vanzetti qualifies this remark so as to acknowledge that, on occasion, some additional information may be obtained from the warmup or cooldown portions of the curve. This information appears in the form of a discontinuity in the heating or cooling rate which seems to signifiy physical movement in a lead which is partly detached form the joint. This movement is attributed to thermal warping of the lead and to a change in its state of mechanical contact with the underlying surface. This motion can occur during the warmup or cooldown or both, and it results in an abrupt change in the apparent thermal mass.

Joint Description and Detectability

The following descriptions develop further the information about the various types of defects which Vanzetti has identified.

Lead Detached from Joint

This type of defect includes the cases of fully detached leads, in which there is no electrical contact, and partly detached leads in which electrical contact is preserved but is of questionable reliability. Such defects are not likely to occur during manufacture, but they might occur with cold or other defective joints under mechanical and thermal cycling in the field and possibly during routine maintenance or repair, such as during removal of the conformal coating. As evidence of the latter, certain cold joints and tilted joints which were prepared as test samples in Phase 1 were inadvertently loosened during examination or cleaning.

As it happened, fully or partly detached leads were not intentionally provided. But, through observation, it was found that Leads Nos. 12 and 13 on Sample E1, which included examples of leads tipped on their pads, were indeed separated from the pads and allowed a piece of paper to be slipped underneath either a part or all of the lead. Laser/thermal tests revealed abnormally high peak temperatures on the detached parts of the leads. Figure 38 is illustrative of the type of behavior which was observed with suchjoints.

Cold Joints

A cold joint is defined as one in which the solder is not properly bonded to the workpiece. It is an unintentional event which can occur in several ways:

1. Soldering iron not fully heated, or not clean, resulting in insufficient solder temperature to permit bonding to metal;
2. Soldering iron used improperly in which the solder is heated but not the workpiece;
3. Joint was inadvertently moved during solder solidification.

Regardless of the method of formation, the joint is not as mechanically durable as a properly formed joint. Although it may show electrical continuity and some mechanical integrity, there is the risk that the joint will open up under thermal cycling or mechanical stress. Occasionally, a cold joint will exhibit an electrical resistance value of anywhere from a few ohms to many ohms, although most of them show less than a milliohm as does a normal joint.

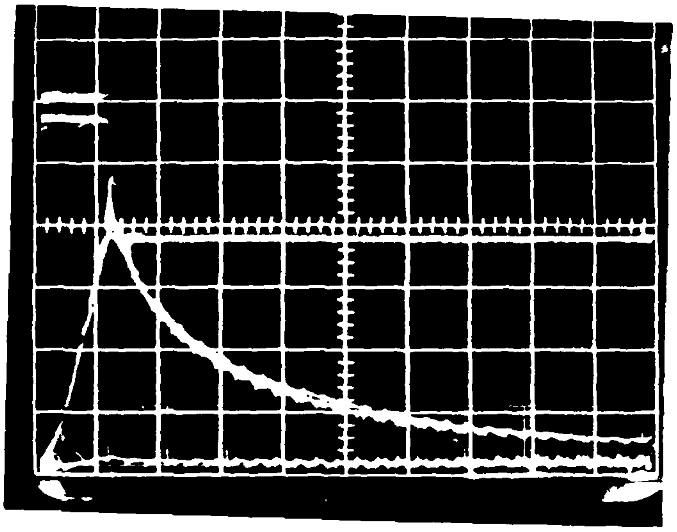

FIGURE 38. THERMAL PROFILE OF A DETACHED LEAD (UPPER TRACE) AND OF A NORMAL JOINT (TRACE CLOSE TO BASELINE).
V: 100. H: 50. E: approx. 50*.

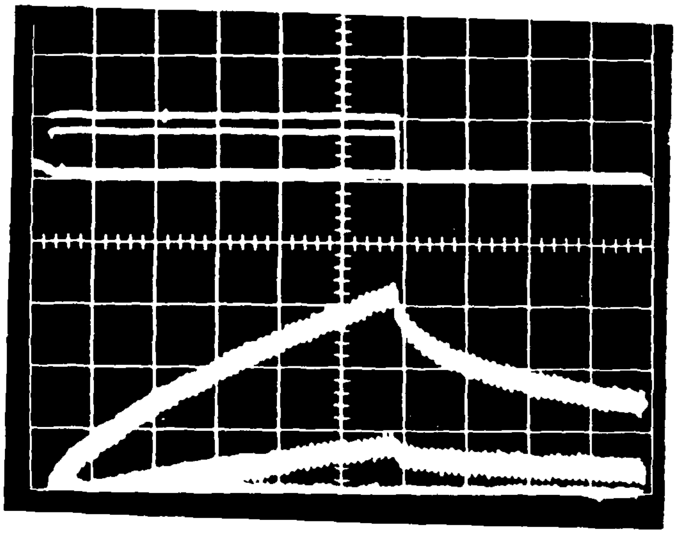

FIGURE 39: A VANZETTI-PREPARED COLD JOINT (UPPER) AND A NORMAL JOINT (LOWER)
V: 50. H: 100 uncal. E: approx. 900.

If a cold joint passes a resistance test, the only way in which it can be recognized visually is by its dull surface, if any. This is due to a granular or crystalline structure formed during solidification, which differs markedly from the shiny appearance of a properly formed joint. However, it is possible for a cold joint to appear shiny and thus to escape visual detection.

Vanzetti's tests included laser inspection of a number of cold-joint test samples which they prepared intentionally so as to appear dull. The microscopic peaks and valleys associated with the dullness serve to increase the effective surface area exposed to the laser beam. The valleys serve as "light traps", allowing multiple reflections to occur within them instead of single reflections as with a smooth surface. The absorption of laser-beam power will thus be greater, allowing more rapid heating and a higher peak temperature.

This is illustrated in Figures 39 through 42, in all of which the thermal signals are higher for the cold joints than for the normal ones. These data were obtained from a set of five cold joints and five normal joints prepared at the Vanzetti Company. The cold joints were prepared so as to appear cloudy. Other cold joint samples were furnished to Vanzetti by Battelle. These were prepared by physical movement of the leads while the solder was cooling, and may be presumed to be mechanically weak. However, the surfaces did not develop the cloudy texture which permits visible detection of such joints and Vanzetti was not able to identify them by laser/thermal means. Electrically, these samples show resistances of less than 0.001 ohm, and must be regarded as being in the rare category of cold joints which are not identifiable by electrical or optical tests.

Note that in all cases the laser pulse is quite long--150 to 900 milliseconds.

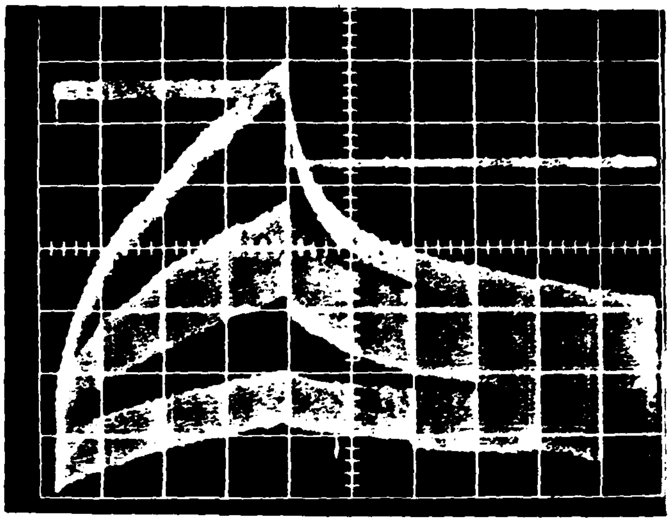

FIGURE 40. FIVE VANZETTI COLD JOINTS (UPPER TWO GROUPS OF TRACES) AND FIVE NORMAL JOINTS (LOWER GROUP).
V: 50. H: 200 uncal. E: approx. 600.

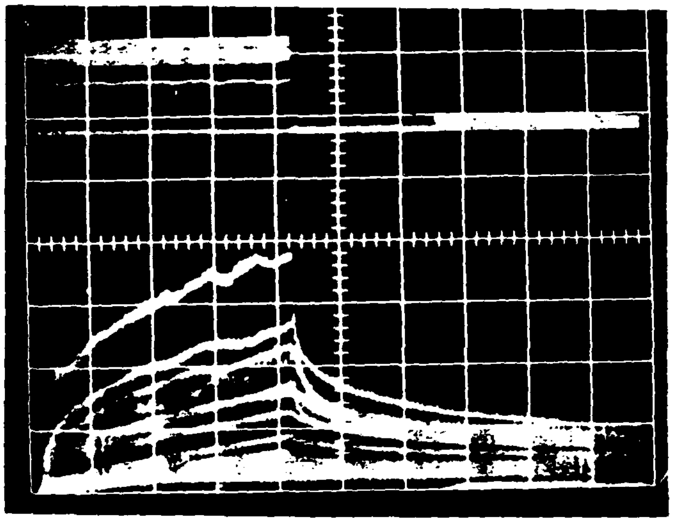

FIGURE 41: A REPEAT OF THE FIGURE 4 TESTS. FIVE COLD JOINTS (ABOVE FIRST DIVISION) AND FIVE NORMAL JOINTS (BELOW). DIFFERENCES FROM FIGURE 4 MAY BE DUE TO TARGET-POINT DIFFERENCES.
V: 100. H: 200. E: 850.

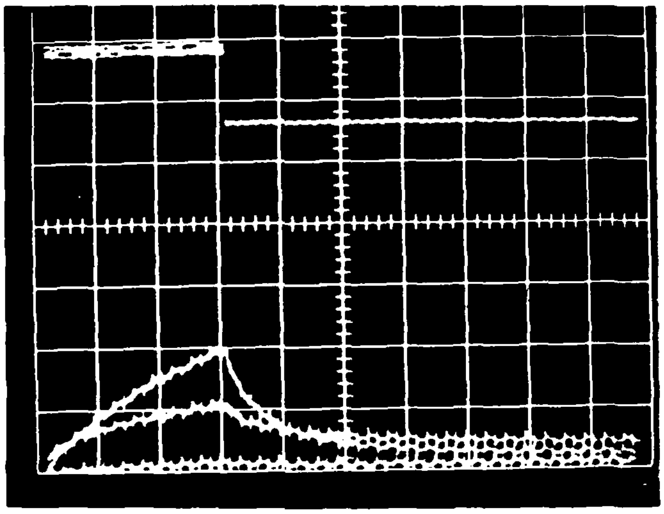

FIGURE 42. COLD JOINTS WITH SHORTER PULSE DURATIONS. TWO COLD JOINTS ARE SHOWN BY THE TWO UPPER TRACES. THE NEARLY FLAT TRACE REPRESENTS A NORMAL JOINT. 120-Hz "PICKUP" IS SEEN.
V: 100. H: 50. E: 150.

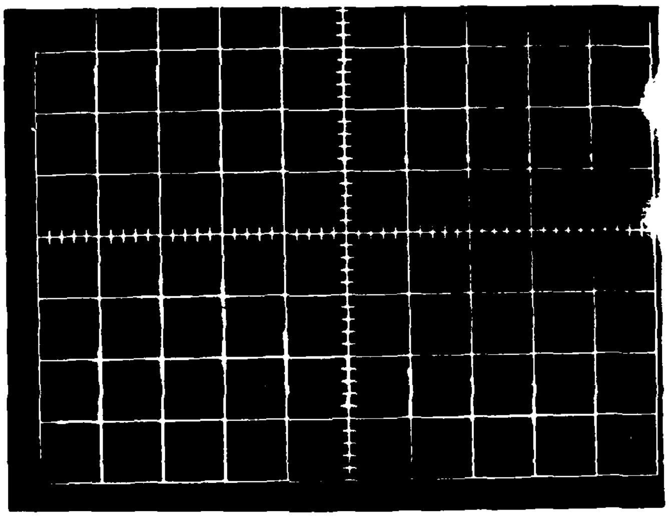

FIGURE 43. FIVE DEWETTED JOINTS (UPPER GROUP OF TRACES) AND TWO NORMAL ONES (LOWER GROUP).
V: 50. H: 500. E: 1,300.

Dewetted Joints

These are joints in which the solder did not properly wet either the lead or the pad or both, due to improper cleaning or to poor use of heat or of flux. As with a cold joint, this defect is associated with reduced mechanical strength.

From the standpoint of laser/thermal tests, the dewetted joint appears as a reduced thermal mass, possibly because of a poor thermal pathway from the lead to the joint or because less solder is present.

Vanzetti has tested the five dewetted joints on Battelle Sample No. D2 as well as the normal joints bordering them. The thermal signatures for all five dewetted joints were very similar (upper family of traces in Figure 43) and were visibly higher than the two normal curves (lower family).

Granular Surfaces

These are similar in appearance to cold joints and exhibit increased absorptivity for the same reasons. Typical test results on Battelle Sample No. E2 appear in Figure 44. The upper group of traces represents five thermal signatures for the granular joints; the lower curves are for their associated normal leads.

Exposed Gold

For the 1.06-um laser beam, the absorptivity of gold is markedly lower than for solder, as Vanzetti has shown through tests on the free part of a lead where it exits the IC, with the tinned part reaching a much higher peak temperature than the bare part. This result is directly applicable to the determination of whether or not a gold surface is exposed over much of the solder joint. In Figure 45 appears an upper trace representing a

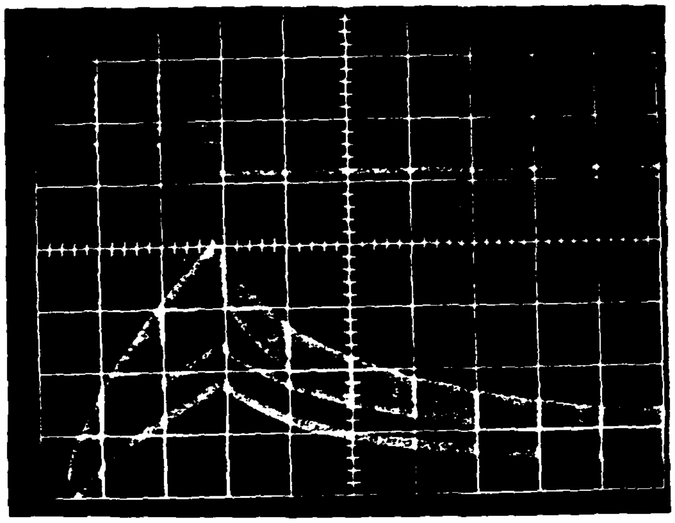

FIGURE 44. FIVE GRANULAR JOINTS (UPPER GROUP) AND TWO NORMAL ONES (TWO LOWER TRACES)
V: 50. H: 500. E: 1,300.

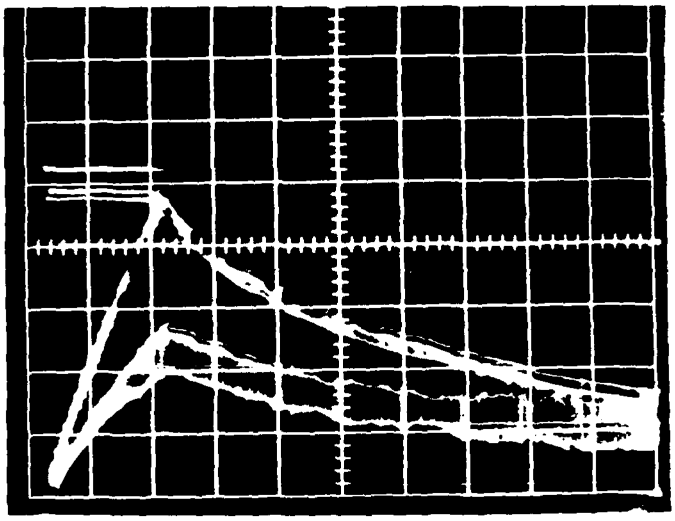

FIGURE 45. ONE NORMAL JOINT (UPPER AND THREE "YELLOW FLAT TOPS" (LOWER GROUP)
V: 20. H: 200. E: 300.

normal lead on Battelle Sample No. D1. Below it is a superposition of three traces from adjacent "yellow flat top of lead" examples on Sample D1.

Excessive Heat

If too much heat is used during joint formation, the bond between the pad and the substrate may be weakened and, also, discoloration of the joint may occur due to deposits of charred flux. In the latter case, a visible discoloration will most likely increase the surface absorptivity at the 1-μm laser wavelength as well as in the visible region, leading to high peak temperatures during exposure.

Battelle Sample B2 includes several joints which are visibly darkened. The thermal signature of one of these is shown in Figure 46, along with that of a normal joint; the two are readily distinguishable.

Insufficient Solder

Here, again, one expects a reduced thermal mass leading to higher peak temperatures.

Figure 47 shows unusually high discriminability between an "insufficient solder" joint and a normal one. This effect was largely repeatable at several locations along the joint and we are led to believe that some other effect is present, such as a poor thermal connection, although it is electrically intact. This is Joint No. 9 in Sample C1.

More typically, the detectability of this type of joint is illustrated by Figure 48.

Lead Half Off Pad

When the overhanging part of the lead serves as the target, high thermal signals would be expected because of reduced thermal mass. Else-

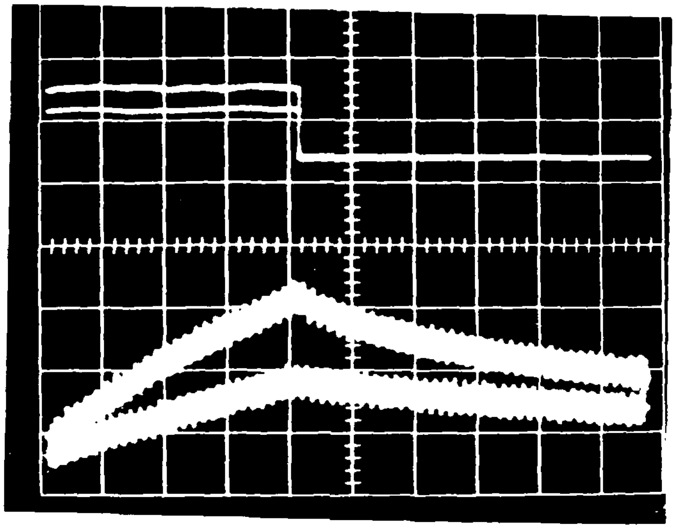

FIGURE 46. AN EXCESSIVELY HEATED JOINT (UPPER) AND A NORMAL ONE (LOWER). V: 50. H: 100. E: 400.

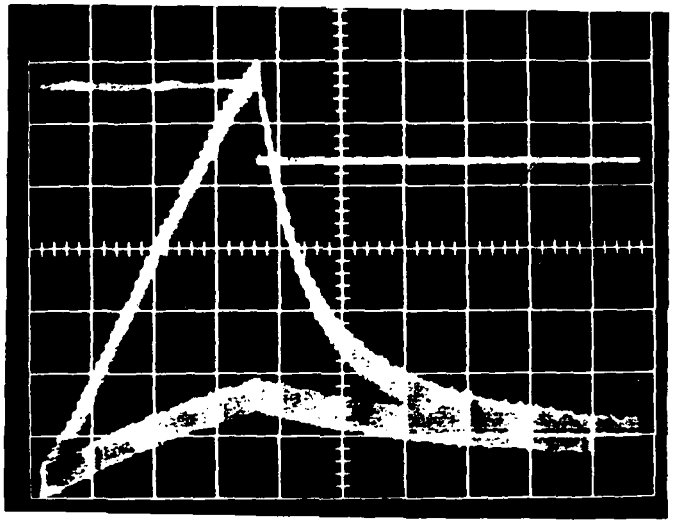

FIGURE 47. AN "INSUFFICIENT SOLDER" JOINT (UPPER) AND A NORMAL ONE (LOWER). ABNORMALLY HIGH DIFFERENCE MAY SIGNIFY A LEAD DETACHMENT (SAMPLE C1, LEAD NO.9). MORE NORMAL RESULT SHOWN IN FIGURE 2. V: 50. H: 200. E: 700.

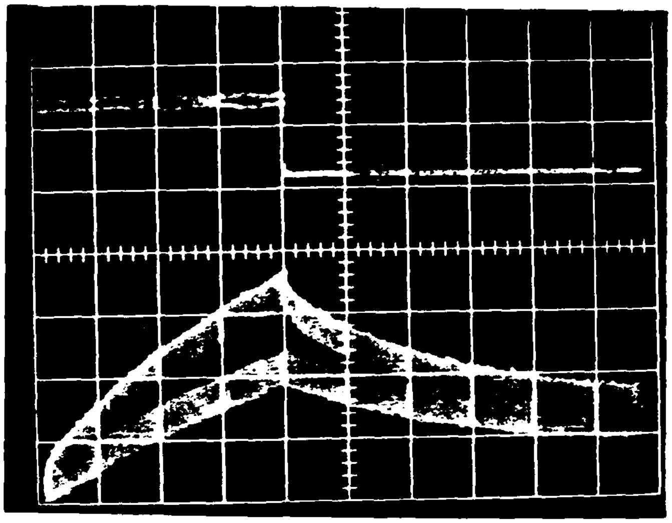

FIGURE 48. ANOTHER "INSUFFICIENT SOLDER" JOINT (NO. C1-11), UPPER TRACE) AND A NORMAL ONE (LOWER).
V: 50.

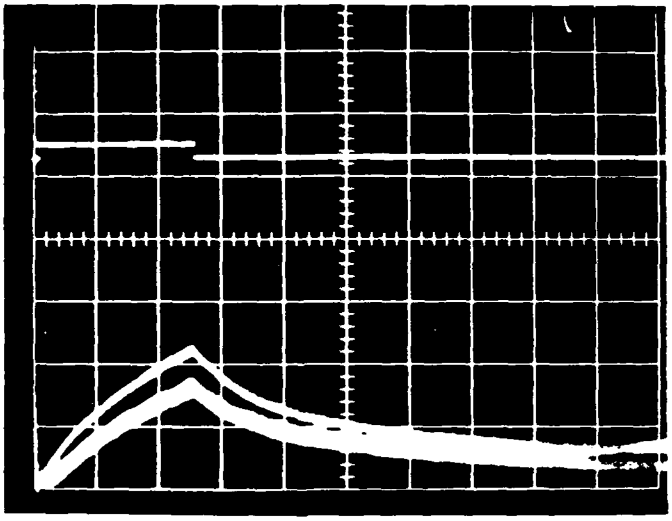

FIGURE 49. LEAD HALF OFF PAD (UPPER TRACE). LOWER GROUP IS TWO SUPERPOSED TRACES AT OTHER POINTS ON SAME JOINT. (UPPER TRACE IS FOR OVERHANG.)
V: 50. H: 500. E: 1,300.

where on the joint, the signals should be lower. This is borne out by Figures 49 and 50 representing two such joints. In both figures, the upper trace represents the overhang and the lower ones are from other parts of the defective joint (instead of from a normal joint).

An anomalous result, as yet unexplained, appears in Figure 51, where a normal joint (No. E2-1) serves as the reference. In this case, the reference trace is the upper one, and below it is the trace from an overhanging portion of Joint No. E2-2. The other normal joint, E2-7, showed a curve similar to the reference curve in the figure.

The laser/thermal technique which has been used in Phase 1 is not addressed specifically to the detection of overhanging leads. This is an accidental result of a decision to measure average effects over a joint and using a central point as the target. However, Figures 49 and 50 show that an overhanging lead is detectable by proper targeting (or by scanning), and an appropriate method could be implemented in Phase 2 is such if deemed desirable.

Moveable Joints

Figure 52 shows a typical example of a heating-rate discontinuity which is attributed to motion of the joint with a consequent change in apparent thermal mass. This is the case of Joint NO. E1-12, of the "lead tipped on pad" type which was found not to be connected to its pad. It is reasonable to speculate that the lead is barely in contact with the underlying solder and that, during warming, the upper surface expands more rapidly than the lower surface. This differential expansion would cause the lead end to bend downward, as would a thermostatic bimetallic strip, thereby causing the end to contact the solder which then reduces the heating rate.

One may speculate as to why the reverse of the process is not apparent in the cooling part of the cycle. However, the physics of the

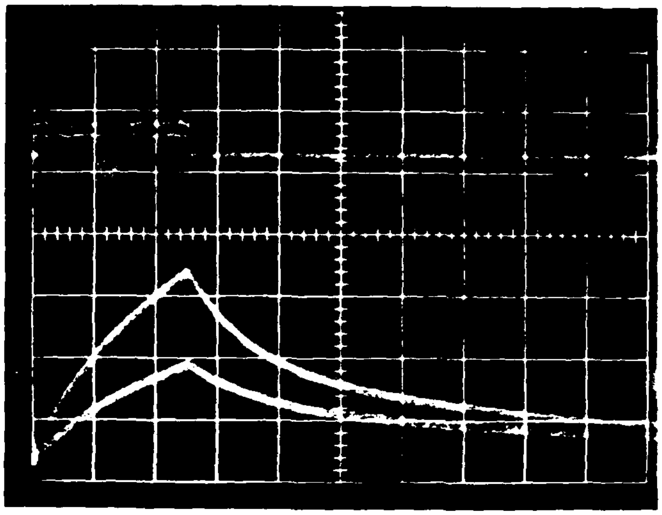

FIGURE 50. A DIFFERENT LEAD HALF OFF PAD. UPPER TRACE IS OVERHANG: LOWER IS AT ANOTHER POINT ON SAME JOINT.
V: 50. H: 500. E: 1,300.

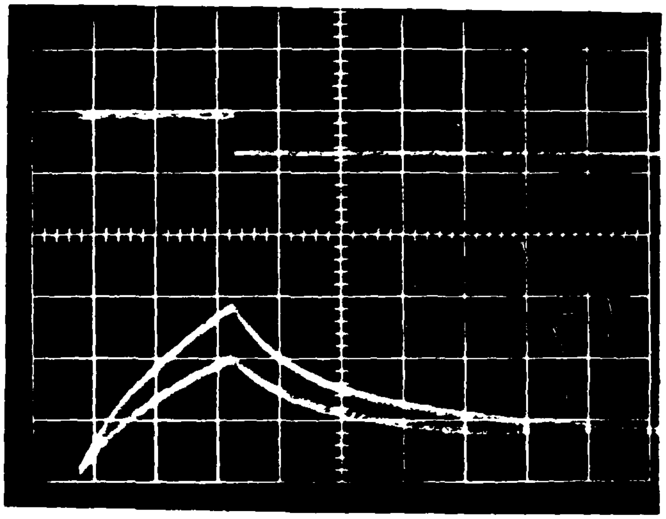

FIGURE 51. ANOMALOUS RESULT FOR LEAD HALF OFF PAD. UPPER TRACE IS A NORMAL JOINT (NO. E2-1). LOWER TRACE IS OVERHANG ON No. E2-2.
V: 50. H: 500. E: 1,300.

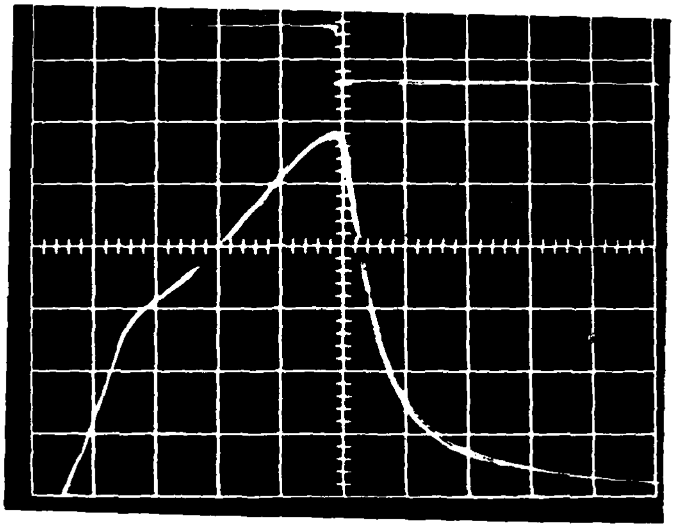

FIGURE 52. EXAMPLE OF HEATING-RATE DISCONTINUITY. DETACHED LEAD ON JOINT NO. E1-12. MOVEMENT OF LEAD DURING HEATING APPARENTLY CAUSES CHANGE IN THERMAL CONTACT WITH JOINT V: 200. H: 200. E: 970.

process does not require the reversal to occur at the same thermal signal level, for the heating and cooling processes as seen at the target surface are not the reverse of each other (note the much higher cooling rate). It is likely that the temporary contact persists until after the target surface has cooled.

Discussion

This section treats a few miscellaneous questions which have been recognized during this study.

Non-Detectable Defects

At the outset of the study, it was recognized that certain types of solder-joint defects were more readily detectable by means other than the proposed thermal method. It was not surprising, then when the tests failed to detect such defects as "toe of lead bent up", "irregular spreading", "no fillet at heel", and certain others.

However, it was believed that certain other types of defects would provide more definitive test results than they have so far. Prominent among these is "voids in solder", a type of joint which had been detected successfully, in scaled-up form, using tungsten-lamp heating. The ability to detect "holes and pits" (by virtue of increased absorptivity) also was expected; "excess solder" because of increased thermal mass, "inclusions" causing reduced thermal conductivity (depending upon the material), and possibly "cracks at heel" if a detachment were involved.

At present, such flaws have not been detected. The experimental work will continue for a time after this report is completed and any significant findings will be reported in a supplemental letter.

Laser Pulse Stability

In the oscillograms shown earlier, a square-pulse oscilloscope trace will be noticed in the upper part of each photograph. This is the unprocessed signal from a silicon photodetector which was used for measuring pulse duration, pulse-power uniformity, and for triggering the oscilloscope sweep. The detector was mounted so as to receive Nd:YAG laser radiation reflected from the target surface.

One of the questions which was of concern early in the program involved the constancy of laser power from pulse to pulse as well as the repeatability of the electronic shutter which produced the pulses. The experience gained during the program has been that there are no significant fluctuations in either of these characteristics over the short term, that is, during a pulse or between pulses within a period of a few hours. Over the long term (several hundred hours), a gradual decline is expected in output power from this type of laser during normal aging of the tungsten-filament pump lamps, which are easily replaceable.

Those oscillograms which display multiple thermal traces also include multiple pulse traces from the silicon detector. In some cases the pulse heights are seen to vary from pulse to pulse. This is indicative of reflectivity differences among the surfaces being probed. The differences are especially noticeable in Figure 44.

Pulse Duration and its Effects

Short laser pulses are desirable in order to maximize the throughput of the final system, and the results suggest that effective fault-detection can be accomplished with pulse durations on the order of 50 milliseconds if sufficient laser power is used. (Excess power and shorter pulses may damage the joints).

The Sylvania Model 607 laser in use at Vanzetti is rated for an eight-watt output when the lamps are new and when the system is operated at a full 240 VAC line voltage. For several reasons, Vanzetti elected to operate the laser at lower voltages, with outputs in the three to five-watt range, and to use correspondingly longer pulses. The main reason for this was to prevent damage to the Battelle solder-joint samples before testing had been completed. Earlier tests, showed that a solder surface could be discolored if part of the laser beam extended into the substrate region. The G-10 material is easily burned by an intense laser beam, and its combustion products settle on nearby solder surfaces from which they are not easily removed.

A second reason for operating at reduced power was to conserve lamp life and shutter life, and to reduce any risk of premature laser failure stemming from operation at maximum power.

When the final experiments are nearly concluded, the laser will be restored to maximum power for some thermal-signal vs. pulseduration tests, to be compared with present test results.

During the present work, the pulse durations ranged from 50 milliseconds (Figure 38) to well over one second. Also note that the heating curves for normal and for faulty joints continue to diverge in the pulse-duration ranges which have been used. That is, they do not level off within these ranges and, as yet, a maximum pulse length beyond which no further change occurs has not been identified.

In the cases of some types of defects, it is clear that shorter pulses might have been used, as in Figure 38. However, this would reduce the detectability of the more difficult defects, depending upon those types which are held to be important. This latter decision and its consequences regarding choice of pulse duration are appropriately left for Phase 2.

Some improvement in detectability will result when steps are taken to improve the amplifier system which processes the indium antimonide detector signal. In the experimental setup, the amplifier and its interconnections are subject to stray electrical noise. With improved shielding and filtering, the noise can be reduced, permitting the detection of smaller thermal-signal differences and allowing shorter pulse lengths to be used.

Variations Along a Joint

Figure 53 is a multiple-exposure (repeated trace) oscillogram in which a fixed point on a normal joint was repeatedly exposed to identical laser pulses, with cooling between. These and similar tests have revealed no observable differences in the peak thermal signals which were obtained under such circumstances.

However, a different situation prevails in Figure 54. Here the heating spot has been moved randomly along the same lead to various target points, and the differences among thermal signals are clearly seen.

Visual inspection of this lead (No. A1-14) and similar ones reveals variations in solder thickness along the length, as well as in topography. The latter item is important because the inclination of the localized target area can affect the amount of laser radiation which is absorbed.

The discussion is continued in the following sub-section.

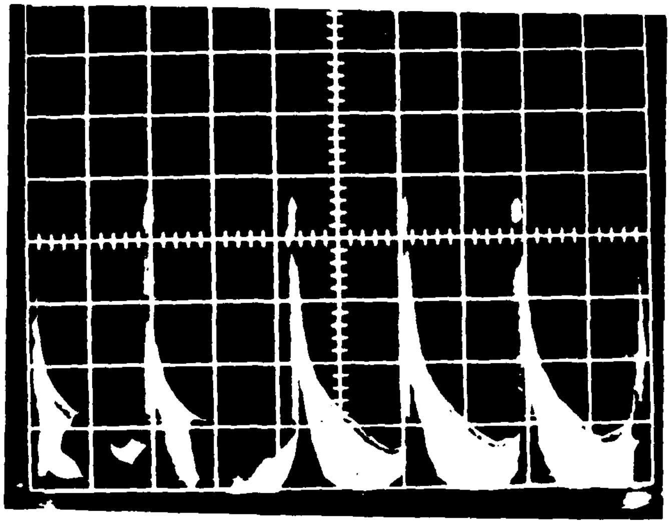

FIGURE 53. REPEATABILITY OF PEAK THERMAL SIGNAL AT FIXED POINT ON A JOINT. MULTIPLE EXPOSURES WITH 10-SECONDS OF
V: 20. H: 5,000 E: 240.

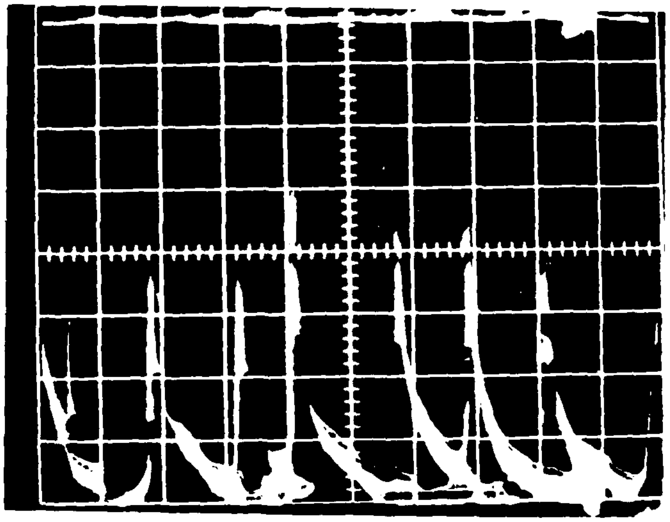

FIGURE 54. VARIABILITY OF THERMAL SIGNAL AT DIFFERENT POINTS ON THE SAME JOINT. TWELVE SECONDS OF COOLING BETWEEN.
V: 50. H: 5,000. E: 500.

Variations Among Joints

Figure 55 is illustrative of several test exposures performed on various normal joints on the Battelle test board. It indicates the same type of variation observed at different points on the same test joint, although it is shown on a different time scale. The joint-to-joint and place-to-place variability is not an unexpected result, considering the thermal-mass and absorptivity variations associated with normal joints.

To place this phenomenon on a quantitative basis, the peak thermal signals on 14 normal joints on the battelle board have been measured using 500 mSec pules. The peak signals ranged from 90 to 250 mV, with an average of 139 mV and with a standard deviation of 40.3 mV.

The question arises as to whether a normalizing procedure can be applied to the test data, using heating-rate and/or cooling-rate information, in order to reduce the variable results to a narrower range of numerical values which will characterize a normal joint. For example, if the heating or cooling curves for all normal joints showed a common rate-characteristic, regardless of peak temperature, then a single number could be used to identify a normal joint, making it more easily distinguishable from a defective joint.

The first attempts to do this have not been successful. By use of scaling factors, Vanzetti attempted to reduce the heating/cooling curves for various normal-joint target areas to a single curve, but they are not satisfied with the "fit" of the results. An example of the calculational results is given in Figure 56. Further scaling efforts will continue through the end of Phase 1 and, if necessary, into Phase 2.

Effects of Absorptivity

As seen in this report, the laser/thermal method is highly sensitive to absorptivity differences among surfaces, allowing discrimina-

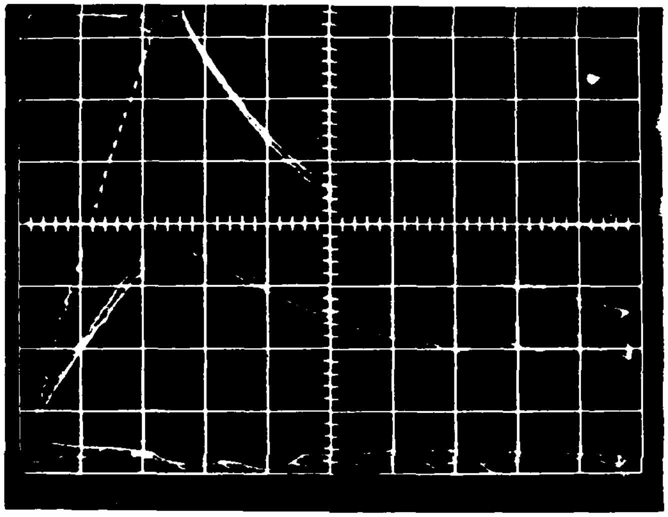

FIGURE 55. VARIABILITY AT CENTERS OF TWO NORMAL JOINTS (E1-9 and EL-14).
V: 20. H: 200. E: 500.

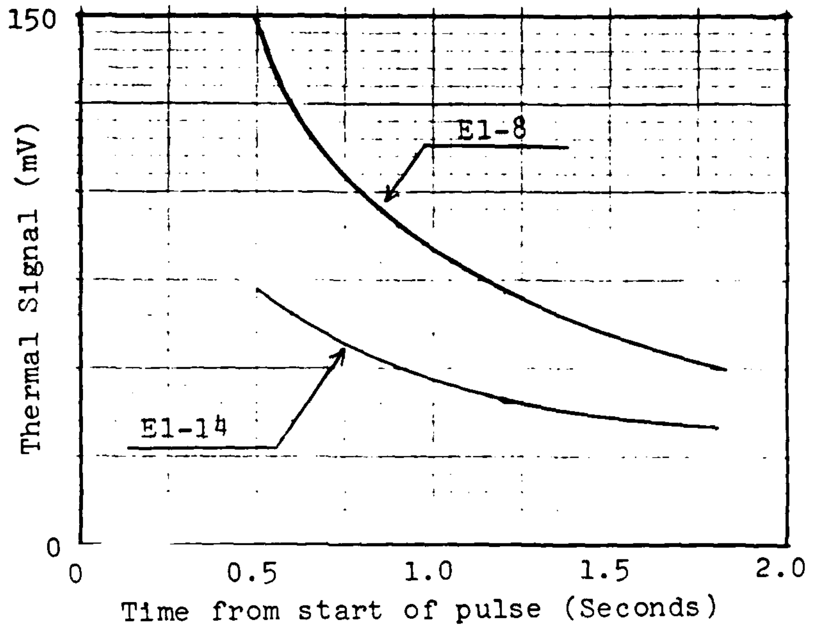

BEFORE NORMALIZATION

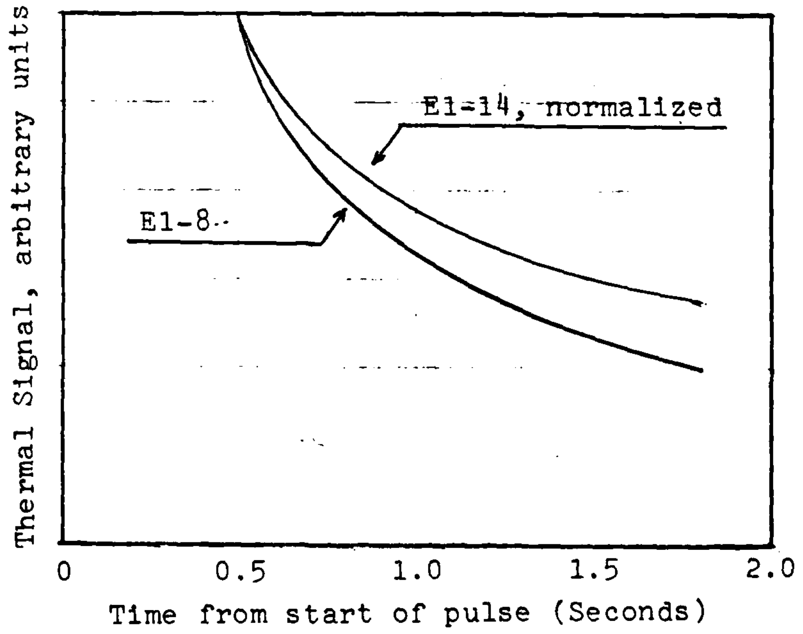

AFTER NORMALIZATION

Figure 56. Early attempt to normalize cooling curves of Figure 19.

tion between normal, dull or discolored, and exposed gold surfaces. This feature can be a detriment in the case of unwanted variations among samples, such as due to tarnish or other coatings of foreign materials. Indeed, even with clean joints there are observed absorptivity differences among normal joints on different circuit boards including the Battelle test board, some earlier Battelle samples, and the board furnished by McClellan AFB after removal of the conformal coating. The variations appear due to the age of the solder joint and are possibly due to variations in solder composition. Therefore, newly prepared joints on an old board undergoing maintenance may yield thermal signatures different from those of the old joints. These normal variations are unavoidable and will have to be taken into account.

What is avoidable, however, is surface contamination, and it is important that joints undergoing laser/thermal tests should be protected as much as is practical from foreign deposits beforehand.

Figure 57 emphasizes the difference in thermal signatures obtainable from lighter and darker surfaces. Two "virgin" pads were used on an early Battelle sample board. These were soldered pads without leads attached and were presumably identical. The lower trace represents a normal, shiny pad while the upper one resulted from an adjoining pad which had been darkened with marking ink. A three-to-one ratio is seen in the peak thermal values.

The purpose of this and similar tests was an attempt to normalize these pairs of curves, as in the previous case, in order to cancel the effects of absorptivity variations. Figure 58 depicts an early attempt to to so, without positive results. This effort will continue.

It should be noted that the effects of surface-absorption variations are enhanced by this method of heating and monitoring the surface by radiant means. The absorption phenomenon plays a double role, first in the

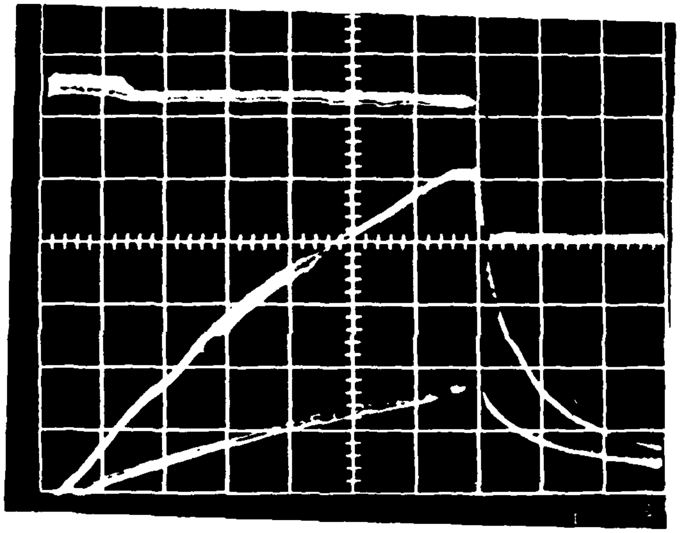

FIGURE 57. AN INK-BLACKENED (UPPER) AND A SHINY (LOWER) VIRGIN SOLDER PAD.
V: 2,000. H: 500. E. 3,500.

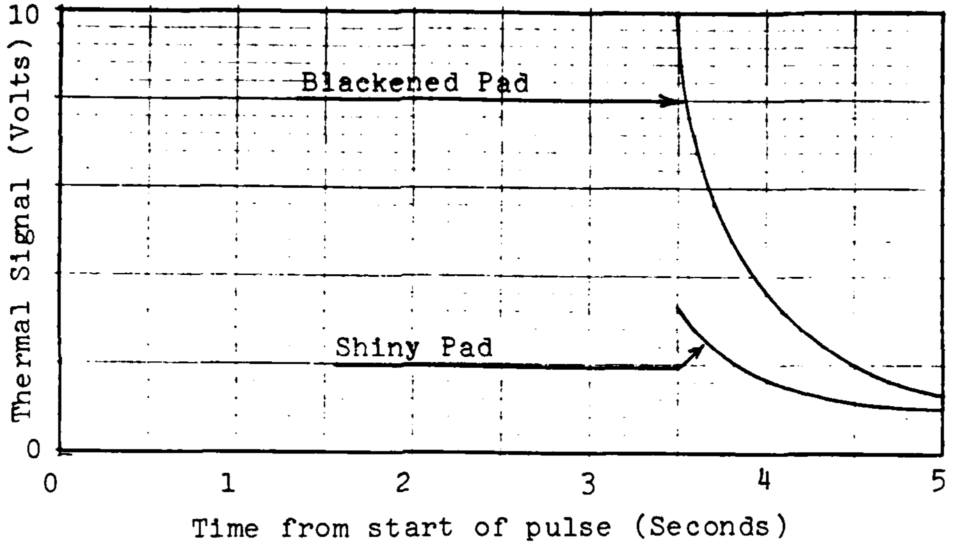

BEFORE NORMALIZATION

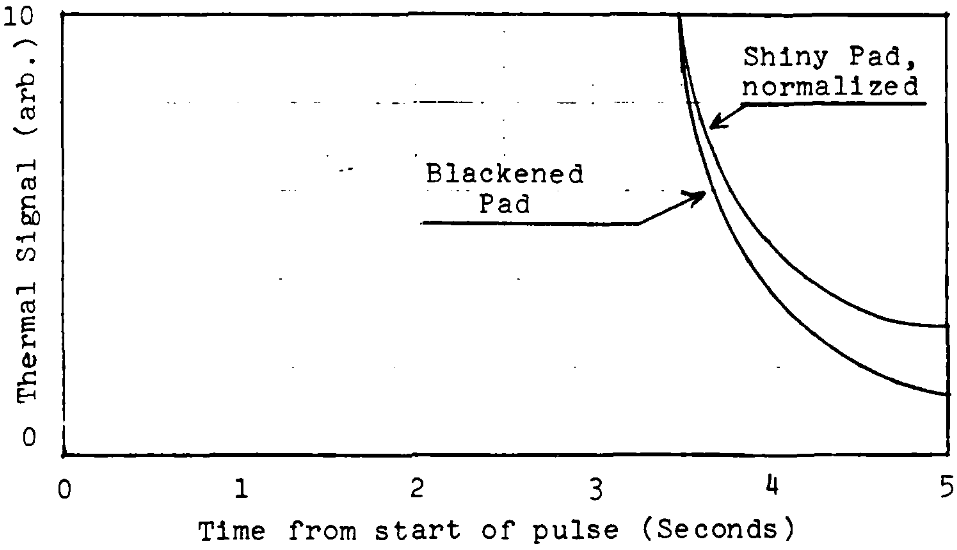

AFTER NORMALIZATION

FIGURE 58. EARLY ATTEMPT TO NORMALIZE COOLING CURVES OF FIGURE 57

form of absorptivity which influences the rate of temperature rise in the sample, and then in the form of emissivity (which is numerically equivalent to absorptivity) which determines the infrared radiation intensity for a given temperature. Thus, in principle, a 20%-absorbing laser-heated surface should provide an infrared signal which is four times greater than that from a 10%-absorbing surface. (In practice, this is not exactly the case, because of other physical phenomena which enter.)

The Micro-Reflectometer

Unless the absorptivity variations among good joints can be normalized, some other means will have to be used to account for them. In anticipation of this, Vanzetti initiated a micro-reflectometer development early in Phase 1. It includes a hemispherical illuminator so designed as to provide uniform irradiation of the sample from all directions in order to eliminate shadowing. The sensor is a specially adapted Vanzetti lens cell and fiber optics combination used with a standard Thermal Monitor. The lens cell is designed to provide a 0.010"diameter target disc at a five-inch working distance. Special straylight baffles within the cell ensure high optical definition. The optical detector operates in the 1 to 1.5 micrometer wavelength region.

Vanzetti is not completely satisfied with the angular uniformity of the radiation provided by the illuminator. Slight shadow areas at steep edges are held responsible for some variability in their test results. A redesign of the illuminator is being considered. This work will continue.

Automatic Sample Centering and Surface Characterization

A helium-neon (HeNe) laser is used as a visible-light pointer so that:

(1) The INSPECT optical axis may be aligned with a heated fine-wire target which is centered in the HeNe focal spot;

(2) The Nd:YAG beam may be centered on the same axis; and

(3) The desired part of the solder joint under test may be aligned precisely with all three optical axes.

In addition, Dr. Traub of Vanzetti has observed that the HeNe beam may serve two other useful purposes in a future system design. Both would make use of the reflected light-beam pattern which results when the laser beam strikes a solder surface. The methods would also use photodetector arrays, either linear or rectangular, in conjunction with microprocessing, in order to

(4) Notify the X,Y-positioning controller when the test lead was centered on the optical axes. This would accommodate leads which were decentered or tilted on their pads

(5) Allow one to derive topographic information about the surface features of the test joint, in support of the other tests. By this means, one could distinguish between a smooth, shiny joint, a dull one, a joint with solder peaks, and so forth.

During Phase 1 visual observations were made of the reflected HeNe pattern and a correlation was observed between certain distinctive patterns with smooth joints, others with rough or contoured joints, and so forth. Also, Vanzetti could find, by this means, when the ridge of the test joint was centered on the optical axes.

Figure 59 illustrates just a few of the patterns which have been observed and whose distinctive properties are well correlated with certain features of the reflecting surface. Included here are patterns representing centered and de-centered flat portions of a joint, a random pattern typical of a surface irregularity, and a horizontal arc characteristic of a smooth, cylindrical solder mound.

Vertical prominence characterizes flat solder joint surface centered on HeNe axis.

Same flat surface but off center.

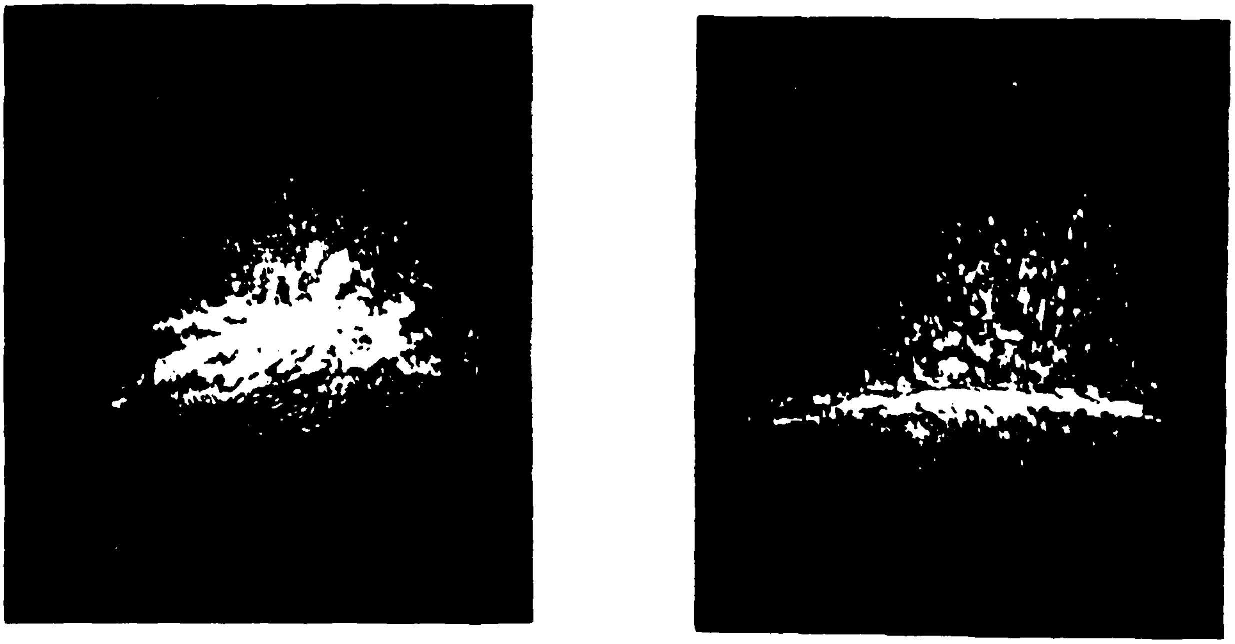

Random pattern results from irregular solder mound.

Cylindrical contour of virgin solder pad yields characteristic horizontal arc.

FIGURE 59. DISTINCTIVE REFLECTION PATTERNS OF HeNe LASER BEAM FROM VARIOUS SOLDER SURFACES.

Continued Efforts

This portion of the Final Report was prepared while the experimental effort was still in progress, and the work will continue to the end of the contract period. New findings, if significant, will be reported to Sacramento ALC by supplemental letter. Following are the continuing tasks which will receive further attention during the last few weeks of the Phase 1 period.

(1) Re-design and fabrication of micro-reflectometer;

(2) Measurement of solder-joint reflectance values and variations therein;

(3) Measurement of the present Nd:YAG-beam focal spot profile;

(4) Elongation of the focal spot to an elliptical configuration, in order to average the test data over the length of the joint

(5) Motor-driven scanning of the circular focal spot along the length of the joint to derive a position-dependent thermal profile

(6) Reduction of pulse durations by increasing the laser power density;

(7) Attempting to normalize the thermal signature variations among normal joints;

(8) Attempting, by normalizing, to cancel the effects of absorptivity differences;

(9) Improvements in the InSb amplifier to reduce noise and, thus, to increase the thermal signal-to-noise ratio in order to shorten the laser pulses.

Technical Discussion

In this section, certain other descriptive information and commentary are discussed to augment the previous information under "Test Results".

Description of Test Arrangement

The bench-top laser/thermal test system has arrived at the configuration shown in Figures 60 and 61 through a continuing series of mechanical, optical and electrical improvements, aimed at better performance.

The principal elements of the system are the two lasers with their shuttering system, the X,Y-positioning table, the INSPECT detection system, and associated optics, mechanics and electronics. The main components are identified in Table 6.

The lens presently being used for focusing the laser beams is an 18-mm diameter by 50 mm focal length airspaced achromat, whose focal length is expected to be somewhat greater than 50 mm at 1.06 μm There is some arbitrariness in the choice of lens focal length. The present choice provides a (nominally) 0.020"-diameter Nd:YAG spot at a two-inch working distance, with most of the heating occurring in the central 0.010" to 0.015" zone. A shorter focal length would provide a smaller spot but at a shorter working distance, and conversely. The 18-mm diameter is unnecessarily large, for the lens need be only slightly greater than about 4 mm to receive the radiation from the Model 607 laser.

The lens and its associated folding mirror are mounted on a 3-axis micro-manipulator manufactured by Line Tool Co.

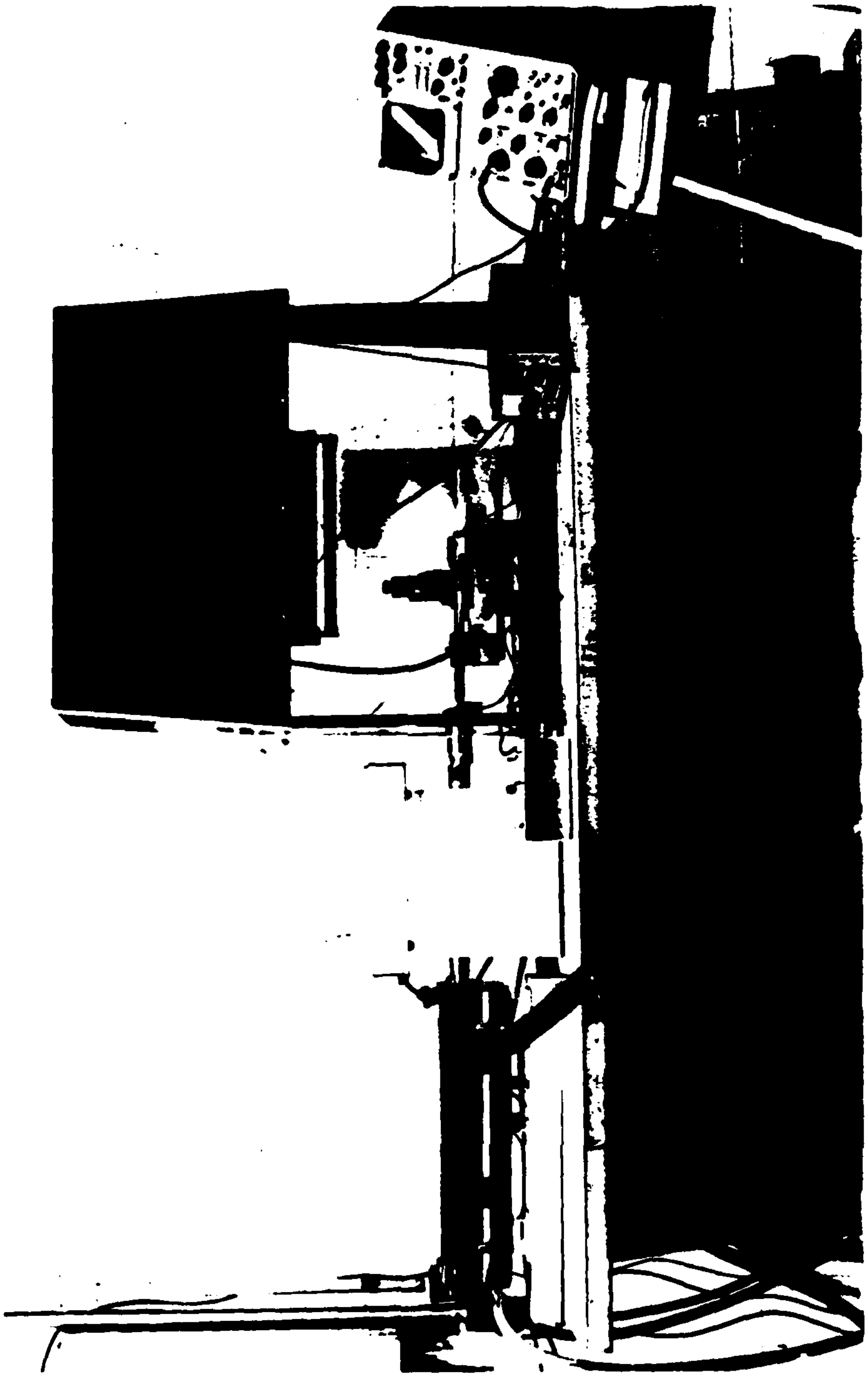

FIGURE 60. PRESENT STATE OF LASER/THERMAL EXPERIMENTAL ARRANGEMENT.

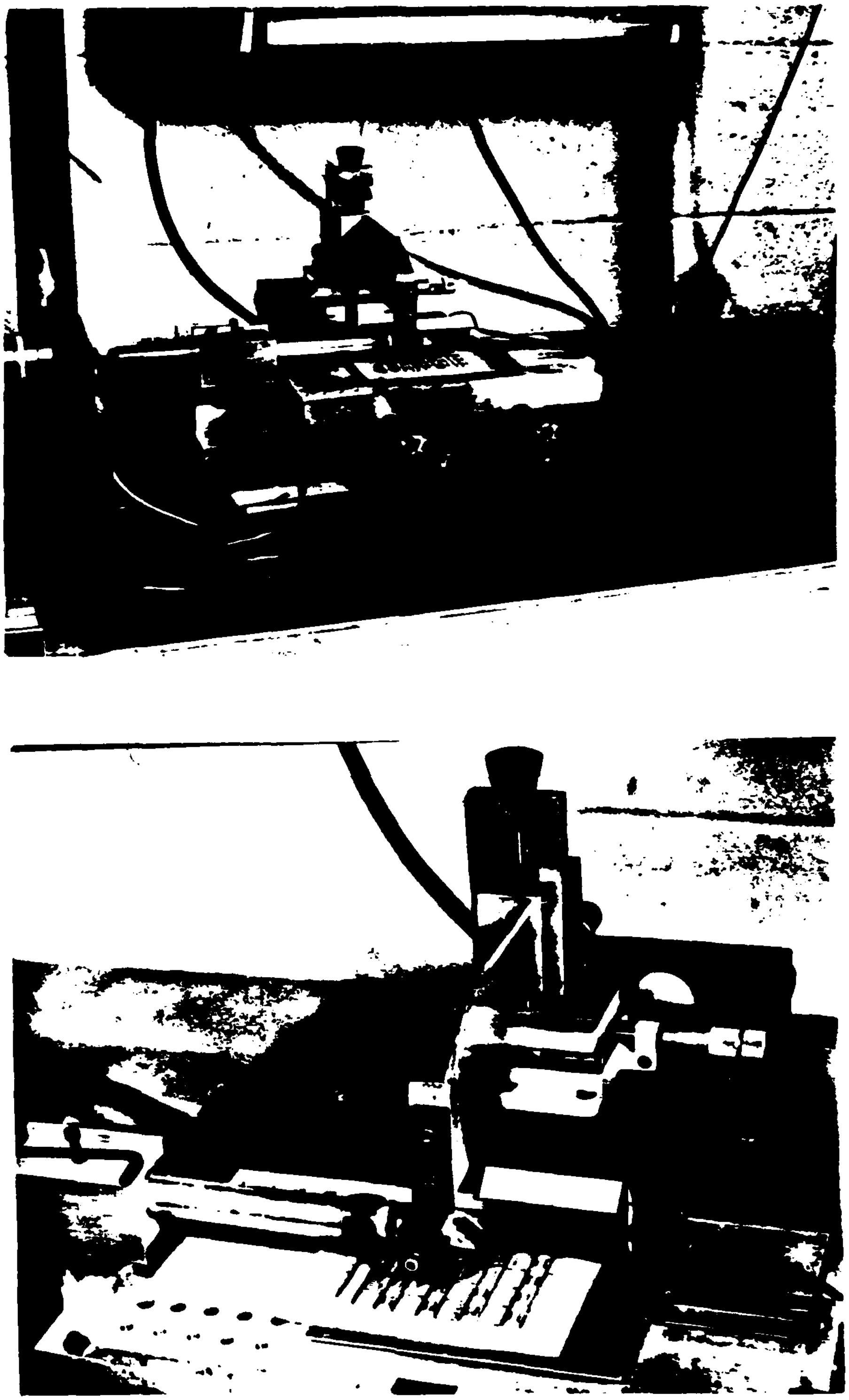

FIGURE 61. TWO VIEWS OF TARGET AREA IN LASER/THERMAL TEST SYSTEM

TABLE 6. MAIN COMPONENTS OF LASER/IR SYSTEM

Item	Purpose	Description
8-watt Nd:YAG laser	Target heating	Sylvania Model 607 1.06-μm, CW, optically pumped
0.0005-watt HeNe laser	Optical pointer, surface-pattern characterization	Spectra-Physics Model 155, 0.6328 μm
Electronic shutter	Laser-beam exposure control	Vincent Associates Model 26L2A1X5 UNIBLITZ
Electronic shutter control	Exposure duration control	Pulse generator, variable, Vanzetti special design
Manual, X,Y-positioner	Locating sample	Vanzetti Part No. 1002D1400
Indium antimonide detector	Thermal	Vanzetti Part No. 1002A1087, Judson Research, photovoltaic, in D05S dewar, D* (500, 900, 1) = 2.3 x 10^{10} 1 μSec maximum, 0.004" x 0.004" sensitive area
INSPECT collecting mirror	Infrared imaging	8" diameter x 8" focal length paraboloid, aluminized and over-coated

Targeting Considerations

At the start of the tests, several options were open with regard to where, on the sample, the laser power was to be injected and at which point the infrared radiation should be monitored. The original concept was to apply heating at one end of the joint and to observe the infrared signal at the other end. Alternatively, the gold-plated lead itself, before it enters the solder mass, might serve as either the power input or output point. Using these methods, one could observe the heat-transfer capability of each joint.

As it happened, it was found to be more effective to apply the heating and to monitor the infrared at the same point. In this way, one would be measuring the amount of thermal mass in contact with the sample surface, while gaining the advantage of achieving higher thermal signals and in shorter time intervals.

Early experiments with the laser verified that this method would eliminate heat-transfer delays and radiative power losses which would be incurred if the injected heat had to flow to a remote monitoring point. This, then, was the method used in the subsequent tests.

Choice of Laser

At the start of the program, three basic laser types were considered for use in the program, all being in the required power-rating range, of the continuous-output type, and being commercially developed types which have been in wide use for many years:

- Argon-ion, emitting in the blue-green region of the visible spectrum;
- Nd:YAG at 1.06 μm in the near infrared; and
- Carbon dioxide at 10.6 μm in the far infrared.

The principal concern in the choice of laser, was that of its wavelength region. It is known that the absorptivity of most metals becomes less at greater infrared wavelengths, so that it would require a mugh higher powered carbon dioxide laser, for example, to provide the same heating as a lower powered argon laser. In the case of electrolytic gold, for example, handbook data indicate an absorptivity of 53% in the blue-green region, less than 5% at 1 μm and less than 2% at 10. Unfortunately, limited such data are available for solder but we expect the same trend to prevail, as it does with most other metals.

We therefore chose a middle course and selected the Nd:YAG laser for the tests. The final choice of laser for the operational system will be made in Phase 2 pending spectroanalytical tests on samples of all materials involved.

Projected System Performance

Following are brief discussions of a few items regarding the expected performance of the final laser/IR system. Reliable predictions about system accuracy, system cost, system failure probabilities, and so forth, are not yet possible because not enough statistical testing information is yet available to permit this. However, a few informed deductions can be made about the likelihoods of detecting certain types of defects. The deductions are based on the firsthand experience with the breadboard system, on the array of samples which have been tested thus far, and on the test conditions which have been used.

The detection probability of the target-portion of a tinned lead that is detached from the underlying surface, will be extremely high, perhaps 99% or greater. However, this value must be modified if the upper or lower surface carries an appreciable solder mass, or if the target area is untinned gold, or for other causes not yet known to us.

In the successful detection of cold solder joints, the peak thermal signals observed, in the best case, are 70% higher than that for a normal joint and, in the worst case, about 20% higher. Intuitively, approximately 75% to 90% of dull or granular surfaces will be reliably detected by this method, depending upon the degree of dullness and upon the amount of variability found in normal joints. The detection probability can be increased if the detection threshold is adjusted so that an occasional normal joint is declared to be faulty.

The detectability of exposed-gold leads will be quite good provided that the gold fills the target area. A detection probability between 70% and 90% is estimated depending upon other variables.

Dewetted or *unwetted joints,* probably will be identified as faulty at least half of the time as will insufficient solder. These are conservative estimates, based on the limited number of samples which have been tested. "Excessive heating" joints which exhibit discoloration are expected also to be more than 50% detectable, again a conservative estimate.

Conclusions and Recommendations

The laser/thermal program was originally proposed by the Vanzetti Company as a means of identifying solder joints containing a limited number of defect-types such as voids and discontinuities. As often happens, certain unanticipated findings are made when the program is actually carried out. In the case of solder joints containing voids, there is some disappointment in not yet having identified those in the Battelle-furnished samples. However, the geometric configuration of the voids in the sample joints would make them difficult to detect. This, coupled with the single-spot heat and detect technique are mutually exclusive of optimum results. We are confident, based on our earlier tests on larger samples, that the principle of laser/thermal void detection is valid although some modifications will be necessary to enhance detectability.

It was rewarding to discover that surface-absorptivity variations, as indicators of questionable joints, are readily detectable by this method. This opens up the possibility of detecting several more types of defect than had been anticipated.

There are some areas that are recommended for further study:

- How "real" are the variations among normal joints which were found in the test samples, and can their effects be suppressed by data processing or by re-shaping of the laser beam spot?
- Can the reflected HeNe laser beam be used with a photodetector array in order to center a misaligned lead on axis? Would useful topographic information also be provided by this technique?
- Would useful information be provided if a laser/thermal scan were made along the length of the joint, as was recently suggested by Battelle? Also, would new information result if an infrared vidicon image of the entire heated joint were to be digitized and processed by computer?

MICROVIDEO STUDY

As stated in the Background discussion, the current method of solder joint inspection is primarily visual. Furthermore, the inspection of solder joints cannot, at least not as yet, be completely freed of the need for visual techniques. There may be certain types of solder joints for which neither the laser/IR nor the ultrasonic technique will provide a definitive test. Therefore, whenever either of these techniques detects solder joints they cannot expressly designate as "bad" or good", those joints will be subjected to a visual examination.

A closed-circuit television, CCTV (color) system is expected to be used as the final inspection of the solder joints identified as questionable by either the laser/IR or ultrasonic technique. The CCTV would be keyed to the mounting stage of the TIS for rapid access to the location of the questionable joints. It is intended that the CCTV would consist of a multilens color subsystem that would permit simultaneous viewing of all visible parts of a solder joint at sufficient magnification to provide good resolution. The display would be either a separate 12-inch color monitor for each lens or a single 25-inch color monitor used in a split-screen mode. In the latter case, there would be the option of using the picture from any of the lenses as a full screen display. This visual system also can be used to inspect the non-lap-type joints on the PCB thus making the TIS a full inspection station for all solder joints.

Battelle has used the CIRCON Corporation, a leader in CCTV inspection, as a technical consultant during this Phase I program. They have shown that a multilens CCTV is a useable tool in a demonstration for BCL and SM/ALC at CIRCON. Further, their color TV camera is the smallest currently on the market and would be the easiest physically to incorporate into the TIS. Therefore, Battelle expects to use the CIRCON equipment as the basis for the visual portion of the TIS.

CONCLUSIONS AND RECOMMENDATIONS

GENERAL CONCLUSION AND RECOMMENDATION

As stated previously, the purpose of this Phase 1 effort was to evaluate the feasibility of using the ultrasonic, laser/IR and microvideo detection techniques as parts of the solder joint inspection station. The general conclusion of this Phase 1 study is that all three techniques are technically feasible and that an inspection station comprised of all three operating together would be significantly more effective than current practices, and more effective than if the techniques were used separately.

The general recommendation is that the Sacramento Air Logistics Center should authorize the Phase 2 effort to fabricate individual usage size models of the detection apparatus and to define the integrated station design.

SPECIFIC CONCLUSIONS

The following specific conclusions address the requirements of the Contract Data Requiremetns List relating to the details to be included in the Final Report. The accuracy percentages stated are based on the number and types of defects examined to date. They are subject to revisions under expanded examinations.

Accuracy of Defect Detection

Ultrasonic Technique

The ultrasonic technique will detect actual open joints with virtually 100 percent accuracy. Further, cracks, voids or inclusions that affect 30 percent or more of a joint can be detected with an estimated accuracy of 95 percent or greater. If the area of the joint affected is from 15 percent to 30 percent for these defect types the estimated accuracy is approximatley 90 percent. Cold solder joints that actually give a granular or cloudy visual appearance can be detected with greater than 90 percent accuracy. Partially cold joints give a lower confidence of detection. Those joints that may be considered "cosmetic" in nature, such as excess solder, irregualr spreading, or toe of lead bent probably will not be detected unless there is some other defect present in the joint.

The overall detection accuracy of the ultrasonic technique, considering all defects, is estimated to exceed 90 percent. A qualitative picture of overall detection capability is shown in Table 7. In Table 7, "YES" indicates near 100 percent detection, "PROBABLE" indicates detection more than 75 percent of time, "POSSIBLE" indicates detection from 50-75 percent of time and "UNLIKELY" indicates detection less than 50 percent of time.

Laser/IR Technique

Actual open joints will be detected with near 100 percent accuracy unless there is an excessive amount of solder or if there is exposed gold on the lead. These conditions could mask the detection by laser/IR alone. The probability of detection of cracks, voids or inclusions that affect 50 percent or more of a joint is estimated to exceed 70 percent with the same constraints as above. Cold solder joints would be detected with about the same accuracy as the ultrasonic technique. The laser/IR technique also will give a warning at least 50 percent of the time that a joint is suspect if there is a significant amount of exposed gold, or if there is excessive solder present, or for many cases of excessive heating.

The overall accuracy of the laser/IR technique cannot be stated with any great confidence until after the results of a cross correlation to be conducted during the beginning of Phase 2.1. However, the current estimate is that the overall accuracy will exceed 70 percent.

TABLE 7. OVERALL DETECTIVE CAPABILITY

		Detection Technique			
	Defect Type	Ultrasonic	Laser/IR	Color Video	Combined
(a)	Cold solder joint	Probable	Probable	Possible	Yes
(b)	Irregular Spreading-Excessive heat	(A)	(A)	Probable	Probable
(c)	Irregular Spreading-Insufficient heat	(A)	(A)	Probable	Probable
(d)	Toe of lead bent up	Possible (A)	Unlikely	Yes	Yes
(e)	Lead soldered 1/2 off pad	Probable	Possible	Yes	Yes
(f)	Tipped lead	Probable	Possible	Yes	Yes
(g)	Yellow flat top visible	Probable	Yes	Yes	Yes
(h)	DELETED	-	-	-	-
(i)	Voids	Yes	Possible	No	Yes
(j)	Cracks at heel	Yes	Possible	Possible	Yes
(k)	Granular appearance	Possible	Yes	Yes	Yes
(l)	Entrapped gold	Possible	No	No	Possible
(m)	DELETED	-	-	-	-
(n_1)	Insufficient solder	Probable	Possible	Yes	Yes
(n_2)	Excess solder	No	Probable	Yes	Yes
(o)	Excessive heat	(A)	(A)	(A)	(A)
(p)	No fillet at heel	Yes	Unlikely	Probable	Yes
(q)	Dewetted	Yes	Possible	Unlikely	Yes
(r)	Holes and/or pits	Probable	Possible	Yes	Yes
(s)	Solder peaks	Unlikely	Possible	Yes	Yes
(t)	Inclusions	Yes	Possible	No	Yes
	Open joint	Yes	Yes	Possible	Yes

(A) Depends on other contributing factors such as severity of defect.

Visual Technique

The visual technique is intended to be complementary to the ultrasonic and laser/IR techniques. Primarily it will resolve the differences between the other two techniques, and will allow assessment of other than lap-type solder joints.

Overall System

The overall inspection system, based on the Phase 1 results, is expected to be at least 90 percent effective in detecting defective solder joints that may affect the operability of a printed circuit board. Essentially 100 percent detection is expected for a solder joint that contains cracks, voids or inclusions that affect 30 percent or more of a joint area. Cold solder joints should be detectable with at least 70 percent accuracy - greater than 90 percent if the joint surface appears granular or cloudy.

The detection accuracy of both the ultrasonic and laser/IR technique is expected to improve somewhat during the Phase 2 program.

Processing Capabilities

Accuracy of Platform Movement

Commercially available positioning tables are capable of stepping-increments of 0.001" with a repeatability of 0.0001". This is more than sufficient in view of the minimum of 0.015" to 0.017" lead widths and their average center-to-center spacing of 0.050".

Throughput Capability, 1000-Joint PCB

Assume 50-mSec laser exposure, recording of peak thermal signal only (no cooldown observations), and moving on to next joint.

Board installation		15 Sec
Testing (per joint)		
Laser Warmup	50 mSec	
Ultrasonic Touch & Go	500 mSec	
Transport	50 mSec	
Computing	20 mSec	
	620 mSec	
	For 100 joints:	620 Sec
Visual Inspection of Estimated 20 Joints @ 5 sec each:		100 Sec
Board Removal		15 Sec
Logging and Data Interpretation		15 Sec
	TOTAL	765 Sec (~ 13 min/bd)

This rate would permit the inspection of approximatley 30 such boards per station per workday.

Number of Allowable PCB Configurations

Board size limited only by table size; 12" x 12" tables are available. Solder joint addresses for each board will be stored on floppy disc. Number of different boards limited only by number of discs stored.

Data Storage Method

Disc data will be loaded into random-access-memory prior to scan of each type of board. Derived data will be stored temporarily on floppy disc for later retrieval and analysis.

Operator Training Requirement

Estimated as two-day hands-on-type seminar.

Marking Methods Considered

There are two marking requirements: (1) a means of marking a printed circuit board (PCB) for permanent identification, and (2) a means of marking replacement parts on a PCB. Little effort was expended on this item during Phase 1. As stated in Battelle's original proposal, this is to be an Auxiliary Task in Phase 2. However, current considerations for marking the PCB range from application of a preprinted sticker, to painting, to modifying the PCB physically. The replacement devices on a PCB probably will be marked by a paint dot or a simple stick-on tag.

Risk Statement

Sensor Techniques

The laser/IR technique is a non-contact method and, thus, there is no wear, as such. The current IR sensor does require cooling (adding refrigerent twice per shift), and the associated optics must be kept clean. Otherwise, the IR sensor is a long-life low maintenance item.

The ultrasonic probe is a small but quite rugged contact system (transceiver assembly). The more fragile parts, e.g., fine wire, piezoelectric materials, etc., will be protected from inadvertant bumping to prevent breakage.

Platform Movement Accuracy

The platform accuracy was discussed earlier. These stages require reasonable care in handling and use. Care should be taken to avoid dropping heavy items on them, and to avoid inadvertant jamming.

Maintenance Calibration

The experience gained during Phase 1 on the laboratory bench models for the inspection techniques indicates that the turn-on and calibration procedure will require from 15-30 minutes at the beginning of a work day plus (possibly) another 10-15 minutes at the midpoint of a shift.

Station Information

General Description

The current concept of the TIS is:

(1) An accurate, programmable x-y stage to hold and position a PCB
(2) An ultrasonic transceiver assembly
(3) A low-power (5-10 watt) laser with shutter to control pulse width (heating)
(4) An infrared detecor
(5) A multilens, color microvideo system for visual examination
(6) A computer to control stage motion, to analyze sensor data and to provide limited temporary memory capability
(7) A floppy disc storage system for permanent storage of desired information

Data Processing Considerations

The consideration of actual data processing techniques (automatic decisions of "good" vs "bad" joint) is not a requirement of Phase 1. However, the determination of feasibility required the evaluation of whether or not the laser/IR and ultrasonic data could be used for automatic decision making. The experimental results, as depicted by the oscillograms in this report, indicate that automatic decision making is quite feasible.

The laser/IR technique apparently needs to consider only the peak temperature reached by a joint due to exposure to a specified laser pulse. This peak temperature then can be compared to the stored peak temperature (actually a narrow range of peak values) for a known good joint. If the observed temperature is wthin the "good" range, the joint is "good". An observed value outside the "good" range would cause the joint to be rejected, or at least, classified as suspect. This is a relatively simple process to implement using digital techniques such as a microprocessor or microcomputer.

The ultrasonic data are somewhat more complex to interpret, but are just as amenable to digital processing. The ultrasonic technique shows that the application of a known ultrasonic pulse to a good solder joint produces a set of resonance frequencies with a range of amplitudes. These frequencies and amplitude ranges could be stored as a comparison key. Three types of response by an inspected joint could result in outright rejection or classificaiton as a suspect joint.

(1) The appearance of additional resonant frequencies with amplitudes above a predetermined level and/or
(2) Significant increases in the amplitudes of the normal resonances beyond the normal range and/or
(3) Broadening of the normal resonant peaks outside the normal envelope.

All of the above responses can be compared to the stored key by digital techniques.

Either of the laser/IR or ultrasonic techniques can cause a joint to be classified as defective. Also, if both techniqeus would classify the same joint as suspect or marginal the joint would be classified defective. In either case, the joint would be subject to repair. If one technique classifies a joint as suspect and the other technique classifies it as good, then the final classification would be made after a visual inspection.

The above is a preliminary discussion only and should not be construed as a fixed committment to a particular procedure.

SPECIFIC RECOMMENDATIONS

The results of the Phase 1 feasibility study suggest the following recommendations.

(1) The program should be continued into Phase 2, the fabrication of usage size models. Phase 2 (12 months) should be divided into two parts.

  (a) Phase 2.1 (5 months) should include
    1. An accuracy refinement task incorporating a correlation between the ultrasonic and laser/IR results with a physical analysis of the tested joints.
    2. A survey of several PCB manufacturers to assure compatability between PCB and the inspection station
    3. The fabrication of an envelope model to give a picture of the overall concept of the TIS. Materials of construction would be plastic, wood, etc., for showing general conformation
    4. Preliminary design documentation
    5. Initiation of actual individual model fabrication.

  (b) Phase 2.2 (7 months) should include:
    1. Completion of fabrication of individual usage size models

2. Completion of design for models and
3. Completion of design for integrated station.

(2) The overall cost for Phase 2 should be approximately $546,000 divided as about $205,000 for Phase 2.1 and about $341,000 for Phase 2.2

(3) Phases 3 and 4, the fabrication, installation and maintenance for 1 year of the TIS will cost on the order of $400,000.

The actual technical details for Phase 2 will be explained more fully and the actual expected cost for Phase 2 will be refined and detailed in Battelle's formal proposal for Phase 2 to be submitted separately from this report.

The details and actual expected cost of Phases 3 and 4 will be provided at the end of Phase 2.